

4-1-1998

Fatigue Related Wind Loads on Highway Support Structures

Kevin W. Johns

Robert J. Dexter

Follow this and additional works at: <http://preserve.lehigh.edu/engr-civil-environmental-atlss-reports>

Recommended Citation

Johns, Kevin W. and Dexter, Robert J., "Fatigue Related Wind Loads on Highway Support Structures" (1998). ATLSS Reports. ATLSS report number 98-03.
<http://preserve.lehigh.edu/engr-civil-environmental-atlss-reports/229>

This Technical Report is brought to you for free and open access by the Civil and Environmental Engineering at Lehigh Preserve. It has been accepted for inclusion in ATLSS Reports by an authorized administrator of Lehigh Preserve. For more information, please contact preserve@lehigh.edu.



ADVANCED TECHNOLOGY FOR
LARGE
STRUCTURAL SYSTEMS

Lehigh University

Fatigue Related Wind Loads on Highway Support Structures

Final Report

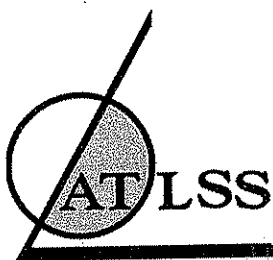
By

Kevin W. Johns
Graduate Research Assistant
Lehigh University

Robert J. Dexter
Associate Professor of Civil Engineering
University of Minnesota

ATLSS Report No. 98-03

April 1998



ADVANCED TECHNOLOGY FOR
LARGE
STRUCTURAL SYSTEMS

Lehigh University

Fatigue Related Wind Loads on Highway Support Structures

Final Report

By

Kevin W. Johns
Graduate Research Assistant
Lehigh University

Robert J. Dexter
Associate Professor of Civil Engineering
University of Minnesota

Prepared for:
New Jersey Department of Transportation
CN 615
Trenton, New Jersey 08625-0615

ATLSS Report No. 98-03

April 1998

ATLSS Engineering Research Center
Lehigh University
117 ATLSS Dr., Imbt Laboratories
Bethlehem, Pennsylvania 18015-4729

Acknowledgments

The research reported herein was performed at the Center for Advanced Technology for Large Structural Systems (ATLSS) at Lehigh University. The project was sponsored by the New Jersey Department of Transportation. The authors would like to acknowledge Professor John W. Fisher for providing invaluable guidance over the course of the research program. Robert Connor assisted with the instrumentation, data acquisition and field testing throughout the duration of the project. Ed Tomlinson assisted in the instrumentation and data acquisition process. John Hoffner, Larry Heffner, Steve Leonard, Roger Moyer, Todd Anthony and other ATLSS technicians provided assistance with all laboratory work.

Table of Contents

List of Tables	v
List of Figures	vi
Abstract	1
Chapter One: Introduction	2
1.1 Problem	2
1.2 Purpose	4
1.3 Scope	4
Chapter Two: Background	6
2.1 Wind Loading Phenomena Relevant to VMS Support Structures	6
2.1.1 Natural Wind Gusts	6
2.1.2 Galloping	9
2.1.3 Truck-Induced Wind Gusts	11
2.2 Background Relevant to Fatigue Resistance of Details	14
Chapter Three: Field Tests and Findings	19
3.1 History of the New Jersey VMS Support Structure	19
3.2 Erection Details	20
3.2.1 Erection Procedures Used on Interstate 80	21
3.2.2 Erection Problems and Recommendations	21
3.2.3 Dead Load Stresses	22
3.3 Field Test Description	23
3.3.1 Short-term Testing Procedures	23
3.3.1.1 Short-term Testing Problems	25
3.3.1.2 Dynamic Characteristics and Static Test Results	25
3.3.2 Long-term testing	26
3.3.2.1 Long-term Testing Problems	26
3.4 Discussion of Field Test Results	27
Chapter 4: Recommendations and Conclusions	70
4.1 Design Load Recommendations	70
4.1.1 Galloping	70
4.1.2 Truck-Induced Gusts	70
4.1.3 Natural Wind Gusts	71
4.2 Conclusions	71
4.3 Recommendations for Future Research	73
4.3.1 Power Supply	73
4.3.2 Communication	73
4.3.3 Pressure Measurements	74

4.3.4 Strain Measurements	74
4.3.5 Additional Truck-Gust Measurements	74
4.3.6 Wind Induced Vibrations	75
References	78
Appendix A – Fatigue Design Load Application	80

List of Tables

Table 2-1 Summary of Pressures from Various Researchers	13
Table 3-1 Test Truck Configurations	28
Table 4-1: Truck-Induced Gust Values	71

List of Figures

Figure 1-1: Cantilevered VMS on Interstate 80 West Bound Mile Marker 48.5.	5
Figure 2-1 Stress Range in a Caltrans Monotube VMS Sign Support Structure.	16
Figure 2-2 Failed VMS Support Structure Due to Anchor Bolt Fatigue.	17
Figure 2-3 Close up of Fractured Anchor Bolts.	17
Figure 2-4 AASHTO S-N Curves for Steel.	18
Figure 3-1 VMS Column Erection on Interstate 80.	31
Figure 3-2 Anchor Bolt Tightening with a Hydraulic Torque Wrench.	32
Figure 3-3 VMS Connected to Truss in Storage Yard.	33
Figure 3-4 VMS and Truss Lifted into Position for Connection to Column.	33
Figure 3-5 Bronze Plate Between Faying Surfaces of Stub and Chord.	34
Figure 3-6 Top Nut Loosened by Hand after being Tightened.	34
Figure 3-7 Gap Between Faying Surfaces Even with Bronze Plate.	35
Figure 3-8 Dead Load Stress in Column.	36
Figure 3-9 Anchor Bolt Numbering Scheme.	37
Figure 3-10 Axial Dead Load Stress in Anchor Bolts.	38
Figure 3-11 Strain Gage Locations on the Column and Truss.	39
Figure 3-12 Strain Gage Locations on Anchor Bolts.	40
Figure 3-13 Pressure Transducer Numbering Scheme.	41
Figure 3-14 Pressure Transducers on the Face of the VMS	42
Figure 3-15 Wind Sentry to Measure Wind Speed and Direction.	42
Figure 3-16 Campbell Scientific CR9000 Digital Data Acquisition System.	43

Figure 3-17 Mobile Field Office for Short-term Testing.	43
Figure 3-18 Location of Load for Static and Pluck Tests.	44
Figure 3-19 Test Trucks Driving Under VMS to Produce Truck-Induced Wind Gusts.	45
Figure 3-20 Damping of Motion is a Column Strain Gage.	46
Figure 3-21 FFT Indicating Natural Frequency in the "Twisting Mode".	47
Figure 3-22 FFT Indicating Natural Frequency in the "Hatchet Mode".	48
Figure 3-23 Stress in Structure from a 1 kN Load.	49
Figure 3-24 Enclosure for Data Acquisition Equipment During the Long-term Testing.	50
Figure 3-25 Random Trucks Under VMS Causing Gusts.	50
Figure 3-26 Pressures from Truck Test One and the Corresponding Column Stress.	51
Figure 3-27 Pressures from Truck Test Two and the Corresponding Column Stress.	52
Figure 3-28 Comparison of Column Response in All Three Truck Tests.	53
Figure 3-29 Pressure Gradient in Truck Test Three.	54
Figure 3-30 Stress Ranges in Column from Truck Test Three.	55
Figure 3-31 Stress Range in Lower Stub and Chord in Truck Test Three.	56
Figure 3-32 Comparison of Structure in "Twisting" and "Hatchet" Modes.	57
Figure 3-33 Random Data File from Long-term Monitoring.	58
Figure 3-34 Close Up of Long-term Data.	59
Figure 3-35 Close Up of Long-term Data.	60
Figure 3-36 Close Up of Long-term Data.	61

Figure 3-37 Random Data File from Long-term Monitoring.	62
Figure 3-38 Close Up of Long-term Data.	63
Figure 3-39 Close Up of Long-term Data.	64
Figure 3-40 Close Up of Long-term Data.	65
Figure 3-41 Maximum Recorded Stress Ranges in Column and Natural Wind Speed.	66
Figure 3-42 Maximum Recorded Stress Range in Top Chord.	67
Figure 3-43 Maximum Recorded Axial Stress Ranges in Anchor Bolts.	68
Figure 3-44 Maximum Wind Speed and Column Response.	69
Figure 4-1 Critical Location Stress Ranges on I-80 Structure.	76
Figure 4-2 Improved Strain Gage Layout for Future Monitoring.	77

Abstract

In order to determine equivalent static pressures for fatigue loads on cantilevered highway sign support structures a cantilevered Variable Message Sign (VMS) located along Interstate 80 westbound at mile marker 48.5 in northern New Jersey was continuously monitored for three months. The structure was instrumented with strain gages, pressure transducers, and a wind sentry. All the data was collected with a Campbell Scientific CR9000 digital data acquisition system. A cellular phone transceiver enabled remote communication with the data logger. The system and instrumentation was powered with solar powers and marine batteries. Short-term testing was performed on the structure to determine the dynamic characteristics such as stiffness, natural frequency, and percent of critical damping. Results of the short-term test indicated that the stiffness was 0.24 kN/mm, the first and second mode natural frequencies were 0.87 cycles/s and 1.22 cycles/s respectively, and the percent of critical damping for the first and second modes were 0.57 percent and 0.25 percent respectively. Long-term monitoring was performed to capture the structure's response to natural wind gusts, galloping, and truck-induced wind gusts. This data would then be used to determine appropriate fatigue design wind loads for future sign support structures. During the three months of monitoring the structure did not experience galloping, which is a phenomena highly dependent on location. A galloping design pressure of 1000 Pa was recommended based on previous research. The summer months, which is when the structure was monitored, were not conducive to the strongest natural wind patterns in northern New Jersey. The highest natural wind speed that was recorded was 7.5 m/s. It is believed that much stronger winds are present in winter and spring, therefore a natural wind gust design pressure of 250 Pa was recommended. Truck-induced gusts were measured and a linear gradient for the truck-induced gust design pressure was determined. The truck-induced gust design pressure ranged linearly from 1760 Pa at 0 to 6 m above the surface of the road to 0 Pa at 10.1 m and over.

Chapter One: Introduction

1.1 Problem

Cantilevered sign and signal support structures are used extensively on major interstate highways and at local intersections for the purposes of traffic control. The cantilevered support structures are attached to a single vertical support as opposed to two supports for traditional overhead structures. The single support increases motorist safety by minimizing the probability of vehicle collision and is more economical than overhead support structures.

The 1994 AASHTO Standard Specifications for Structural Supports for Highway Signs, Luminaires, and Traffic Signals offers little guidance in the design for fatigue. The specification is currently being revised and will have better guidance for fatigue design. Until the new specification is available, designers do not have adequate guidance for fatigue related design issues in signs, signals and luminaire support structures. Consequently, many cantilevered sign and signal support structures across the country have exhibited excessive displacement due to wind-induced vibration and several have even failed due to fatigue cracking. In Michigan, fatigue cracks developed in the anchor bolts of a cantilevered sign support structure, resulting in the death of a motorist. Cracking has also occurred in many of the welded details of cantilevered sign and signal support structures, such as the connection of the mast arm or truss to the column, or the connection of the column to the base plate.

There are some obvious reasons for the sensitivity to vibration of cantilevered support structures. The single support significantly increases the flexibility of the cantilevered structures relative to overhead structures. The flexibility of these structures has increased over the years due to longer span lengths to accommodate more traffic lanes and a desire to set the column farther away from the road to increase motorist safety. Today, it is not unusual for the cantilever to span more than 12 meters (40 ft). The ratio of stiffness to mass consistently gives these structures a low natural frequency of about 1.0 Hz. These cantilevered support structures also have extremely low critical damping ratios, typically less than one percent of critical damping. These conditions make cantilevered support structures particularly susceptible to large-amplitude vibration and/or fatigue cracking due to wind loading.

The wind-induced vibration of cantilevered support structures was recently studied at the Center for Advanced Technology for Large Structural Systems (ATLSS) for the National Cooperative Highway Research Program (NCHRP). The project was NCHRP 10-38, "Fatigue-Resistance Design of Cantilevered Signal, Sign, and Light Supports". It was found that excessive vibration of cantilevered sign and signal support structures may be due to three different phenomena, possibly acting together at times. These three phenomena are 1) buffeting by natural-wind gusts; 2) buffeting by gusts caused by trucks passing under the structure; and 3) galloping. Any of these

may cause large-amplitude displacement ranges and associated stress ranges in sign and signal support structures. Therefore, the details of these structures must be designed for fatigue resistance by considering typical stress ranges resulting from these phenomena.

Equivalent static load ranges were recommended in the NCHRP Project 10-38 final report which can be used to estimate stress ranges at details for the three wind-loading phenomena. These fatigue design loads are less than the ultimate design loads used for strength design, and therefore should not be considered in the strength design checks.

Depending on their geometry, sign and signal support structures may be more or less affected by the three wind-loading phenomena. For example, truck-induced wind gusts act primarily vertically upward on the projected area on a horizontal plane. Flat signs, signals, and their support structures are not susceptible to truck-induced wind gusts, due to their relatively small area projected on a horizontal plane. Variable message signs (VMS) are potentially susceptible to truck-induced wind gusts, because of their width in the direction of traffic and the large area projected on a horizontal plane.

The VMS is a relatively new type of sign that is capable of displaying any message on an electronic LED face. This feature enables motorists to be provided with the most recent information regarding road conditions and traffic flow. The sign is controlled from an office that is given information such as traffic speed and congestion from cameras and radar guns that are mounted beside the VMS. The research described in this report was motivated by reported large-amplitude vibration of a VMS support structure in New Jersey.

Many other VMS have had problems with excessive vibration and fatigue. Failures of cantilevered support structures for VMS have occurred in Virginia¹⁶ and California¹⁷. A second California cantilevered VMS support structure was instrumented and monitored. Stress ranges of 140 MPa (20 ksi) were recorded during one wind event, which is well above the fatigue threshold for typical details. Truck-induced wind gusts are believed to have been the problem in New Jersey and in Virginia, whereas galloping was identified as the cause of the excessive vibration in the California VMS. The California VMS are mounted on a curved monotube support structure, which is much different and more susceptible to galloping due to the low torsional rigidity of the mast arm. A typical truss-type structure, such as is used in New Jersey, is torsionally stiff and is therefore not as susceptible to galloping.

The 10-38 research was focussed primarily on galloping. The recommended fatigue design load range for truck-induced wind gusts was based on some uncertain assumptions. Therefore, this additional research was sponsored by New Jersey DOT (NJDOT) to gather additional data on the magnitude of the truck-induced wind gust loads.

This research also addresses anchor bolt tightening and tightening of the truss to stub connections at the column. The anchor bolts used in these structures are as large as three inches in diameter. There was not much guidance available on the

proper tightening procedure for this size of bolt. Improper tightening of the anchor bolts can cause changes in the dynamic characteristics of the sign support structure.

There was also concern about the amount of contact on the faying surfaces for the truss to stub connection. The concern was over the fact that it is near impossible to get 100 percent mating between the two surfaces, therefore different alternatives were looked at to solve this problem.

1.2 Purpose

The primary objective of the research described in this report was to gather data on the magnitude of truck-induced gust loads and, if necessary, refine the equivalent static load range for truck-induced wind gusts recommended in NCHRP 10-38. To accomplish this objective, a cantilevered VMS was instrumented and monitored. The VMS that was chosen by NJDOT spans Interstate 80 West at mile marker 48.5 in northern New Jersey (Figure 1-1). Short-term and long-term field tests were conducted. The short-term test had two main goals: 1) to obtain the static and dynamic characteristics of the support structure, such as stiffness, natural frequency, and damping ratio; and, 2) to drive trucks under the sign in an attempt to quantify the magnitude of the truck-induced gusts. The long-term test lasted three months and would attempt to measure any significant dynamic response from random truck traffic and other wind-loading phenomena.

1.3 Scope

This report summarizes previous research relevant to the design of VMS support structures to resist truck-induced gusts and other wind-loading phenomena. The measurements included pressures near the VMS and strains at all critical locations. Pressure transducers were intended to measure the pressure resulting from the upward gust of air that large trucks produce when going under the signs at high speeds. The stress ranges deduced from the strain histories would be compared to stress ranges calculated using the fatigue design load ranges recommended in NCHRP 10-38. The design guidelines recommended herein can be used to design future structures to be resistant to fatigue and excessive dynamic displacement despite the worst-case truck-induced wind loads. This research was not concerned with changing the geometry or adding damping devices to mitigate the vibration problems. Mitigation is to be addressed in the phase two studies of project 10-38, which are ongoing at the University of Minnesota under the direction of Robert Dexter.

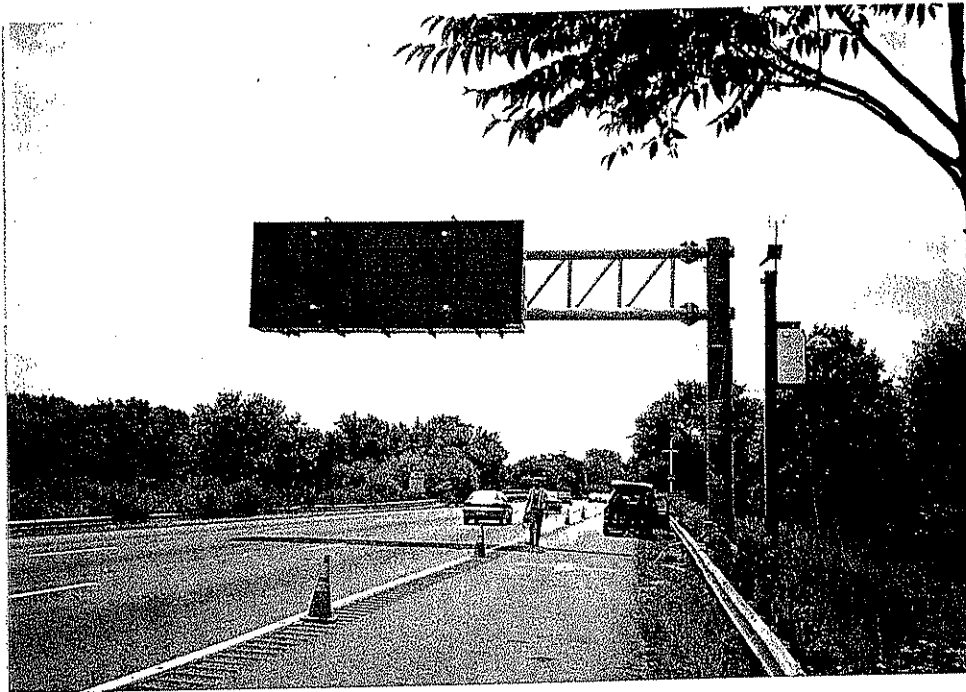


Figure 1-1: Cantilevered VMS on Interstate 80 West Bound Mile Marker 48.5.

Chapter Two: Background

2.1 Wind Loading Phenomena Relevant to VMS Support Structures

All types of support structures are potentially susceptible to natural wind gusts and truck-induced wind gusts. In cantilevered structures it is easier for the mast arm to twist (i.e. for the sign panel to change angle of attack relative to the wind) than it is in overhead structures. This change in angle of attack facilitates galloping, as is explained below. Therefore, in cantilevered structures, galloping is also a primary concern, in addition to natural and truck-induced gust loading. Vortex shedding is a different phenomenon than galloping but also results in vertical displacements; therefore, these phenomena are often confused. Previous research in Project 10-38 showed that vortex shedding did not occur in cantilevered sign and signal support structures as long as the sign or signal was attached, presumably because the galloping began to occur first.

Because overhead support structures are not susceptible to galloping, they are potentially susceptible to vortex shedding. Irwin and Peeters¹ discovered a problem with vortex shedding in an overhead sign support structure that failed in Calgary, Canada. The vortex shedding occurred from two 8 m (25 ft) long sign panels mounted on the structure.

To our knowledge vortex shedding has never been reported to be a problem for cantilevered support structures and therefore, vortex shedding will not be discussed further.

2.1.1 Natural Wind Gusts

The response of typical cantilevered support structures to natural wind gusts was modeled using spectral finite-element analysis. The structure is broken up into several continuous areas such as signs or exposed portions of the structure. The fluctuating wind force on each area and the resulting response variables (such as column base moment) during a short interval are characterized as stationary random processes. The response spectrum can be related back to the expected variable-amplitude history of the response as a function of time. Specifically, the root-mean-square (RMS) of the random response time history is found from the integration of the response spectrum over all significant frequencies. In the case of cantilevered support structures, there are only a few significant frequencies; therefore, the integration is performed by simply summing the response at these frequencies.

The wind force spectrum is derived from the velocity spectrum. A standard wind velocity spectrum (which depends on the mean hourly wind velocity) was selected from the literature⁷:

$$S_v(f) = \frac{4KV_{10}^2 x^2}{f(1+x^2)^{4/3}} \quad (2-1)$$

where $S_v(f)$ is the spectral density of the velocity (which has units of velocity squared multiplied by time), f is the cyclic frequency (cycles/s), K is a terrain coefficient $(m/s)^2$, V_{10} is the mean wind velocity (m/s) at a reference height of 10 meters, and x is the quantity $(1200 \text{ meters} * f)/V_{10}$ (dimensionless for V_{10} in m/s). The terrain coefficient K was taken as 0.005 which is typical for open grassy terrain^{7,8}.

The drag force is proportional to the square of the velocity and both the force and the velocity can be represented as the sum of their mean and fluctuating components. Through algebraic manipulation of these relationships, the following relations can be obtained⁸:

$$\left(\frac{d}{v}\right)^2 = \frac{4 D^2}{V^2} = 4 C^2 A^2 V^2 \quad (2-2)$$

where d and D are the fluctuating and mean value of the drag force respectively, v and V are the fluctuating and mean value of the wind velocity respectively, A is the total frontal area of the surface which is causing the drag, and C is a constant equal to $0.5\rho C_d$ with ρ equal to the density of air and C_d equal to the drag force coefficient. The density was taken as 1.22 kg/m^3 which is the value for "standard air" (one atmosphere pressure at 14°C).

The force and velocity spectra are proportional to the square of the fluctuating components of force or velocity, therefore the ratio of these spectra is equal to the ratio in Equation 2-3, i.e.:

$$S_F(f) = 4 C^2 A^2 V^2 S_v(f) \quad (2-3)$$

The force spectrum must be calculated for the total frontal area of a surface and cannot be broken down into sub-areas. One spectrum is calculated for each sign and signal attachment. Additional spectra are calculated for each continuous exposed portion of the mast arm or column. These spectra must be completely correlated to each other in the analysis.

Important assumptions must be made regarding 1) the mean wind velocity at which the support structures should be analyzed; and, 2) estimating the effective stress range from the RMS of the variable amplitude response. It is impractical to forecast the future wind history at each location for cantilevered support structures therefore, some very simple assumptions were made. The design procedure is based on a spectral analysis using the mean hourly wind velocity, which was exceeded in only 0.01 percent of all hours. It is accepted that the probability of exceedence of mean hourly wind velocity at a location is a Rayleigh distribution, which depends only on the yearly mean wind velocity V_m ⁹, i.e.:

$$P_E(v) = e^{\frac{-\pi v^2}{4V_m^2}} \quad (2-4)$$

where $P_E(v)$ is the probability that a randomly-occurring mean hourly velocity is greater than the velocity magnitude v and e is the base of the natural logarithms. The limit-state mean hourly velocity is found by setting P_E equal to 0.01 percent and solving for v .

The yearly mean wind velocity also varies from place to place. A collection of yearly mean wind speed data from weather stations at 59 cities across the U.S. was examined. Most weather stations are located at airports, therefore the data should be representative of most open terrain. The data showed that 81 percent of the cities had a mean wind velocity of less than 5 m/s (11 mph) at 10 m (33 ft) above the ground. It was decided to use 5 m/s (11 mph), which was exceeded in only 19 percent of U.S. cities, as the baseline case for a static design pressure in the specifications. The mean hourly wind velocity for this yearly mean wind speed is 17 m/s (37 mph).

The result of the analysis, the spectral density of the response, has units of the response (such as moment or stress) squared multiplied by time. When the spectral density of the response is integrated across a range of frequencies, the result (the area under the spectrum) is equivalent to the variance of the response about the mean. The square root of this area is the root-mean-square (RMS) of the response. The time history of the response is narrow-banded (concentrated about one frequency), since the response is still dominated by the resonant frequency. For random, narrow-band time histories, the average or effective stress range S_r^{eff} can be estimated from the relationship which gives the stress range for a constant-amplitude response in terms of the rms of the stress response σ_{rms} ¹⁰, i.e.:

$$S_r^{\text{eff}} = 2.8 \sigma_{\text{rms}} \quad (2-5)$$

A variety of sign, signal, and luminaire support structures were analyzed at a mean wind velocity of 17 m/s and values of normalized equivalent static pressures for these structures ranged from 170 to 300 Pa (3.6 to 6.3 psf). Considering the numerous uncertainties in this analysis, not enough is known to assign greater or lesser loads to different types of structures. Also, separate loading for different types of structures would unnecessarily complicate the design process. Therefore, these values were averaged and rounded to 250 Pa (5.2 psf), which is recommended for design. This natural wind gust pressure must be applied to a variety of surfaces with widely varying drag coefficients. Therefore the recommended static design pressure must be multiplied by the appropriate drag coefficient and then may be applied to the surface. The structures should be designed so that the stress ranges resulting from the application of this load range are below the CAFL⁶.

These calculations indicate that most structures will eventually be susceptible to cracking from natural wind gusts, but the recommended loads are not so large as to

predict rapid failure. These results are consistent with observed service fatigue failures that can be attributed to natural wind gusts. Because of the uncertainty in these assumptions, the recommended equivalent static load range can be easily adjusted for other mean wind speeds.

2.1.2 Galloping

Galloping, also known as Den Hartog instability, is an areoelastic phenomenon caused by a coupling between the aerodynamic forces which act on a structure (caused by the action of wind) and the structural vibrations². Galloping is characterized by large amplitude, vibrations normal to the direction of wind flow. Galloping-induced oscillations primarily occur in flexible, lightly damped structures with non-symmetrical cross-sections (e.g. circular cylinders are not susceptible to galloping-induced vibrations because they are symmetric).

Galloping-induced oscillations are caused by forces, which act on a structural element as it is subjected to periodic variations in the angle of attack of the wind flow. The periodically varying angle of attack is generated by across-wind oscillation of the structure. When the forces are aligned with the direction of across-wind motion, the result is successively larger amplitudes of oscillation, i.e. galloping.

The potential susceptibility of a structure to galloping from the equilibrium position is evaluated using the Den Hartog stability criterion⁴.

$$\left(\frac{dC_{Fy}}{d\alpha}\right)\bigg|_{\alpha=0} = -\left(\frac{dC_L}{d\alpha} + C_D\right)\bigg|_{\alpha=0} > 0 \quad (2-6)$$

where C_{Fy} is the aerodynamic lift force coefficient acting normal to the free stream velocity, α is the angle of attack, C_L is the lift force coefficient, and C_D is the drag force coefficient which acts in respect to the relative wind velocity. The free stream velocity is defined as the relative wind velocity times the cosine of the angle of attack. The Den Hartog stability criterion states that "a section is dynamically unstable if the negative slope of the lift curve is greater than the ordinate of the drag curve." As is evident from Equation 2-6, this condition is satisfied when the slope of the lift force coefficient normal to the free-stream velocity, $dC_{Fy}/d\alpha$, is positive (in other words, when the term $dC_L/d\alpha + C_D$ is negative). This condition is referred to as "negative aerodynamic damping".

Galloping from the equilibrium position can only occur if the magnitude of the negative aerodynamic damping is greater than the magnitude of the positive mechanical damping possessed by the structure (i.e. galloping can only occur if the effective damping is less than zero). Therefore, the minimum wind velocity required to initiate galloping is directly proportional to the mechanical damping possessed by the structure³. This onset wind velocity is also proportional to the mass and stiffness of the structure and the inverse of the slope of the lift force coefficient curve, C_{Fy} .

Thus, a highly flexible structure with low damping (such as a typical cantilevered support structure) will be susceptible to galloping-induced oscillations at relatively low wind velocities provided, of course, that the Den Hartog stability criterion is satisfied.

Although the structure on Interstate 80 never experienced galloping while it was monitored, there has been other very recent research that has been investigated to formulate a recommended fatigue design galloping pressure range.

A majority of cantilevered support structures are composed of structural members with circular cross-sections. Circular cylinders are not susceptible to the galloping instability. This fact is important because it indicates that the across-wind vibrations observed in the cantilevered support structures in the field are the result of the aerodynamic characteristics possessed by the attachments to these structures (i.e. signs/signals).

This fact was confirmed by McDonald et al.⁵ at Texas Tech University. McDonald's tests indicated that the configuration of the signal attachments and the direction of flow significantly influence the susceptibility for galloping. Signal attachments configured with backplates and subjected to flow from the rear were found to be most susceptible to galloping (i.e. the slope of the lift force coefficient curve, C_{Fy} , was greatest for this configuration and flow direction).

A full-scale 12.2 m (40 ft) structure configured with signal attachments was observed to experience galloping oscillations with displacement amplitudes at the tip of the horizontal support estimated at between 300 to 400 mm (12 to 16 in). The results of tests on a 14.6 m (48 ft) structure were similar. Galloping was observed in this structure at a wind velocity equal to 4.5 m/s (10 mph) with a maximum measured stress range in the vertical support (at a location 330 mm (13 in) from the base) equal to approximately 34 MPa (4.9 ksi).

These observations regarding signals with backplates were confirmed in wind-tunnel tests conducted at the Wright Brothers facility at M.I.T. as part of the NCHRP project 10-38. These wind-tunnel experiments were such that the scaled up cantilevered sign and signal support structures would be subjected to equivalent static lift-pressure ranges between 1150 and 1770 Pa (24 and 37 psf) during occurrences of galloping-induced vibrations. These pressures were derived from the maximum loads obtained at the highest wind velocities (about 13 m/s) applied in the tests. It was observed that the magnitude of the loads increases with wind velocity, such that much larger loads are theoretically possible at higher wind velocities. However, larger velocities were not used in the wind-tunnel tests in order to minimize potential damage to the test specimens.

Finite-element models were prepared for several structures that were observed to gallop in the field. In the Texas Tech tests, strain measurements at the column base were available. In other cases mast arm displacement amplitudes were estimated from videotapes. The finite-element analyses showed that these structures were subjected to equivalent static pressure ranges from 775 to 1290 Pa (16.2 to 27.0 psf) during the

observed galloping. Thus, the wind-tunnel data are conservative and reasonably consistent with respect to the field observations.

The most recent research that has obtained data on galloping was done in California. Caltrans has instrumented a cantilevered VMS that is supported by a monotube structure. Figure 2-1 shows a stress range of 145 MPa (21 ksi) in the column of the Caltrans VMS support structure. VMS on monotubes will be more susceptible to galloping due to their lack of stiffness in the cantilevered section. This lack of stiffness allows the sign to easily change angle relative to the oncoming wind. As described previously, this circumstance is required for galloping to occur. The equivalent static galloping pressure that would cause this stress in the column is about 2000 Pa (42 psf).

Considering the inherent variability in the response of a structure to galloping, the variation in equivalent static pressure ranges observed in NCHRP 10-38 where remarkably consistent. Based upon these results, it is recommended that an equivalent static lift-pressure range equal to 1000 Pa (21 psf) be used in the design of cantilevered sign and signal support structures for galloping-induced fatigue. The stress ranges resulting from the application of this load range should be less than the constant amplitude fatigue limit (CAFL), to obtain essentially infinite life⁶.

The value of 1000 Pa (21 psf) is the median (rounded to two significant figures) of the loads from the field observations (775 to 1290 Pa). This equivalent static lift-pressure range should be applied vertically as a shear stress on the surface area of all sign and signal attachments mounted to the horizontal mast arm as seen in the normal elevation.

Of course it would be preferred to mitigate or prevent the galloping. It is theoretically possible, that much larger loads could be experienced if the wind velocity increases significantly. Several research efforts are currently underway to investigate ways to mitigate galloping. However at this time none of these have been shown to be effective. Without a reliable and cost effective means of mitigation, it is advised that structures be designed to resist these recommended fatigue loads.

Most present structures are not designed to withstand this large a load and will require more fatigue resistant details and possibly increased sections in order to meet these criteria. Therefore, many agencies are concerned that these loads are too conservative. On the other hand, the Caltrans measurements show the galloping loads could be as high as twice the recommended value of 1000 Pa in some cases. Larger design loads may be appropriate for monotube cantilevered support structures such as those used in California. However, this is believed to be a special case that is not applicable to the much stiffer truss-type structures. Therefore, the recommended load of 1000 Pa represents a compromise between safety and practicality.

2.1.3 Truck-Induced Wind Gusts

The passage of trucks beneath cantilevered support structures tends to induce gust loads on the frontal area and the underside of the members and the attachments

mounted on the mast arms of these structures. The magnitude of a natural wind gust pressure is much larger than the pressures from truck-induced loading (in the horizontal direction). Therefore, for the purposes of fatigue design, truck-induced wind loads normal to the sign are not critical.

The VMS are particularly susceptible to truck-induced wind gusts. These signs have a relatively large width (up to approximately 1.2 m or 4 ft) in the direction parallel to traffic flow. Figure 2-2 is a VMS structure that failed due to anchor bolt fatigue. Figure 2-3 shows a closer view of the fractured anchor bolts. Prior to failure, VMS structures in Virginia and California were observed to be vibrating in the vertical plane. Therefore, it is believed to be the vertical pressure acting on the horizontal area that caused these vibrations.

A study by Creamer, Frank, and Klingner¹³ has been the most extensive program performed to date on the subject of truck-induced gust loads. This study's suggested loading function is represented by a horizontal triangular pressure distribution applied to the face of the sign panel with a peak pressure of 60 Pa (1.25 psf) and a vertical uniform pressure distribution of 60 Pa (1.25 psf) applied to any walkways or lighting fixtures. The development of this forcing function was based upon the maximum loading event observed in the field and corresponds to a gust velocity of approximately 8.5 m/s (19 mph).

In addition to the above research program, several other studies have been conducted which support the conclusions drawn by Creamer. For example, field testing of one support structure conducted by the University of North Carolina determined that the maximum pressure induced on the face of the sign was equal to 67.5 Pa (1.41 psf)¹⁴. Another field study conducted by the Michigan Department of Transportation determined that the maximum axial stress range, induced in the anchor bolts of a cantilevered sign support structure, is equal to just over 21 MPa (3 ksi)¹⁵. This axial stress range was observed during the simultaneous passage of two trucks beneath the structure.

Wind tunnel data from a test on a two dimensional one-eighth model cantilevered sign and signal support structure performed at M.I.T.'s Wright Brothers Facility by Philip Mark Cali and Eugene Covert¹² indicates that the shape of the truck had a large influence on the magnitude and shape of the graph of the pressure ranges created by the truck-induced wind gusts. M.I.T. used two different model test trucks—one box-shaped and one source-shaped. The box truck produced the maximum pressure. It is confirmed by this data that the maximum pressure on the vertical area of the signs acts toward the trucks. The interesting observation of M.I.T. was that this negative truck gust came when the leading edge of the truck was in the vicinity of the edge of the sign.

A range of cantilevered sign and signal support structures were analyzed including a fatigue damaged VMS. The resulting stress ranges caused by the loads suggested by Creamer et al¹⁰ in both the horizontal and vertical direction were very small, which is not consistent with the failures that have occurred.

Ronald Cook, et al¹¹, (University of Florida) measured pressures from truck-gusts by mounting pressure transducers on the side of an overpass. By measuring the pressures at varying elevations, Cook observed a vertical gradient in the pressure from truck-induced gusts. The maximum observed pressure by Cook was about 50 Pa, which is much higher than observed on Interstate 80. However, Cook's measurements were taken about 600 mm closer to the trucks.

Desantis¹⁶ modeled the sign structure that failed in Virginia. He used a simple model for the truck-gust load that assumed the velocity of the wind in the upward direction is equal to the truck velocity. The equivalent static truck-gust pressure is determined by using the static wind pressure formula where $V = 105$ kph (65 mph). To account for an increase in the relative truck speed due to head winds, the gust factor of 1.3 is also included. Since the applied truck-gust pressure will lift the mast arm vertically, the pressure obtained above is doubled to represent the entire truck-gust pressure range. This doubling of the pressure is based on the assumption that on the first cycle the downward and upward forces are equal. Based on these assumptions, an equivalent static vertical pressure range of 1760 Pa (36.6 psf) can be obtained. This pressure range must be multiplied by the appropriate drag coefficient and horizontally projected area in order to determine the proposed vertical truck-gust load. Using this equivalent static pressure Desantis was able to match the displacement ranges observed for the structure in Virginia that failed. Table 2-1 shows a comparison of the different pressures measured by different researchers.

Table 2-1 Summary of Pressures from Various Researchers		
Researcher	Model	Pressure
Creamer et al	Uniform vertical loading based on maximum loading event observed in the field	60 Pa
Univ. of North Carolina	Max pressure on the face of a sign	67.5 Pa
Cook et al	Pressure transducers at various heights and angles	*50 Pa
Desantis	Upward wind gust is equal to truck velocity	1760 Pa
ATLSS	Back calculated from strain gage data	525 Pa

* Measured dynamic pressure, not an equivalent static pressure.

In the NCHRP project Desantis' model was recommended for truck-gust loading. The structures should be designed so that their stress ranges resulting from the application of this load range are below the CAFL. In order to check the Desantis model it was applied to the two structures that failed. One structure was observed vibrating immediately after installation and developed fatigue cracks after approximately six months of service. The other structure failed after approximately 18 months of service. From analysis, the ratio of the stress ranges to the fatigue thresholds was 5.2 and 2.7. The predicted fatigue lives are consistent with the relative

service lives prior to failure. Therefore, the simple Desantis model seems reasonable for design purposes.

Assuming a drag coefficient of 1.45 the Desantis model would imply an equivalent static pressure of 2550 Pa. Note that this is almost five times bigger than the maximum equivalent static pressure from strain gage data in the New Jersey research. However, during the monitoring in New Jersey there were no significant headwinds and it is not known what synergetic effect this may have.

2.2 Background Relevant to Fatigue Resistance of Details

Fatigue cracks can form and propagate from weld discontinuities and/or stress concentrations if a member is subjected to significant cyclic live loads, even if the maximum stresses are well below the yield strength.^{18, 21} Testing on full-scale welded members has indicated that the primary effect of constant amplitude loading can be accounted for in the live-load stress range, i.e. the mean stress is not significant. The reason that the dead load has little effect on the lower bound of the results is that, locally, there are very high residual stresses in welded details. Therefore, the mean of the total stresses (applied plus residual stresses) is relatively high regardless of the dead load. In details that are not welded, such as anchor bolts, there is a strong mean stress effect. A worst-case conservative assumption, i.e. a high tensile mean stress, is made in the testing and in the design of these nonwelded details.

When structural members are tested, the loading is characterized in terms of the nominal stress in the structural member remote from the weld detail. The local stress concentration effect associated with the shape of the weld is considered part of the fatigue resistance. The nominal stress is conveniently obtained from standard design equations using member forces and moments from a global analysis.

Experience with multiaxial loading experiments on large-scale welded structural details indicates the loading perpendicular to the local notch or the weld toe dominates the fatigue life. The cyclic stress in the other direction has no effect if the stress range is below 83 MPa (12 ksi) and only a small influence above 83 MPa (12 ksi). Since the combination of multiaxial loading does not have to be considered. The recommended approach for multiaxial loads is:

- 1) decide which loading (primary or secondary) dominates the fatigue cracking problem (typically the loading perpendicular to the weld axis or perpendicular to where cracks have previously occurred in similar details); and,
- 2) perform the fatigue analysis using the stress range in this direction (i.e. ignore the stresses in the orthogonal directions)¹⁸.

The strength and type of steel have only a negligible effect on the fatigue resistance expected for a particular detail. The welding process also does not typically have an effect on the fatigue resistance. The independence of the fatigue resistance from

the type of steel greatly simplifies the development of design rules for fatigue since it eliminates the need to generate data for every type of steel.

Fatigue test data generally consist of the number of cycles to failure for a particular detail subjected to a particular constant amplitude stress range. The results are in general highly variable, therefore a statistically significant number of replicate tests must be performed. The large variance in the number of cycles to failure is primarily due to variance in both the weld geometry and weld discontinuities. This large variance makes it difficult to distinguish the secondary effects of many variables such as type of steel and filler metal, rate of loading, mean stress, and the environment.

Fatigue tests are performed at a number of different stress ranges and the data are generally plotted with the logarithm of the nominal stress range on the ordinate and the logarithm of the number of cycles to failure on the abscissa (even though the number of cycles is the dependent variable). The relationship used to represent the lower bound to these data is referred to as an S-N curve (see Figure 2-4. An S-N curve is an exponential equation of the form:

$$N = C \times S^{-m} \quad (2-7)$$

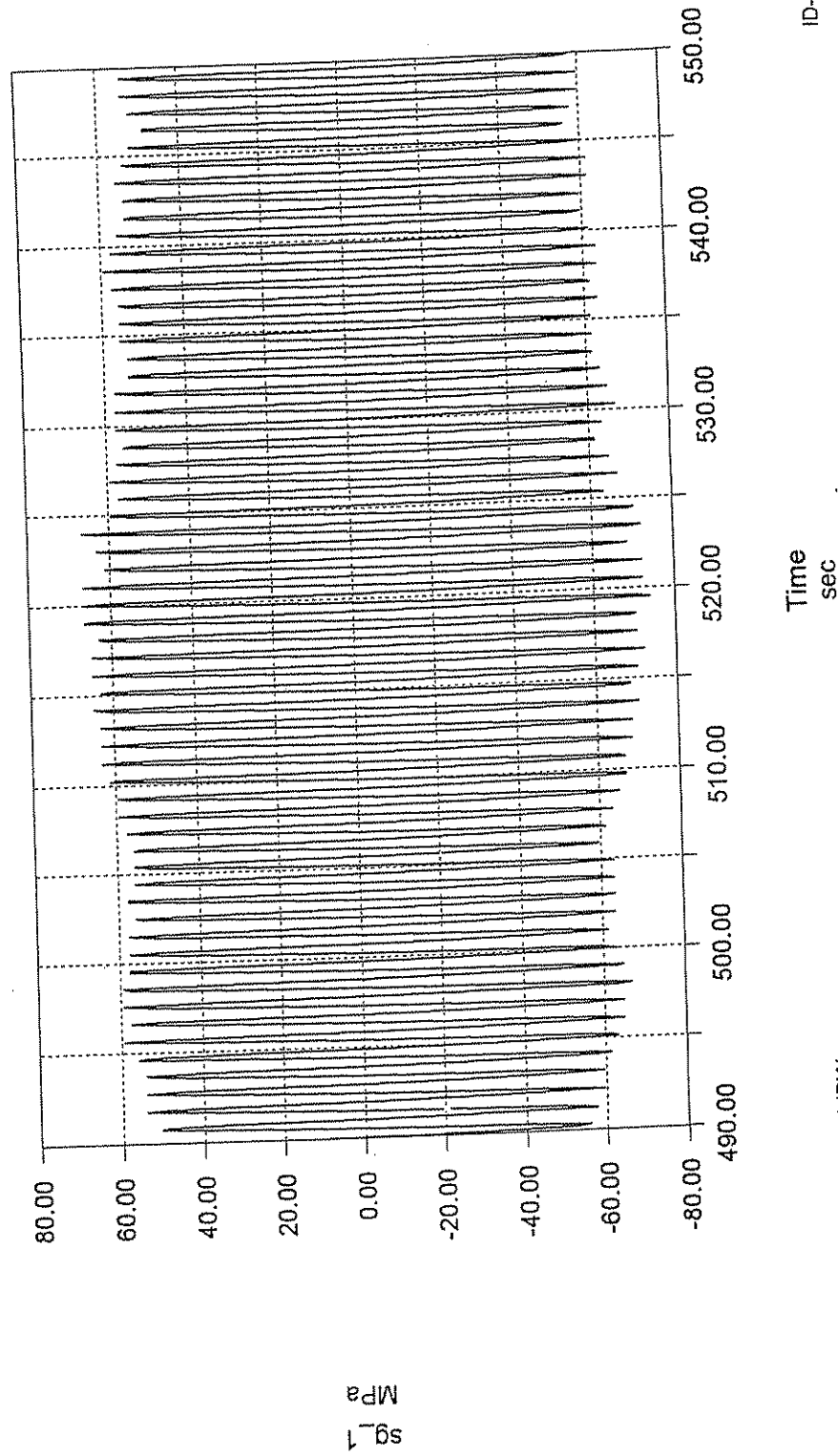
or

$$\log N = \log C - m \log S$$

where N is the number of cycles to failure, C is a constant dependent on detail category, S is the applied constant amplitude stress range, and m is the inverse of the slope of the S-N curve. In the AISC and AASHTO codes as well as in Eurocode 3²⁰, m is standardized at 3.0 for steel.

Figure 2-4 shows the constant amplitude fatigue limits (CAFL) for each category as horizontal dashed lines. When constant amplitude tests are performed at stress ranges below the CAFL, noticeable cracking does not occur. Sign support structures experience what is known as long-life variable-amplitude loading, i.e. very large numbers of random amplitude cycles greater than the number of cycles associated with the CAFL. In this case, the fatigue design consists of making sure that the upper bound stress range, as defined by the recommended fatigue design load ranges, is less than the CAFL. If this is true, then the fatigue life should be essentially infinite.

Galloping Induced Oscillations in a Caltrans VMS Sign Support Structure



D:\CALTRANS\IONTARI-1\IONT102-1.IDW

Time
sec

ID-2000

Figure 2-1 Stress Range in a Caltrans Monotube VMS Sign Support Structure.

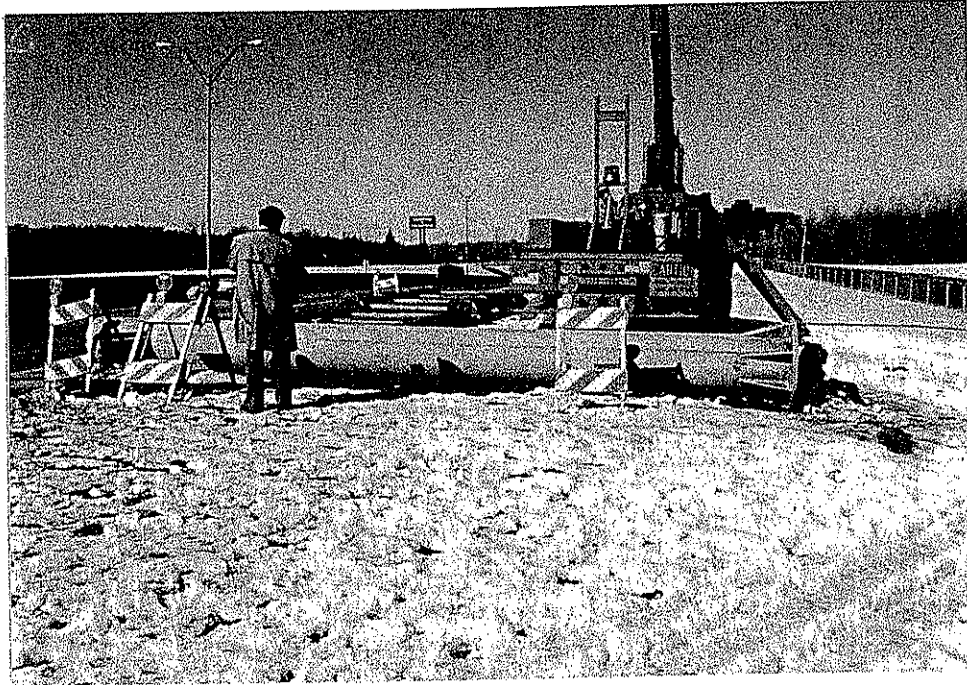


Figure 2-2 Failed VMS Support Structure Due to Anchor Bolt Fatigue

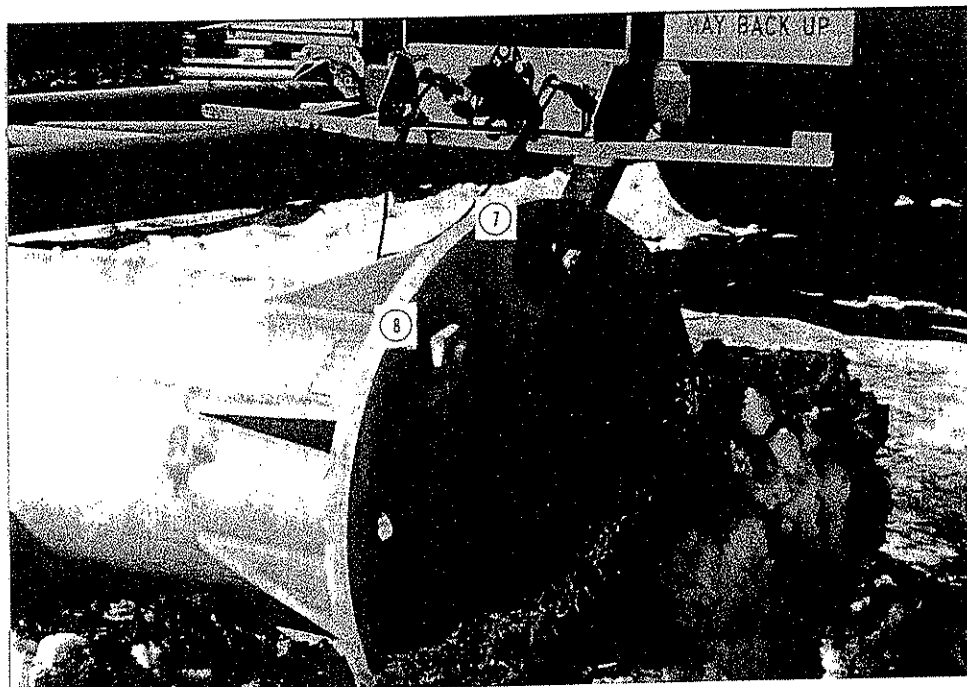


Figure 2-3 Close up of Fractured Anchor Bolts.

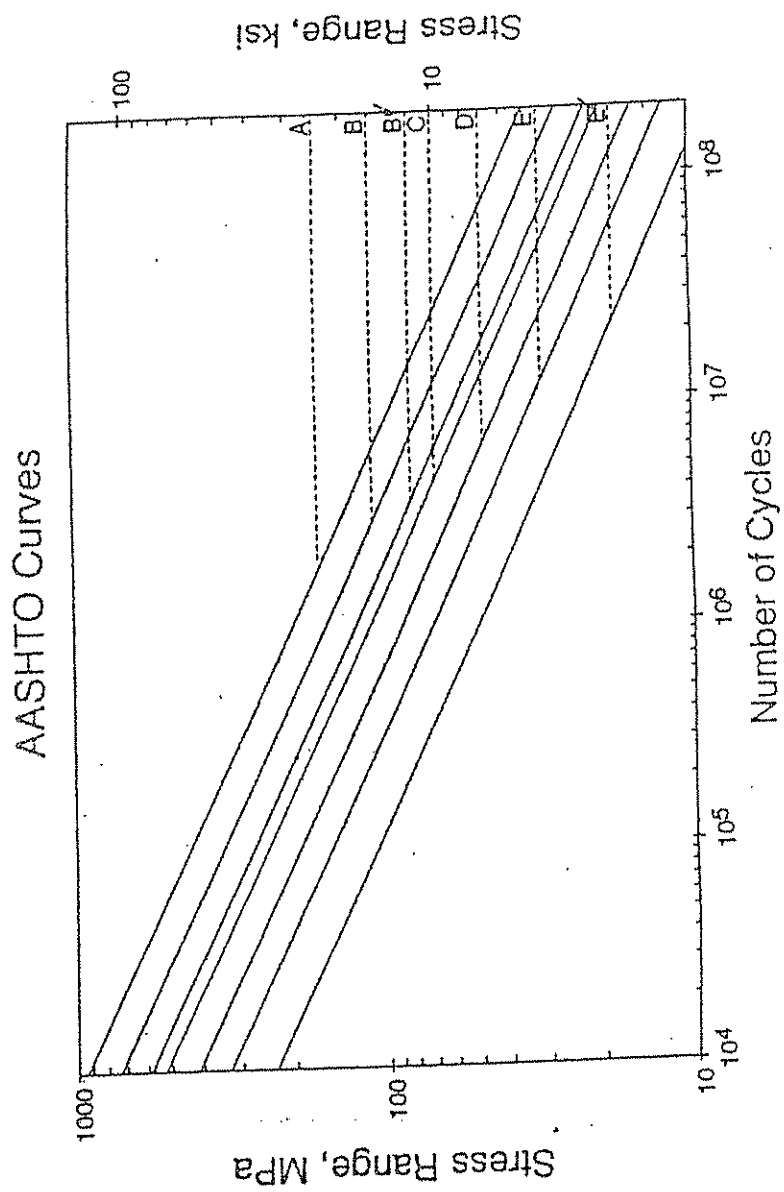


Figure 2-4 AASHTO S-N Curves for Steel.

Chapter Three: Field Tests and Findings

3.1 History of the New Jersey VMS Support Structure

The VMS that was monitored on Interstate 80 was originally on State Route 17 in northern New Jersey. At its original location on Route 17 it was reported to experience large amplitude vertical displacements at the end of the cantilever. One report from a New Jersey DOT worker alleged that the displacement was approximately four feet at the tip of the cantilever. Other reports were in the neighborhood of one to two feet of displacement at the tip. These displacements were large enough that concern for motorist safety forced the DOT to take down the VMS and support structure. Because the displacements were reported to be in the vertical direction, truck induced wind gusts were suspected. However, Richard Janacek of Edwards and Kelcey reported that the displacements might have been more elliptical, containing a horizontal component as well as a vertical component. This observation might indicate that the vibration could be due to natural wind gusts alone or in combination with truck-induced wind gusts. Although Route 17 is a north-south route and Interstate 80 is an east-west route there are some curves in the roads that have traffic going perpendicular to the main direction of travel. Because of these curves, the location of the sign on Route 17 and on Interstate 80 was such that a wind going in a northeast direction would be directed toward the front of the sign. This is a favorable orientation because the prevailing winds in northern New Jersey come from the west and the strong winds are more likely from the south.

NJDOT has temporarily stopped the deployment of the VMS on cantilevered support structures and is using overhead support structures for VMS. However, the overhead support structures are reported to cost about 2.5 times that of the cantilevered support structures. Therefore, it was decided to perform this research to validate the fatigue design criteria for cantilevered VMS support structures. As long as the cantilevered support structures are designed to meet the criteria described in Chapter 4 of this report, they will be resistant to fatigue and excessive dynamic displacement and therefore, it will not be necessary to use overhead support structures.

The VMS that was observed to vibrate on Route 17 was to be erected again for the field tests. However, there were several changes that made the situation different for the field tests than it was when the problem was observed. The first change was that the VMS could not be erected back on its original foundation because an overhead support structure had already been erected there. The alternate location on Interstate 80 was chosen because the anchor bolt pattern matched the bolt pattern in the column base plate from the Route 17 structure. The terrain may have a significant effect on the wind characteristics, and the natural wind may have been a significant factor in the problem, which occurred on Route 17.

The second significant change was that the column of the Route 17 support structure was two feet shorter than the one that was called for on Interstate 80. This

meant the mandatory 17 ft 9 in of clearance under the sign would not be met if the Route 17 column were used. Therefore, the longer column was used, not the original Route 17 column. The longer column did not make the structure farther from the trucks than they were on Route 17, it simply maintained the 17 ft 9 in clearance that was called for on Route 17 and Interstate 80. The longer column did effect the stiffness of the structure. The dynamic characteristics of these types of structures are very sensitive to changes in stiffness.

A third change that can effect the behavior of the structure is the erection procedures. The tightness of bolts in the structure can change the damping ratio, which will significantly affect the behavior of the structure. The contractor that erected the VMS support structure on Route 17 was different than the contractor that erected it on Interstate 80. The erection at the Interstate 80 location was scrutinized carefully and there was significant attention paid to bolt tightening. There were no clear guidelines with respect to the appropriate amount of torque to place on the anchor bolts, even at the time of the Interstate 80 erection.

The fourth change from the original structure on Route 17 was the absence of the walkway in front of the sign when it was erected on Interstate 80. On route 17 there was a walkway that spanned the front of the VMS box. The walkway was intended for access to maintenance the front of the sign. The usefulness of these walkways was questioned because of the concerns about working above open traffic, and therefore a decision was reached not to use them in the future. If traffic has to be closed in order to work on the sign, a bucket truck might as well be used and the expense of the walkway spared. However, the walkway presents significant additional projected area on a horizontal plane and therefore could have contributed to the truck-gust loading problem on Route 17. The walkway was positioned 18 inches below the bottom edge of the sign. Therefore part of the structure was 18 inches closer to the trucks on Route 17 than on Interstate 80 which could also contribute to the truck-induced response.

These changes mean that the conditions on Interstate 80 were not identical to the conditions that existed on Route 17 that caused the large-amplitude displacements. The ideal situation would have been to monitor the structure on its original foundation before it was taken down.

3.2 Erection Details

The following sections describe the erection procedures that were used on interstate 80 when the VMS and support structure were installed. The problems, and possible solutions, that were associated with this erection procedure will also be discussed. When the truss and VMS box were connected to the column dead load stresses were recorded in the column and anchor bolts. This data is also presented and discussed in this section.

3.2.1 Erection Procedures Used on Interstate 80

The erection procedure for the VMS and sign support structure was as follows. The leveling nuts were placed on the anchor bolts and made level. Next, the column was brought in and positioned with a crane (Figure 3-1). The top nuts were all placed on the anchor bolts and tightened with a hydraulic torque wrench. The bolts were tightened in a star pattern and in increments of 350 foot pounds so as to keep the column plumb while the nuts were tightened. The nuts were torqued to 750 foot pounds (Figure 3-2). Next the truss and VMS were brought in. The VMS was already attached to the truss at the storage yard (Figure 3-3). The VMS and truss were simultaneously lifted and positioned at the stubs (Figure 3-4). A bronze plate was placed between the flanges of the truss and stub to try to increase the mount of contact between these two surfaces (Figure 3-5). According to fabricators it is almost impossible to achieve a perfect surface so there is 100 percent mating between the two flanges. The bronze plate is suppose to smash itself into the gaps when the flanges are torqued together. The final step is to tighten the bolts that connect the truss to the stubs. All the bolts on one side of the truss were tightened then the bucket truck was moved to the other side to tighten these bolts.

New Jersey DOT performed ultrasonic testing on all the anchor bolts and the bolts in the stub-truss connection to determine their elongation due to tightening. Unfortunately, this data was never made available to determine precisely how much tension was in the bolts.

3.2.2 Erection Problems and Recommendations

There are some definite problems in the anchor bolt tightening procedures. A total torque of 750 foot pounds is insufficient for a 3 inch diameter bolt. Two weeks after the structure was erected a site visit was made to collect data and inspect the structure. One of the top nuts could be removed by hand (Figure 3-6). This indicated a definite lack of tension in the anchor bolts. A second problem with the anchor bolts was the leveling nuts. The erection procedure never included coming back through to tighten the leveling nuts against the bottom of the base plate. Four of the eight leveling nuts could be turned by hand after the structure was erected.

The anchor bolts that are used by NJDOT for the VMS structures are A36 steel. The minimum amount of tensile stress that should be in a high strength bolt is 70 percent of the ultimate strength, however these anchor bolts are not high strength bolts. Using 70 percent of the ultimate strength for mild steel would still be above the yield point; therefore, a minimum tensile stress of 60 percent of ultimate shall be used on the anchor bolts. Equation 3-1 gives the amount of preload that corresponds to 60 percent of the ultimate strength.

$$F_t = 0.6 \times F_u \times A_t \quad (3-1)$$

where F_I is the bolt preload, F_u is the ultimate tensile strength, and A_T is the bolt tensile stress area. The tensile stress area can be calculated using equation 3-2

$$A_T = \frac{\pi}{4} \left(d - \frac{0.9743}{n} \right)^2 \quad (\text{in}^2) \quad (3-2)$$

or

$$A_T = \frac{\pi}{4} (d - 0.938P)^2 \quad (\text{mm}^2)$$

where d is the bolt diameter in the unthreaded portion, n is the number of threads per inch, and P is the thread pitch. Equation 3-3 relates the bolt preload to torque.

$$F_I = \frac{T}{K \times d} \quad (3-3)$$

where T is the torque, and K is a friction coefficient depending on thread lubrication. For the A36, three inch diameter anchor bolts used in this structure, using a value of 0.2 for K , the minimum torque is 11,700 ft lbs. Future anchor bolts could be made of a higher strength steel to allow for more clamping force.

It is recommended that the bronze plate should be left out and the fact that there will not be 100 percent mating between the surfaces should be accepted. The Research Council on Structural Connections specifically states in section 3 part (a) "All material within the grip of the bolt shall be steel"¹⁹. This statement is made to guard against the potential for creep in the softer metal, which could cause a loss of pretension in the bolts. The effectiveness of these plates was in question anyway due to the fact that daylight could be seen between the two flanges (Figure 3-7). The fact that gaps may exist in the faying surfaces does not prevent the bolt preload from being developed. The end plate thickness is enough to bridge the gaps and develop the desired bolt tension.

The tightening pattern of the bolts in the stub to truss-chord connection should be in a star pattern the same as the anchor bolts. This could be facilitated by having two bucket trucks, one on each side of the truss. Each person should take a turn tightening the appropriate bolt. These bolts should also be incrementally tightened when going through the star pattern.

3.2.3 Dead Load Stresses

During the connection of the truss and VMS box to the column the strain gages in the column and anchor bolts were monitored; this allowed the dead load stresses in the column and anchor bolts to be recorded. Knowing the dead load

stresses is not needed for a fatigue assessment, however it was a good opportunity to test some of the strain gages and data acquisition equipment.

Figure 3-8 shows that the dead load stress in the column was 90 MPa (13 ksi). This was larger than expected, but still within the allowable bounds. Figure 3-9 shows the numbering scheme for the anchor bolts. Figure 3-10 shows the axial dead load stress in anchor bolts 2, 3, and 4. As can be seen in Figure 3-10 the maximum axial dead load stress of 85 MPa (12.5 ksi) was in anchor bolt two. It is reasonable that anchor bolt two had more dead load stress than the others because of the eccentricity of the VMS box on the truss. This eccentricity should cause the maximum dead load stress to be on anchor bolt two.

3.3 Field Test Description

This section describes the test setup and procedure that was implemented in the short and long-term testing.

3.3.1 Short-term Testing Procedures

Short-term field tests were performed to obtain the dynamic characteristics of the sign structure on Interstate 80 in northern New Jersey; as well as the response to truck gusts. Strain gages were placed on the anchor bolts, column, stubs, and truss to obtain strain measurements. There were 25 gages on the column, stubs and truss (Figure 3-11). Twenty-one of the strain gages were CEA-06-W250A-350 Measurements Group, Inc. strain gages. These are uniaxial, weldable, 350-ohm strain gages; temperature compensated for structural steel. The remaining four gages were CEA-06-250UR-350. These are three-element, single-plane 45-degree rosettes; temperature compensated for structural steel. There were eight bondable strain gages placed on the four anchor bolts on the tension side of the column (Figure 3-12). These gages were positioned 180 degrees apart in order to resolve out bending of the anchor bolts if necessary. Strain gaging of the column and truss took place while they were still in the storage yard. With the column and truss up on blocks, it was easier to install the gages. The anchor bolt gages were installed before the column was placed on the foundation. All the strain gages were installed and protected as is described in the Measurements Group installation procedures.

Eight Omega PX163 differential pressure transducers, with a measurement range of plus to minus 1250 Pa, were placed on the front face of the sign. Their locations were 0.3 m and 2.67 m up from the bottom edge of the sign; two sets above the centerline of the two lanes under the sign (Figure 3-13). The pressure transducers were intended to measure the pressure from truck-induced gusts. The transducers were placed inside of four-inch diameter PVC pipe. The truck-induced gusts were directed to the pressure transducers through pitot tubes and a short section of quarter inch diameter tubing. The

pitot tubes were oriented to capture flow that was both parallel and perpendicular to the face of the sign (Figure 3-14). They were positioned at different elevations to obtain the pressure gradient over the face of the sign.

A wind sentry equipped to measure wind speed and direction was employed to determine the effects of the natural wind on the sign support structure. The wind sentry was positioned on top of the column that supported data acquisition equipment for the long term testing (Figure 3-15).

All data was collected with a Campbell Scientific CR9000 Data Logger (Figure 3-16). This data logger was designed with remote monitoring in mind and was capable of measuring at up to 100,000 samples a second. It came equipped to measure 42 differential voltage measurements and 7 pulse counting channels. The pulse counter was required for the wind speed, all other measurements were made as differential voltage. The data logger was operated from the back of a moving van for the short-term test (Figure 3-17). All strain gages were wired into the logger using a three wire, quarter bridge setup. All voltage measurements were taken differentially. All sampling in the short-term testing was done at 20 samples per second.

The first step of the short-term test was to establish the stiffness, natural frequency, and damping ratio of the sign support structure. A pull test was performed on the structure to determine these dynamic characteristics. A heavy rope was attached to the bottom chord of the truss at the position shown in Figure 3-18. The rope was attached to a come-a-long with a quick release hook and a load cell. The load cell was monitored to track the force that was being applied to the structure. A large flat bed truck acted as a counter weight during the pull test. The rope would be ratcheted to a specific load with the come-a-long and then released with the quick-release mechanism. This allowed the structure to vibrate at its natural frequency and dampen down at its critical damping ratio.

This test was performed with two different configurations. One the sign was pulled straight down and the second the sign was pulled at a 45-degree angle. This would enable determination of the dynamic characteristics in the two primary modes of vibration, the "twisting mode" and the "hatchet mode". The "twisting mode" describes the sign rotating about the z-axis. The "hatchet mode" describes an up and down movement in the x-y plane. Figure 3-18 shows an axis for reference to these modes.

The second phase of the test was to determine the effect of the truck-induced wind gusts on the structure. Two trucks were hired to drive under the sign and the upward gusts from these trucks would be measured with pressure transducers (Figure 3-19). The drivers were instructed to note their speed and radio it back so a correlation could be made with truck-induced wind gusts and truck speed. The two lanes of Interstate 80 under the VMS box were closed so the trucks could easily get up to speed and position themselves correctly in their lane.

3.3.1.1 Short-term Testing Problems

There were some problems with the short-term testing that did not allow for as much data to be collected as would have liked. Delays in equipment, such as bucket trucks, to the site pushed the schedule back by about 7 hours. Instrumentation could not be connected until well after dark because of this.

A second problem was the test trucks could not run as much as was agreed upon to collect truck-induced wind gust data. Originally, two lanes of Interstate 80 were to be reserved until 6:00 P.M. for the trucks to drive under the sign. The testing was forced to stop by 11:00 A.M. This lack of time did not allow for all the truck runs that were originally planned upon.

3.3.1.2 Dynamic Characteristics and Static Test Results

The short-term test successfully determined the dynamic characteristics of the VMS support structure

Data indicated that the stiffness was 0.24 kN/mm (1.38 kip/in.).

The log-decrement equation, Equation 3-4, was used to determine the percent of critical damping in the sign support structure

$$\frac{1}{j} \ln \frac{u_1}{u_{1+j}} = \frac{2\pi\zeta}{\sqrt{1-\zeta^2}} \quad (3-4)$$

where j is the number of cycles being considered, u_1 is the amplitude at peak 1, u_{1+j} is the amplitude j cycles later, and ζ is the critical damping ratio. The percent of critical damping in the “twisting mode” and “hatchet mode” was 0.57 percent and 0.25 percent respectively. The larger damping in the “twisting mode” is from the large frontal area of the sign box moving through the air. The sign has an easier time slicing through the air in the “hatchet mode”. Figure 3-20 shows the damping of motion in one of the strain gages on the column.

A Fast Fourier Transform was performed on data from a strain gage while the structure oscillated at its natural frequencies. The natural frequency in the “twisting mode” and “hatchet mode” was 0.87 cycles/s and 1.22 cycles/s respectively (Figures 3-21 and 3-22)

The pull test enabled a static calibration to be performed on the structure as well. This enabled a comparison of calculated to measured stresses in the structure. Figure 3-23 is a graph of the calculated stresses in the structure from a 1 kN force applied at the same load point as in the short-term testing. The dots indicate strain gage readings from when the load cell indicated there was 1 kN of force being applied to the structure. Figure 3-23 shows that the actual stresses are typically less than the calculated stresses. In part because of the location of the gages, the column appears to agree, but the truss gages do not seem to capture the bending components.

3.3.2 Long-term testing

Long-term testing was intended to collect data from any significant event on the VMS for three months from June to August 1997. The data logger was placed in an enclosure that was mounted to the column erected next to the VMS support structure (Figure 3-24). The wind sentry, two solar panels, a cell phone antenna, and a lightning rod were placed on top of this column.

The long-term test monitored gages that were determined to be critical from the results of the short-term test. Column gages 9, 10, 11, and 12 were monitored in the long-term testing (Figure 3-11). Upper chord gages 33, 34, 35, and 36 were monitored (Figure 3-11). Strain gages 52 and 53 from anchor bolt 2 were monitored (Figure 3-12). All of the pressure transducers were monitored (Figures 3-13 and 3-14). The wind speed, and wind direction were also monitored in the long-term testing (Figure 3-15). The logger was programmed to monitor these gages continuously, however it was triggered to record events only when predetermined thresholds were exceeded. The logger would be triggered to record if any column gage exceeded 7 MPa (1 ksi) or the wind speed was in excess of 10 m/s. (20 mph). Thirty seconds of pre-triggered data would be recorded to capture the events that led to the triggering. The logger was also programmed to turn on at certain times of day that were determined to have heavy truck traffic. This allowed inspection of the gages on a daily basis if no event triggered recording occurred that day. The sampling rate for all the channels of the long-term testing was 40 samples per second. There were no filters used on the data that was collected in the long-term test.

The data that was collected in the long-term testing was to be transmitted back to the lab through a cellular phone link. The logger was connected to a cellular phone transceiver and cellular phone modem that would enable remote communications with the logger. Not only could data be received from the logger, new programs could be sent to make any necessary changes.

Two 20-watt solar panels were connected to two deep-cycle marine batteries that helped support the logger's battery. The marine batteries were intended to provide reserve power at night and on days when there was not much sun.

There were no significant events that occurred during the long-term monitoring. More truck-induced gusts were able to be collected from random trucks under the sign (Figure 3-25). Galloping never did occur while the structure was being monitored. The structure is always undergoing some low amplitude vibrations that appear to be from a combination of natural wind and truck-induced gusts, however these stress ranges did not appear large enough to cause any immediate damage.

3.3.2.1 Long-term Testing Problems

There was a lot of variability in the quality of cell phone communication with the logger. The antenna that was purchased was a directional antenna. A directional

antenna is intended to be pointed in the direction that the signal is going to be sent and received from. The antenna was pointed at the closest cell phone tower to the VMS; this, however might not be the tower that the signal is sent and received from. The tower that the call was sent to is a function of distance as well as the number of people using that tower. If there was heavy cell phone traffic on the closest tower the call may be bumped to a different tower. When this occurred, the directional antenna was pointed incorrectly for the best signal. In hindsight a non-directional antenna would have been better suited.

There was significantly more power needed to run all the instrumentation and equipment than was previously suspected. The solar panels could not adequately replace power that was being consumed. This did not result in the loss of any data; it simply meant regular trips with a generator and battery charger were required to recharge the batteries. This was not a real problem because it gave opportunities to visually inspect the sign support structure for any cracking; none was found.

There were occasions when the strain gages started to drift from the zero position. This gage response is not due to a strain in the structure, but is usually due to an environmental or electrical condition. This drifting was responsible for some instances of recorded data because the data logger would be triggered to record if certain channels exceeded a predetermined value. This was not a serious concern due to the extremely large amount of memory in the data logger. The data logger was programmed to zero all the channels every six hours, which would correct for any drifting. Zeroing could have been done more often to keep unnecessary data from being recorded. A better way to trigger would have been to use the standard deviation or root mean square (RMS) as the trigger. Equation 3-5 describes the relationship between the RMS stress range and the effective stress range

$$S_R^{\text{eff}} = 2.8 S_R^{\text{RMS}} \quad (3-5)$$

where S_R^{eff} is the effective stress range and S_R^{RMS} is the RMS stress range.

3.4 Discussion of Field Test Results

The data that was collected on Interstate 80 enabled a decision to be made on the appropriate fatigue design pressures for truck-induced gusts. The appropriate truck-induced gust pressure was calculated using strain gage data rather than the pressure transducers. Based on data taken from the test trucks, the data from the pressure transducers was unpredictable in most cases. Table 3-1 shows the configurations of the test trucks as they went under the VMS. Figure 3-26 shows data from the first run of our test trucks. As can be seen in Figure 3-26 the primary pressure recorded by the pressure transducers was a push on the bottom of the sign. Strain gage 9 is plotted to show the response of the column to the truck-induced gust. Figure 3-27 shows data from the second run of our test trucks. This time the pressure transducers indicate suction as the primary gust. The configurations of the trucks

were the same in the first and second test truck runs, however the magnitudes and directions of the pressures were drastically different. This indicated a problem with the data from the pressure transducers. Unfortunately, as was described in section “3.3.2.1 Long-term Testing Problems”, the opportunity to perform additional tests under this truck configuration did not exist.

Table 3-1 Test Truck Configurations		
Test Number	Truck Configuration	Truck Speed (MPH)
1	Conventional Cab First Cabover Followed Second Both in First Lane	Conventional = 54 Cabover = 64
2	Conventional Cab First Cabover Followed Second Both in First Lane	Conventional = 54 Cabover = 55
3	Conventional Cab in First Lane Cabover in Second Lane Trucks Side-By-Side	Both = 51

There is some evidence that suggests the initial gust pressure is a suction on the sign, Figure 3-28 shows the response of strain gage 9 to the truck-induced gusts from all three of the test truck runs. To cause strain gage 9 to go into tension at the beginning of the first cycle, as it does in all three test runs in Figure 3-28, there must be an initial suction on the VMS. As was described in section “2.1.3 Truck-Induced Wind Gusts”, Cook¹¹ also discovered that there was a strong suction that preceded the upward gust of air on the soffit area of the VMS.

Figure 3-28 also shows a correlation between truck configuration and the response of the sign. Test truck run 1 and 2 has a stress range of 1.5 MPa while test truck run 3 has a stress range of 3 MPa. All three runs were performed at approximately 55 MPH, however in test truck run 3 the trucks were running side by side instead of one behind the other as in test truck runs 1 and 2 (Table 3-1). This data indicates that trucks running side by side under the VMS may have twice the effect on the structure as two trucks running one behind the other. If more truck runs could have been performed a stronger correlation might have been reached.

One reason the pressure transducers connected to pitot tubes may not have given reliable results was because of the extreme turbulence in the truck gust. This type of apparatus is more reliable in a situation where the flow is extremely laminar, such as in ventilation ducts. When the gust leaves the truck and goes toward the soffit area of the VMS there would probably be a severe amount of swirling in the upward air movement. If a swirl goes past the pitot tube's entrance port in such a way that it does not enter directly into the tube the recorded pressures would not be accurate. By

this reasoning, the pressure transducers were not relied upon to give a magnitude of truck-induced gust pressure.

Although the pressure transducers were not relied upon to give a magnitude of truck-gust pressure they were used to try to quantify a pressure gradient at different elevations above the truck. Figure 3-29 shows pressure transducer data from above each of the lanes in the third truck test run. The pressure from the truck gust above lane one ranged from 4 Pa (0.08 psf) to 2.5 Pa (0.05 psf) at heights of 0.3 m to 2.67 m up from the bottom of the sign respectively. The pressure from the truck gust above lane two ranged from 6 Pa (0.13 psf) to 3 Pa (0.06 psf) at heights of 0.3 m to 2.67 m up from the bottom of the sign respectively. This data indicates that at a height of 4.5 m above the bottom of the existing VMS box the pressure would go to essentially zero. This gradient will be incorporated into the design recommendations for truck-induced wind gusts.

Figure 3-30 shows a stress range of about 3.5 MPa (0.6 ksi) in the column from the third truck test run. The response of the lower stub and chord was recorded and is displayed in Figure 3-31. The lower stub shows signs of considerable bending as well as axial stress. This response was typical of all the truck-induced gust data.

Figure 3-32 shows a comparison of the structure in the "hatchet" and "twisting" modes to the third truck test run. Strain gages 9 and 11 represent the "hatchet" mode and strain gages 10 and 12 represent the "twisting" mode. The structure has about four times the stress range in the "hatchet" mode as it does in the "twisting" mode. Figure 3-32 also shows the large amount of damping after the first cycle in the "twisting" mode. This is due to the large amount wind resistance on the front face of the sign as it tries to move through the air in this mode. The stress range in the "twisting" mode is less than half of that in the "hatchet" mode. This proves that it is not necessary to apply the truck-induced gust loads to the front of the structure because a natural wind gust will undoubtedly govern in this direction.

A stress range of about 4 MPa (0.5 ksi) in the column seemed to be the typical range from truck-induced gusts. Figure 3-33 shows about 45 minutes of triggered truck-induced gust data from the long-term monitoring. The stress range does not usually exceed about 6 MPa. Figures 3-34, 3-35 and 3-36 show a zoomed in view of Figure 3-33 to prove that the signal is not just noise being recorded. The close-up views represent some of the higher stress ranges in Figure 3-33. As can be seen from these figures, the stress range was about the same as indicated in the test truck data. Figure 3-37 shows about 45 minutes of a different file that indicates a similar situation from other long-term triggered data. Figures 3-38, 3-39, and 3-40 are zoomed in view of Figure 3-37 to show the validity of this triggered file. As was typically the case, the stress range does not usually exceed about 6 MPa.

Although the typical truck-induced stress range may have not been very high, Figure 3-41 shows measured column stress ranges from other random truck-induced wind gusts reached as high as 10 MPa (1.5 ksi) and the accompanying natural wind speed of 2.5 m/s. Figure 3-42 shows the stress range in the top chord of the truss is 1.5 MPa. Figure 3-43 shows the axial stress range in anchor bolt 2 is 11 MPa. It is

reasonable to assume that with any significant head wind this stress range in the column could have easily reached 14 MPa. The equivalent static pressure on the horizontal area of the sign and truss that would cause the stress range of 14 MPa in the column is 525 Pa (11 psf). This pressure is the worst case equivalent static pressure that was deduced from the long-term monitoring.

In order to compare this equivalent static pressure to the measured dynamic pressures from the pressure transducers the measured dynamic pressures must be multiplied by the dynamic amplification factor. The measured damping ratio was 0.25 percent of critical, the low damping implies a dynamic amplification factor of about 200 (at the natural frequency the dynamic amplification factor equals $1/2\zeta$, where ζ is the critical damping ratio). Therefore, the typical dynamic pressure of 6 Pa shown in Figure 3-29 corresponds to an equivalent static pressure of 1200 Pa (25 psf).

The equivalent static pressure, deduced from the pressure transducer data, significantly exceeds the equivalent static pressure deduced from the strain gage data. As was described above it is believed that the strain gage data corresponds to the average pressure over the entire horizontal area and is more representative of the average applied pressure, which could be used for design criteria. On the other hand, the pressure transducers measured the pressure at only one specific point in space.

The back calculated pressure of 525 Pa is about 3.3 times less than Desantis' recommendation of 1760 Pa (Table 2-1). The exact reason for this is not known, however there are some plausible explanations for it. The structure that Desantis modeled may have been closer to the trucks. The structure could have been more flexible than the one monitored on Interstate 80. If there was more ambient wind this could have a synergetic effect that is still not fully quantifiable.

The largest natural wind gust recorded was about 7.5 m/s (Figure 3-44). As can be seen in Figure 3-44, there was a definite increase in the stress range to about 4 MPa when the wind gusted from a mean of about 4 m/s to 7.5 m/s. The direction of the wind was about 45 degrees to the face of the sign when it was gusting up to 7.5 m/s. It is believed that stronger wind gusts could be measured at other times of the year in this same location. According to records of natural wind patterns in northern New Jersey the strongest winds occur in winter and spring, as was previously noted this research was performed in the summer.

The concerns of airfoils on the cabs of the trucks causing a higher truck-induced pressure was also investigated. The Interstate 80 study indicated that the airfoils were not a problem. The point of the airfoils is to increase the fuel efficiency of the trucks. In order to do this the air must be kept laminar as it flows over the trailer behind the cab. If the flow is kept laminar the upward gust will be lessened because instead of going turbulently up into the bottom of the sign it flows along the trailer. Conversations with researchers at Mack Trucking helped to confirm this. These researchers have done wind tunnel tests on trucks with and without airfoils. Their data confirms that the flow stays laminar along the trailer when airfoils are used. This information suggests that the presence of airfoils does not increase the dynamic pressure acting on the sign.



Figure 3-1 VMS Column Erection on Interstate 80.

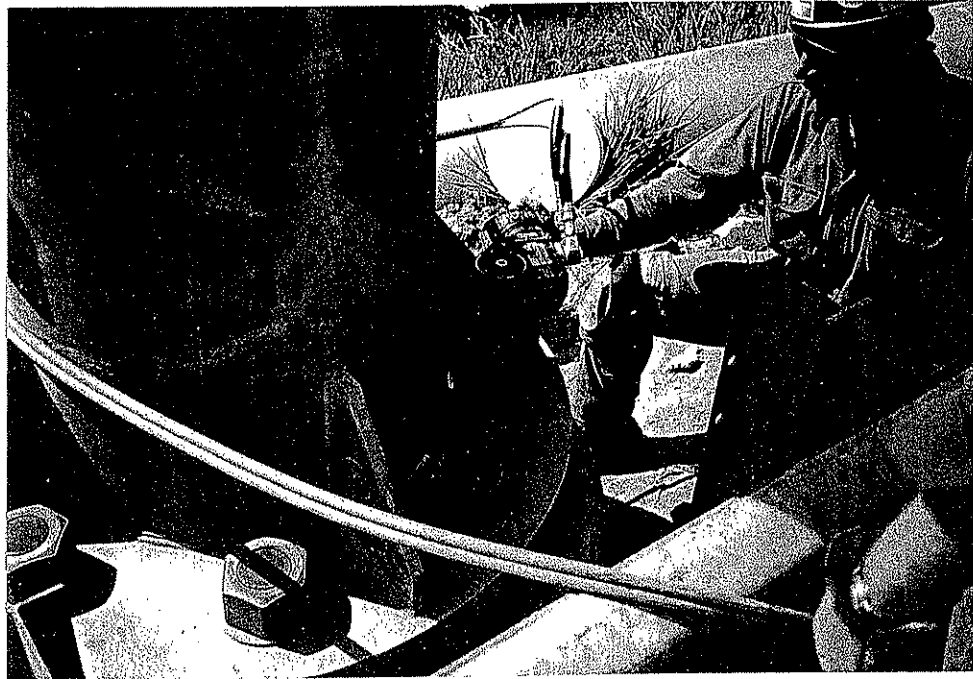


Figure 3-2 Anchor Bolt Tightening with a Hydraulic Torque Wrench.

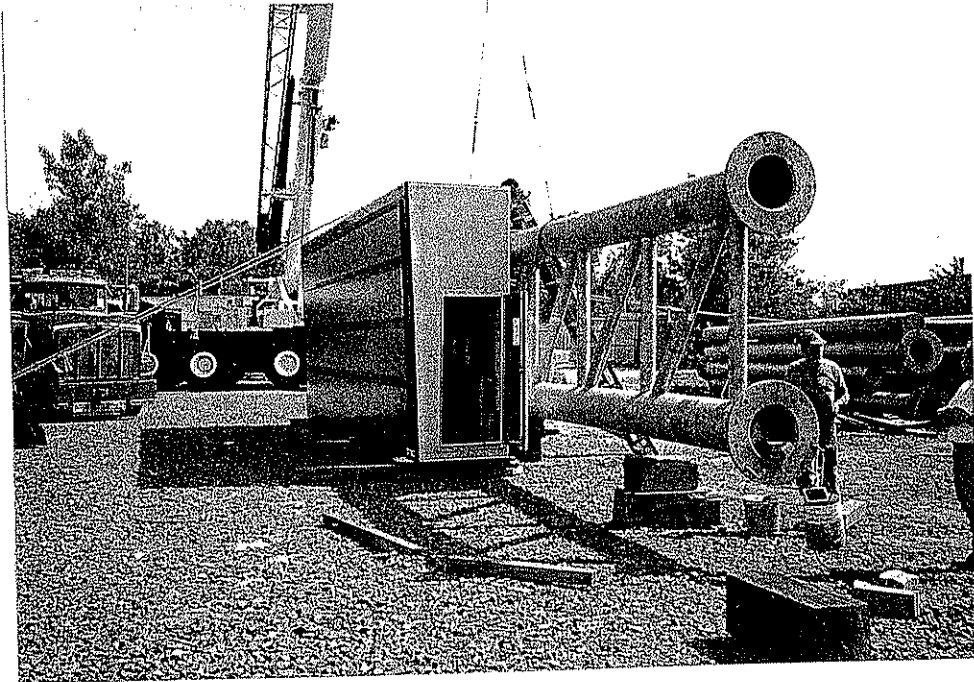


Figure 3-3 VMS Connected to Truss in Storage Yard.

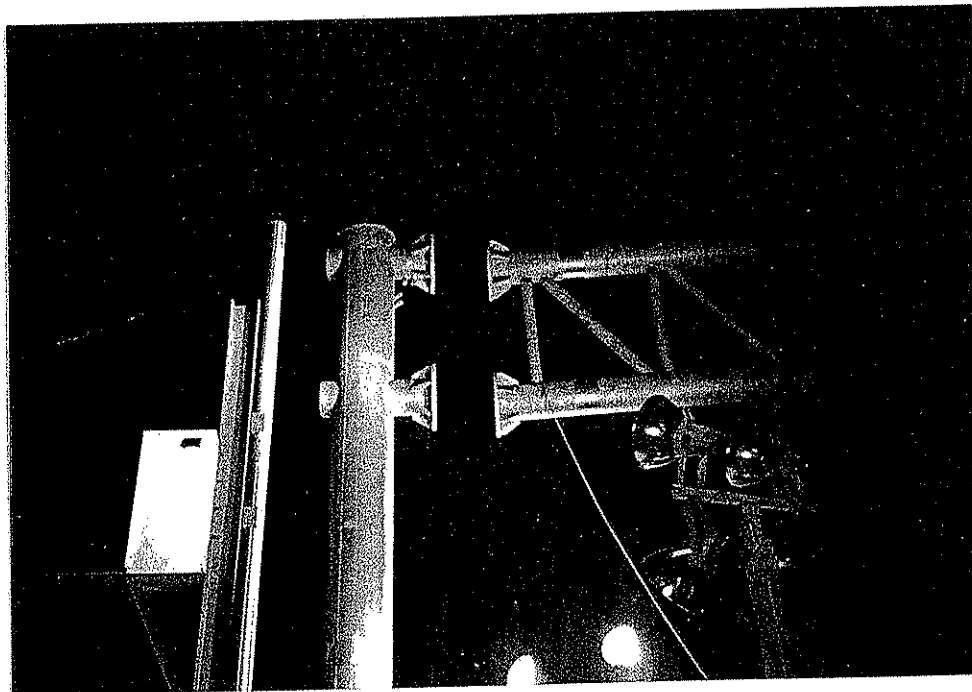


Figure 3-4 VMS and Truss Lifted into Position for Connection to Column.

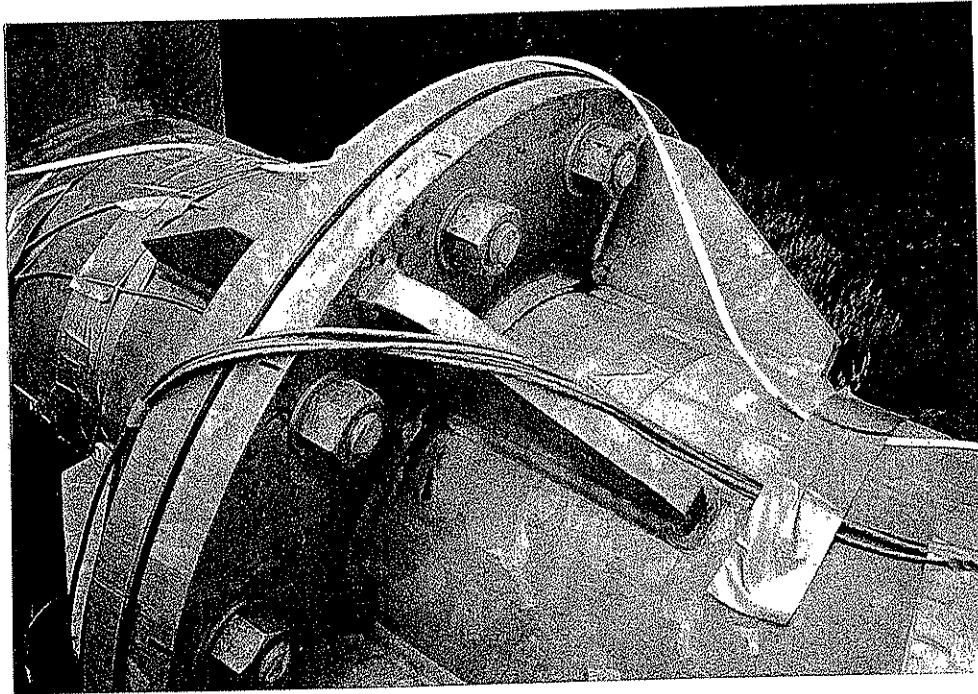


Figure 3-5 Bronze Plate Between Faying Surfaces of Stub and Chord.

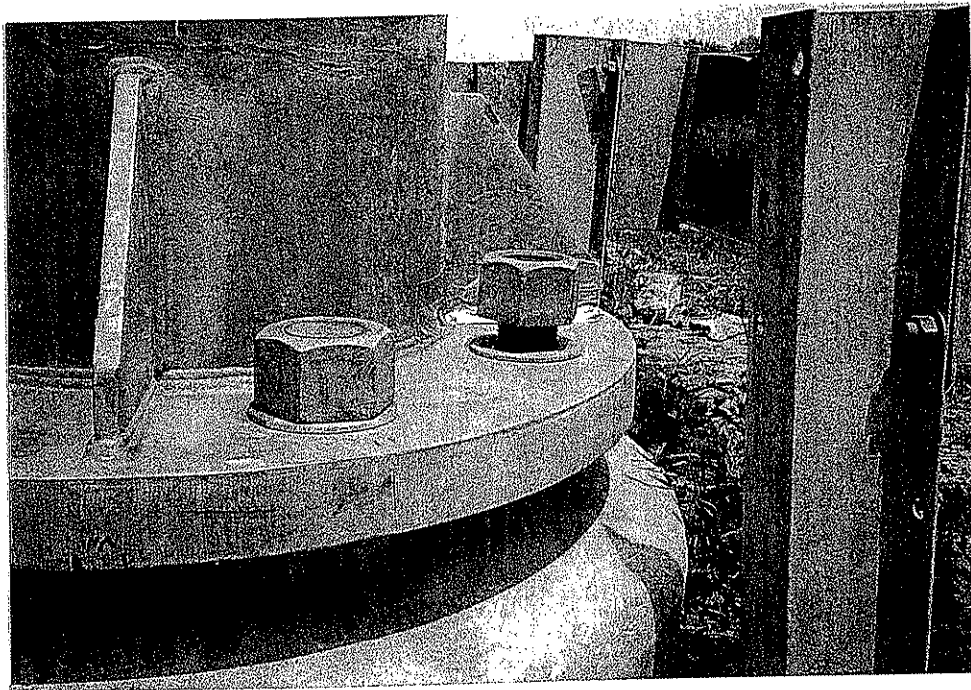


Figure 3-6 Top Nut Loosened by Hand after being Tightened.

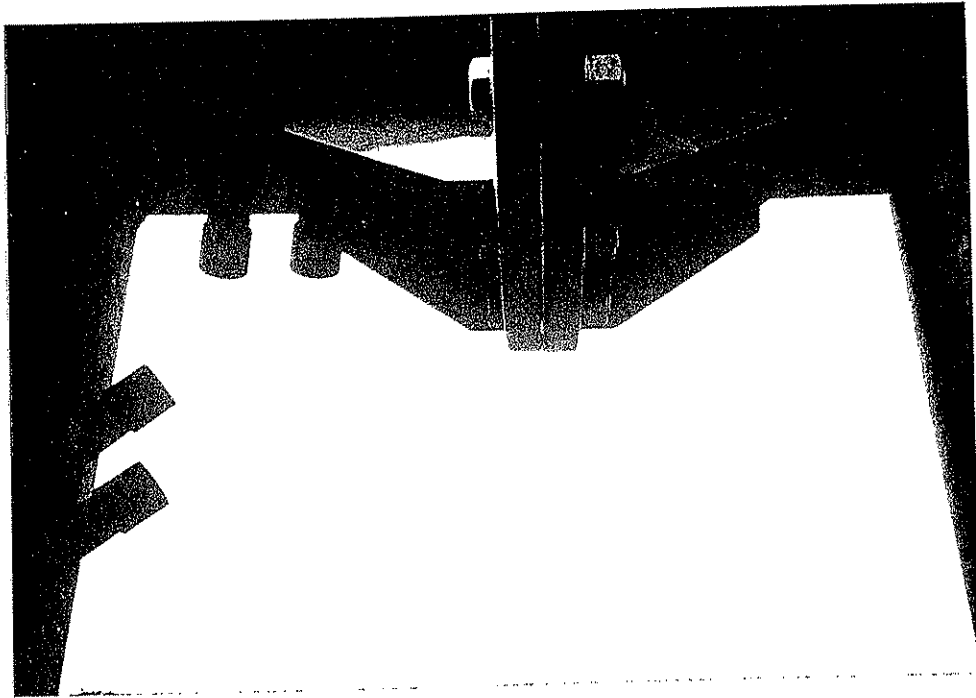
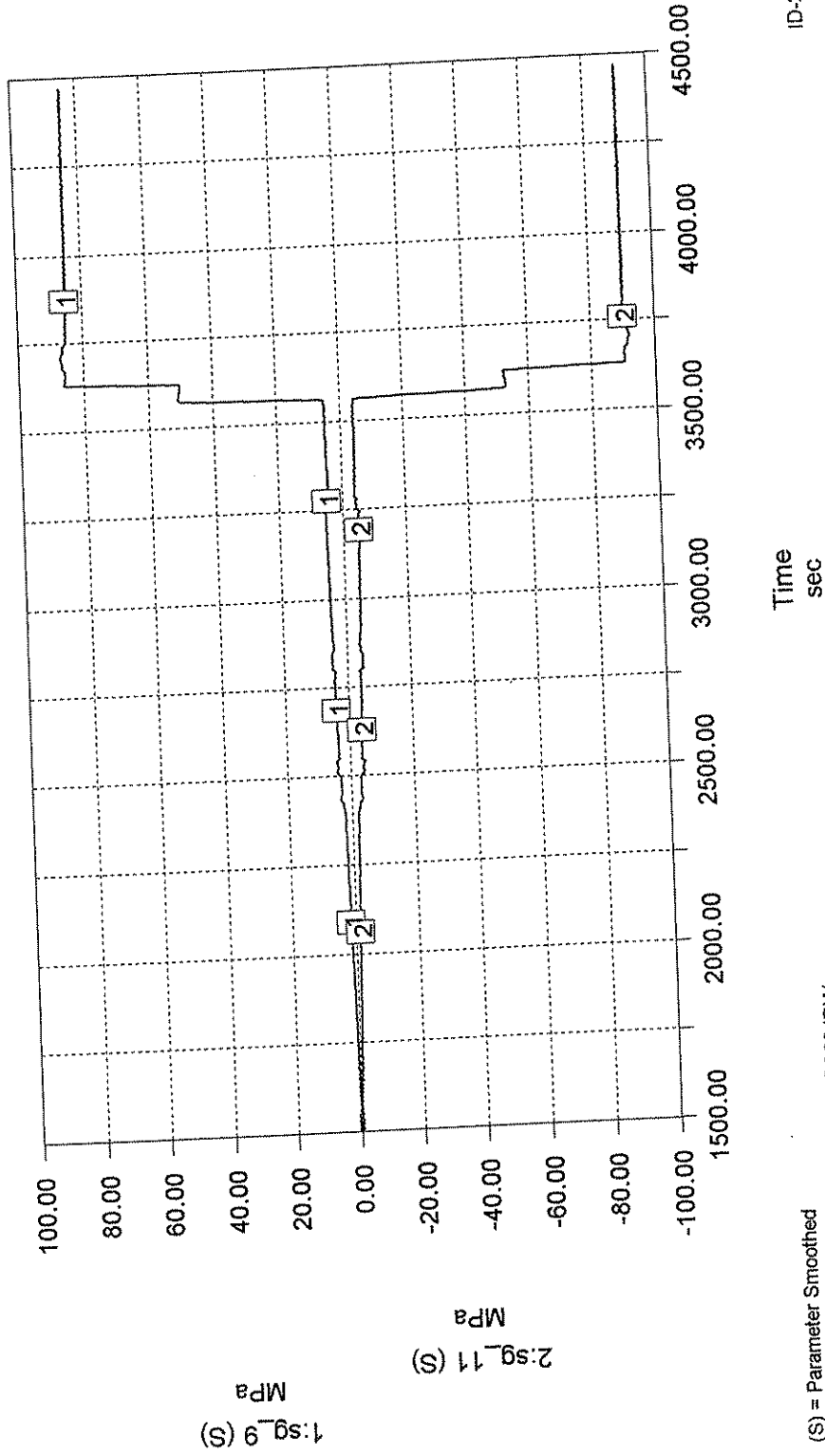


Figure 3-7 Gap Between Faying Surfaces Even with Bronze Plate.

Dead Load Stress in Column from Weight of Truss and VMS Box



(S) = Parameter Smoothed
D:\NJ_SHO-1\SHORT_~1\DEADLOAD\BC02.IDW

ID-2000

Figure 3-8 Dead Load Stress in Column.

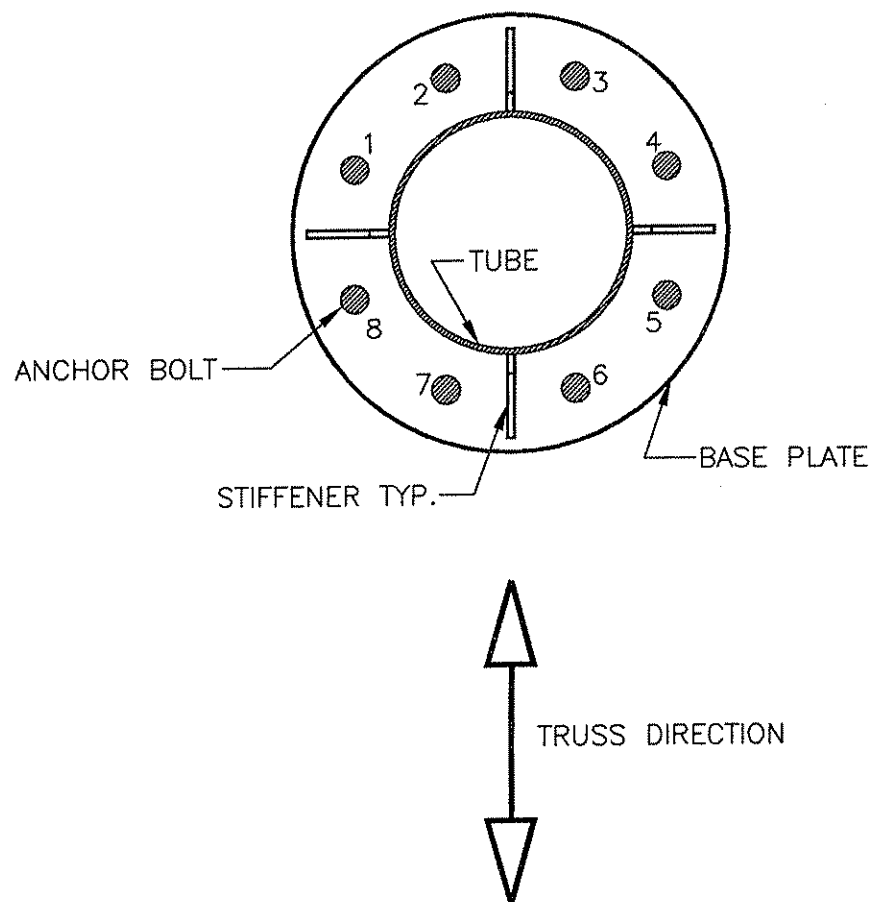
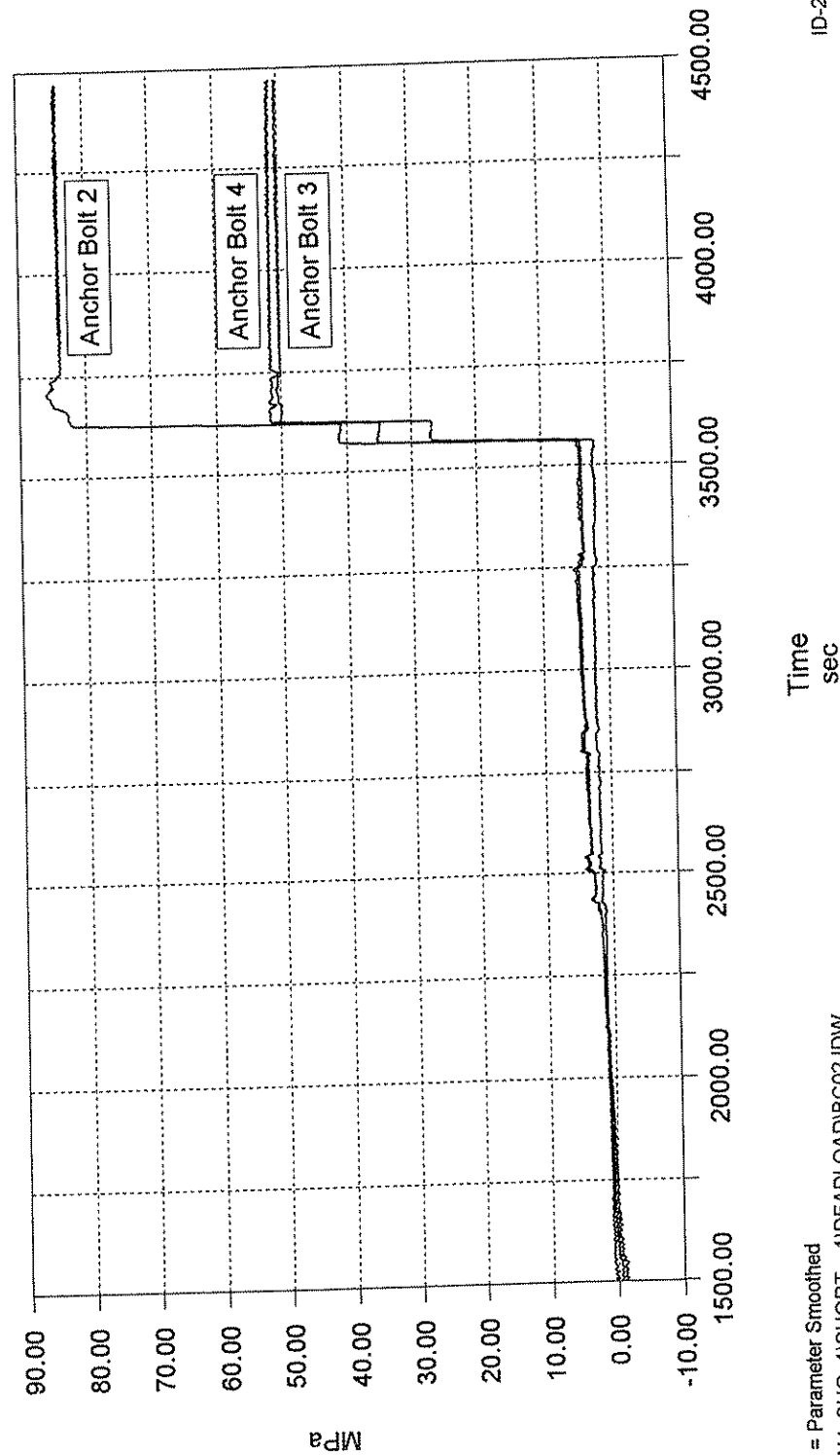


Figure 3-9 Anchor Bolt Numbering Scheme.

Dead Load Axial Stress in Anchor Bolts from Weight of Truss and VMS Box



(S) = Parameter Smoothed
D:\NJ_SHO~1\SHORT_~1\DEADLOAD\BC02.IDW

ID-2000

Figure 3-10 Axial Dead Load Stress in Anchor Bolts.

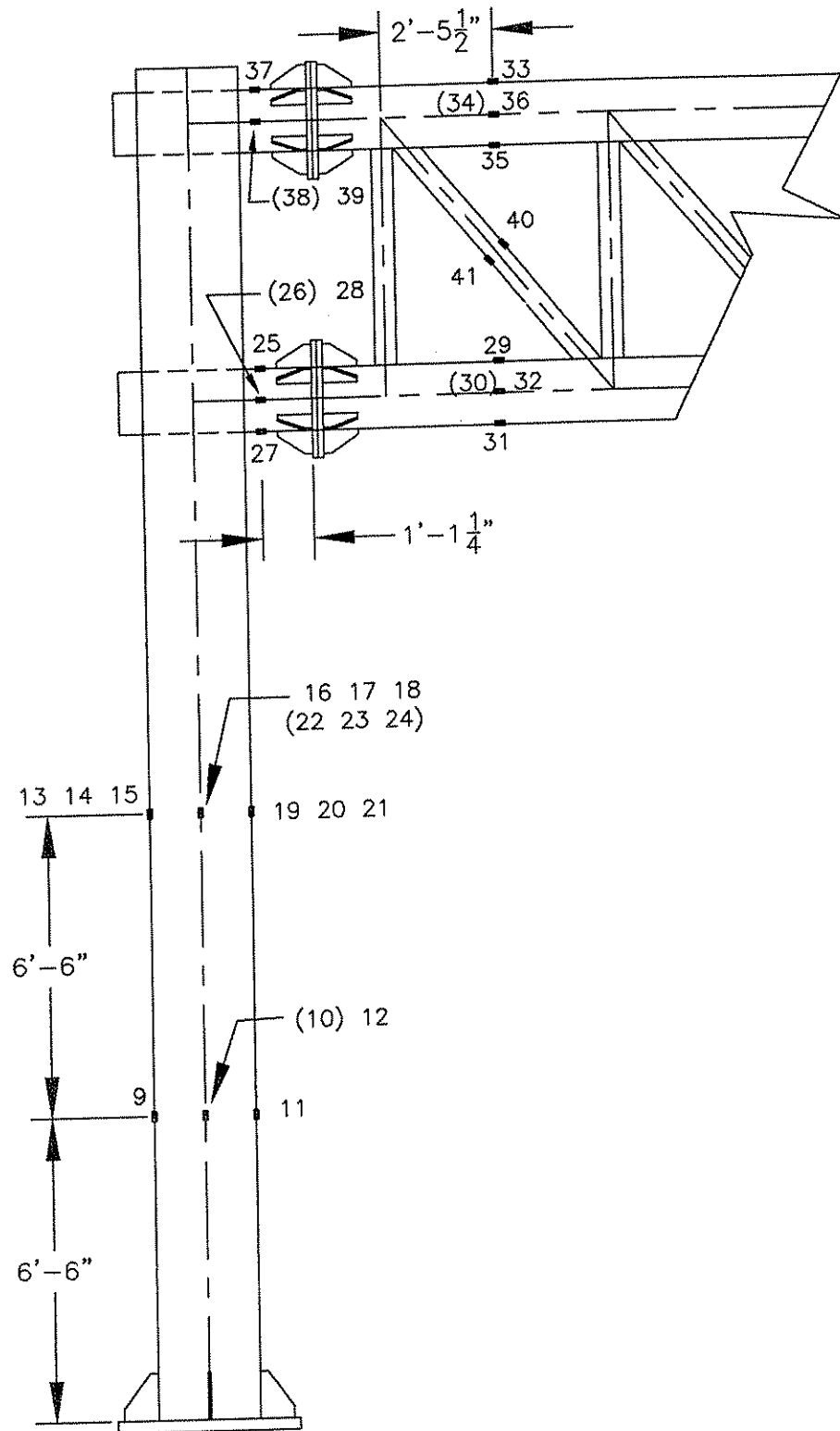


Figure 3-11 Strain Gage Locations on the Column and Truss.

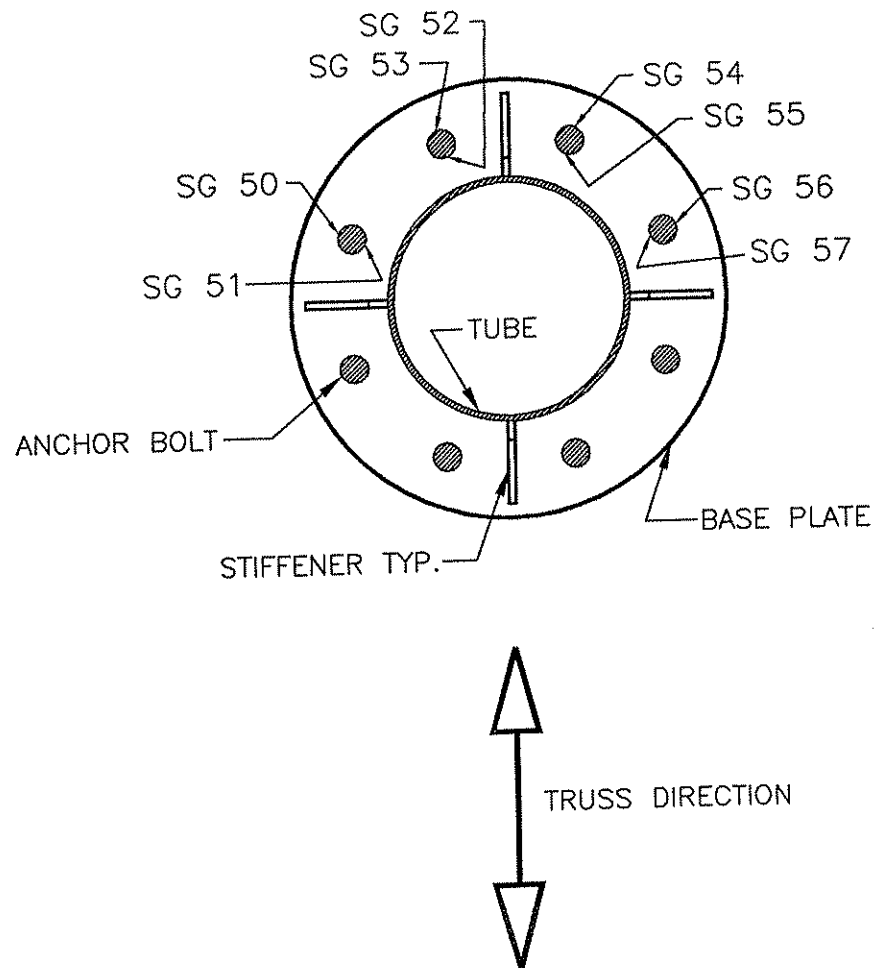


Figure 3-12 Strain Gage Locations on Anchor Bolts.

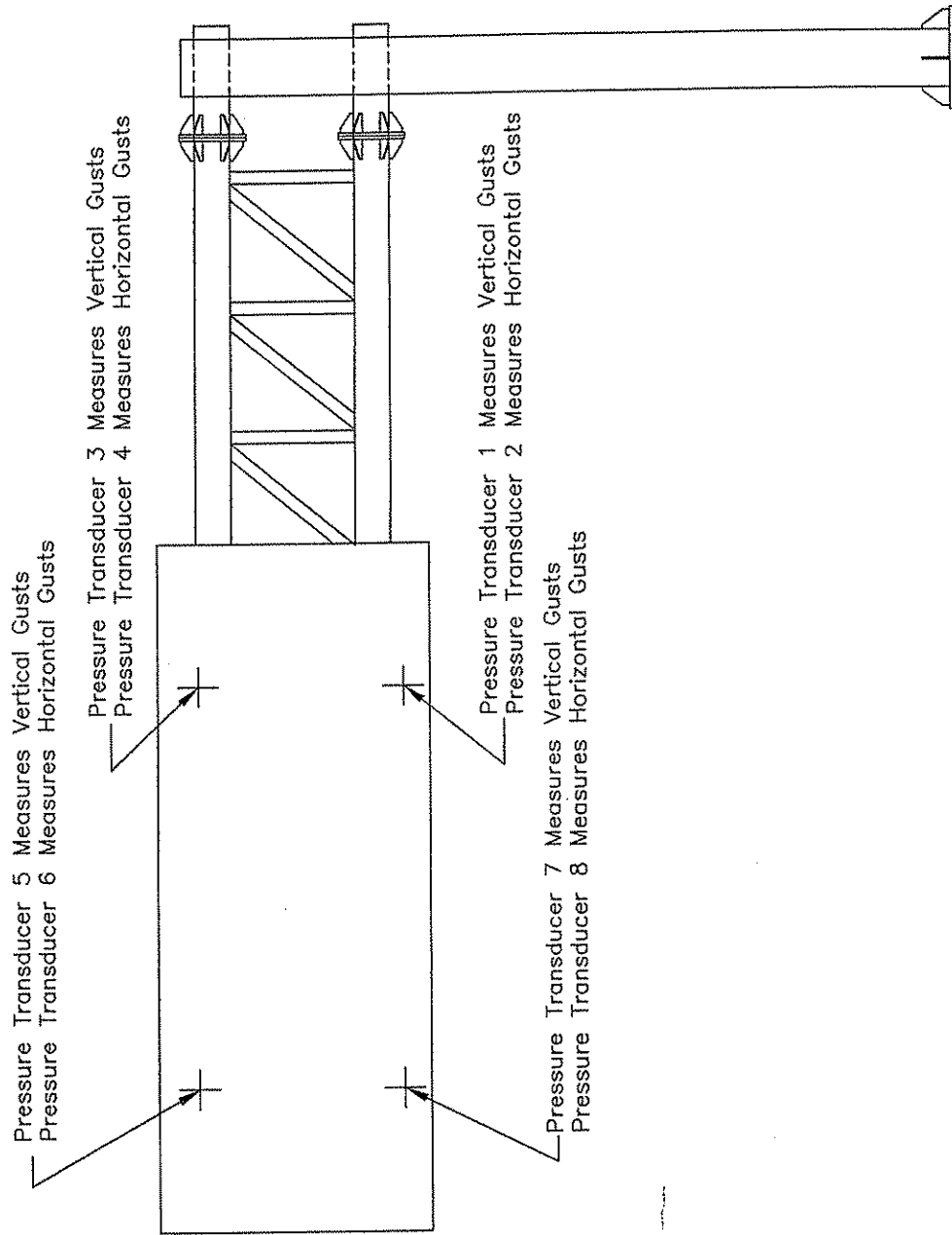


Figure 3-13 Pressure Transducer Numbering Scheme.

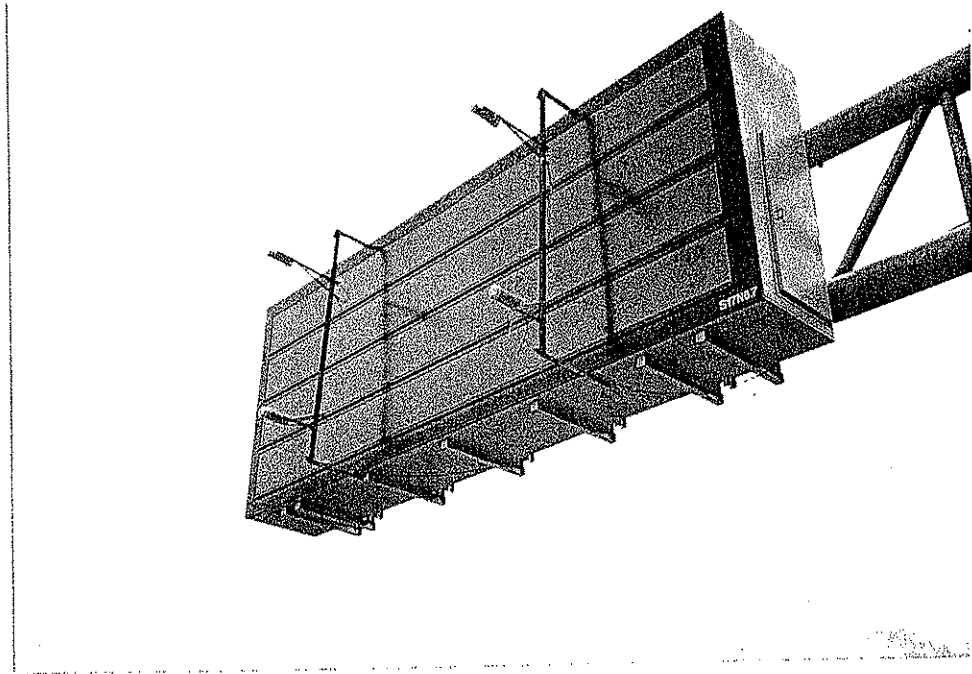


Figure 3-14 Pressure Transducers on the Face of the VMS.

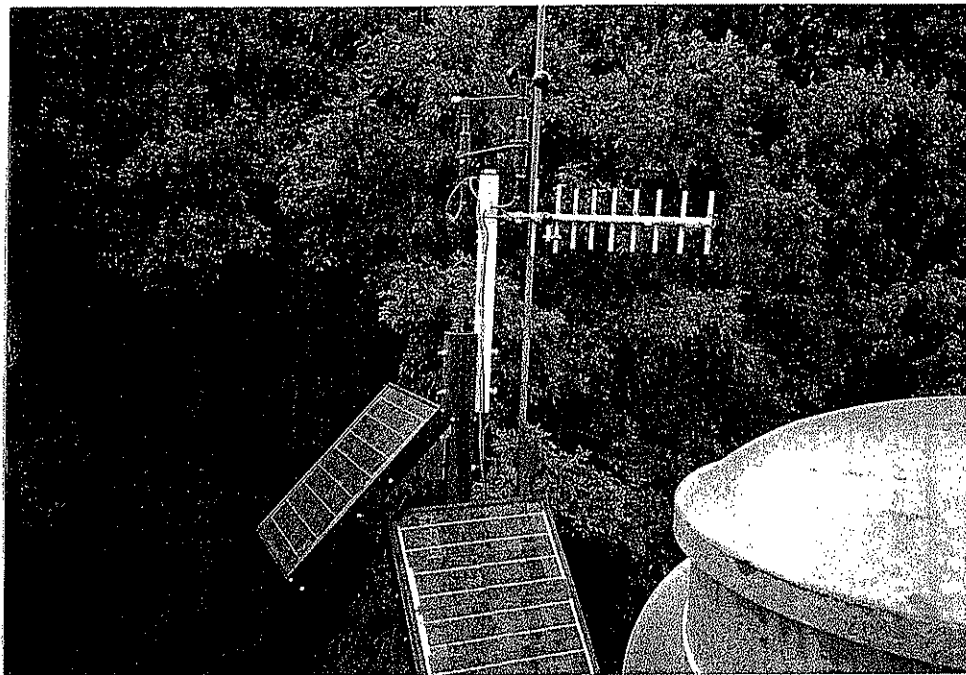


Figure 3-15 Wind Sentry to Measure Wind Speed and Direction.

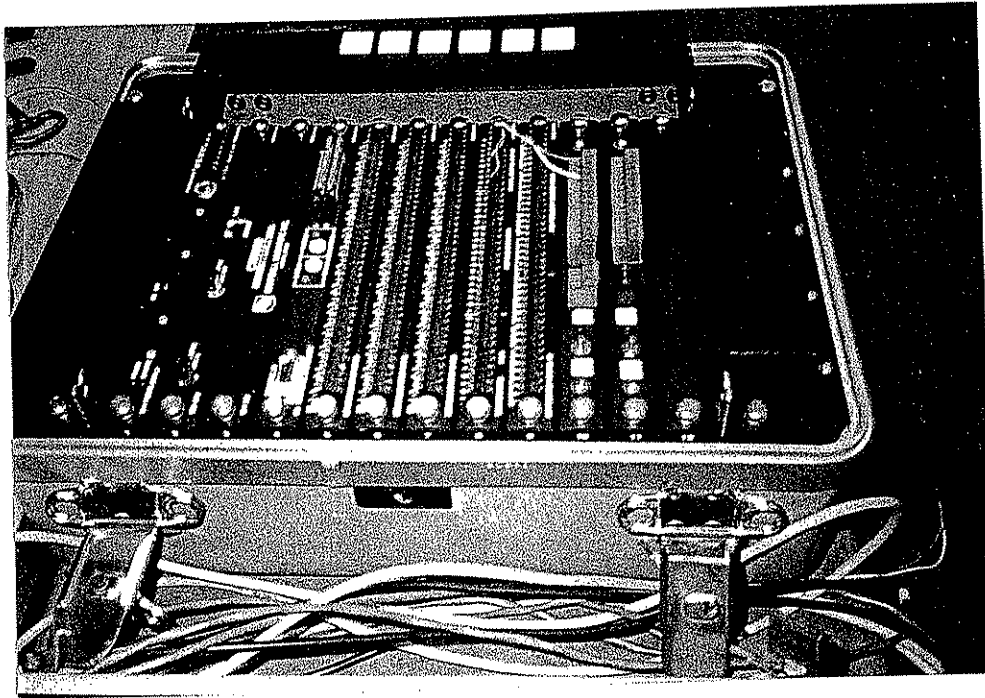


Figure 3-16 Campbell Scientific CR9000 Digital Data Acquisition System.

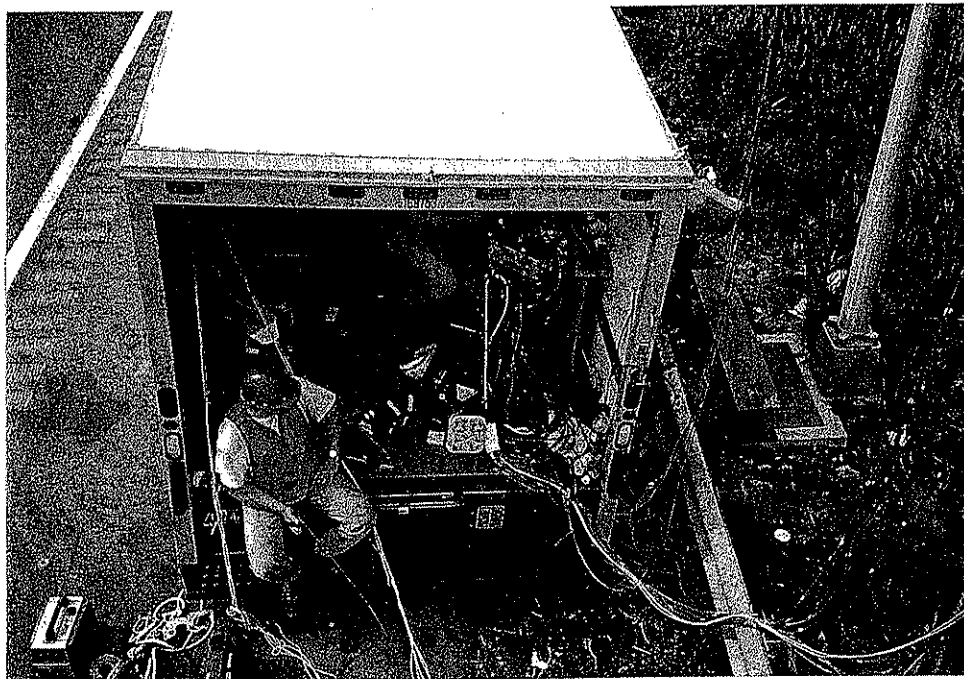


Figure 3-17 Mobile Field Office for Short-Term Testing.

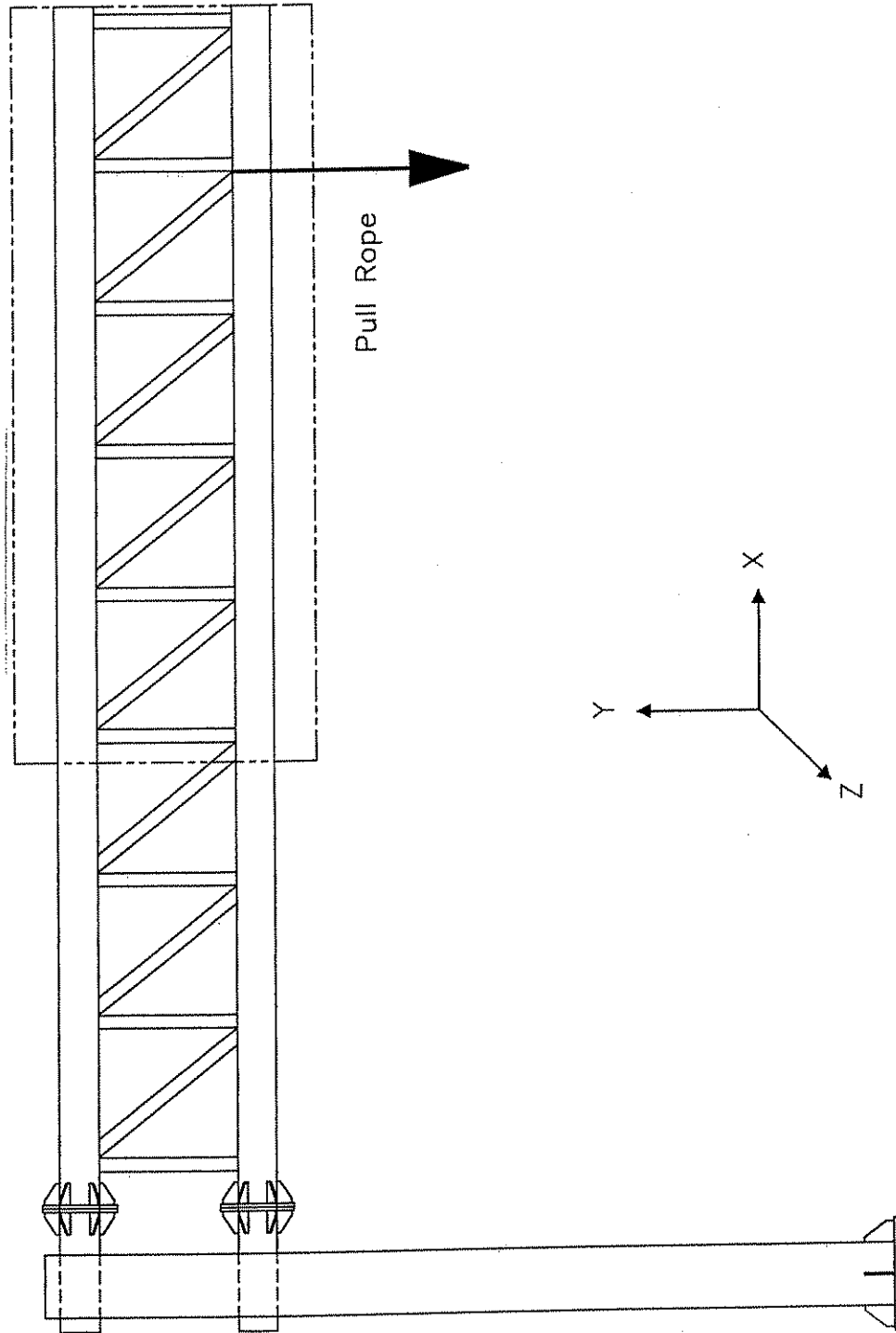


Figure 3-18 Location of Load for Static and Pluck Tests.

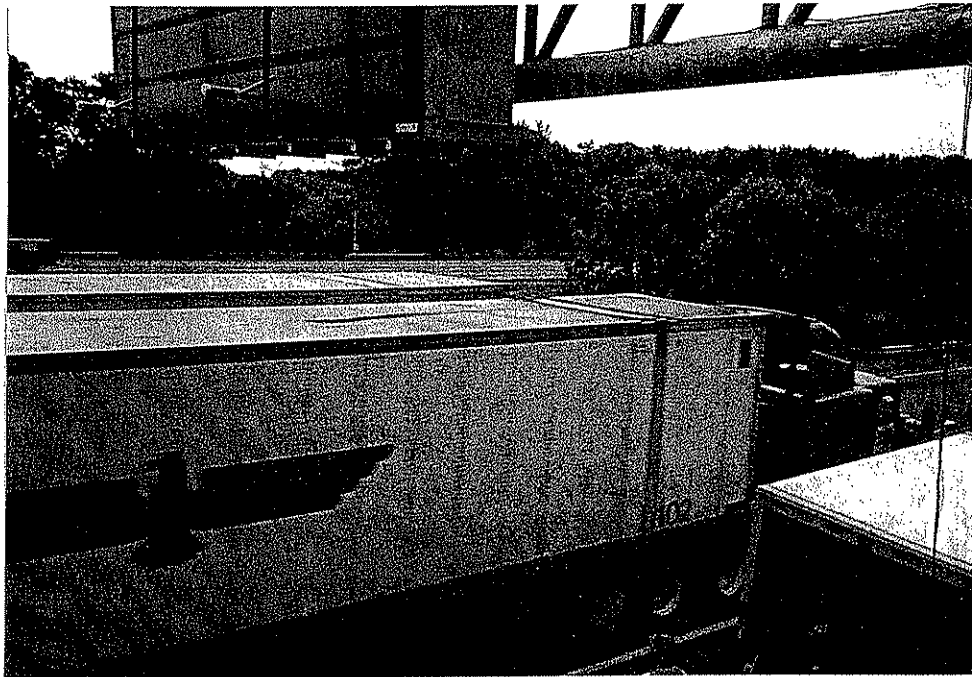
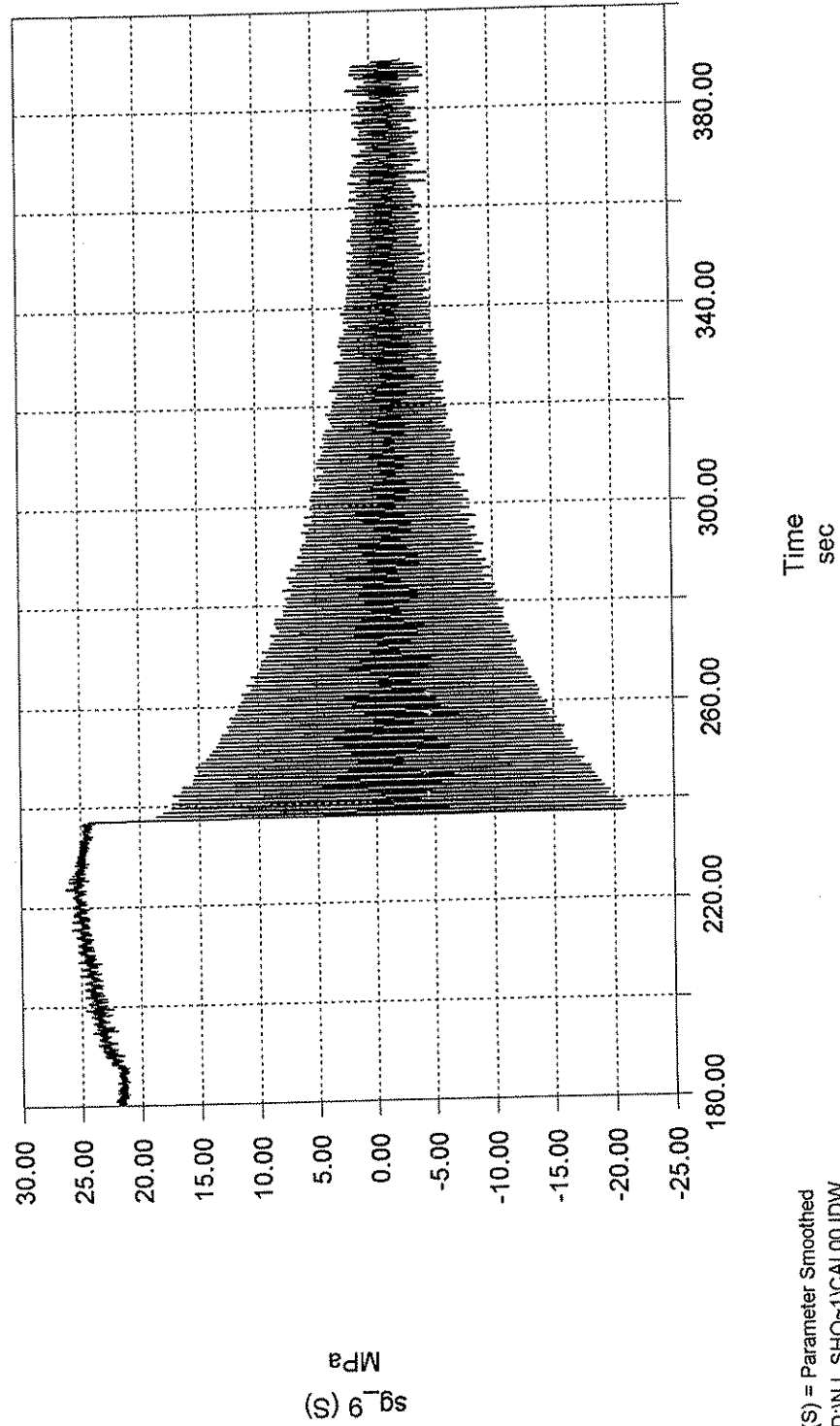


Figure 3-19 Test Trucks Driving Under VMS to Produce Truck-Induced Wind Gusts.

Decay of Motion in a Column Strain Gage

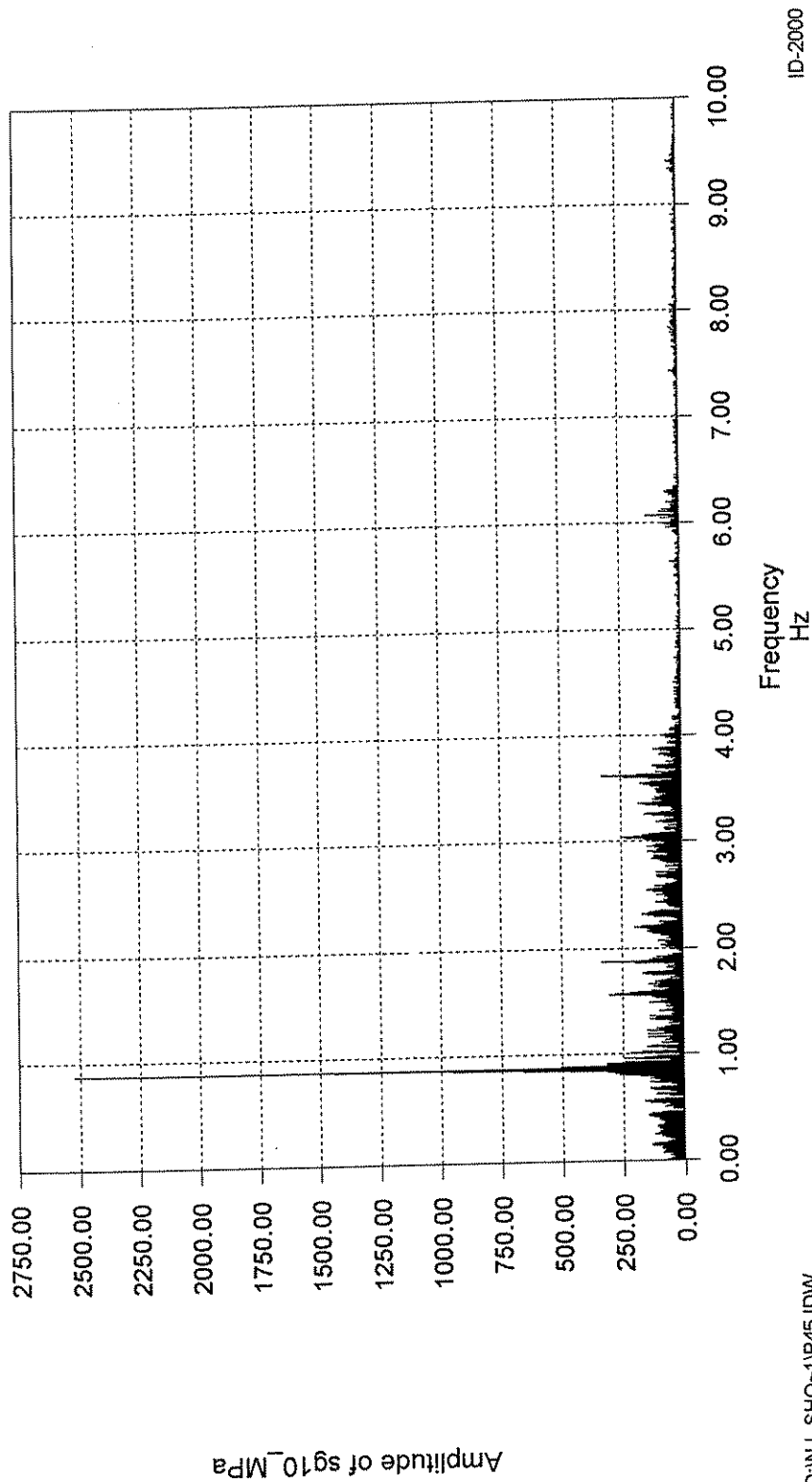


(S) = Parameter Smoothed
D:\NJ_SHO~1\CAL00.IDW

ID-2000

Figure 3-20 Damping of Motion in a Column Strain Gage.

Amplitude Spectrum of sg10_MPa Time: 211.95 to 314.40
FFT Size: 2048 FFT Window Type: Rectangle/None
Peak of 2524.09 at 0.87 Hz



D:\NJ_SHO-1\p45.IDW

Figure 3-21 FFT Indicating Natural Frequency in the "Twisting Mode".

Amplitude Spectrum of sg_9 Time: 240.10 to 342.55
FFT Size: 2048 FFT Window Type: Rectangle/None
Peak of 11984.99 at 1.22 Hz.

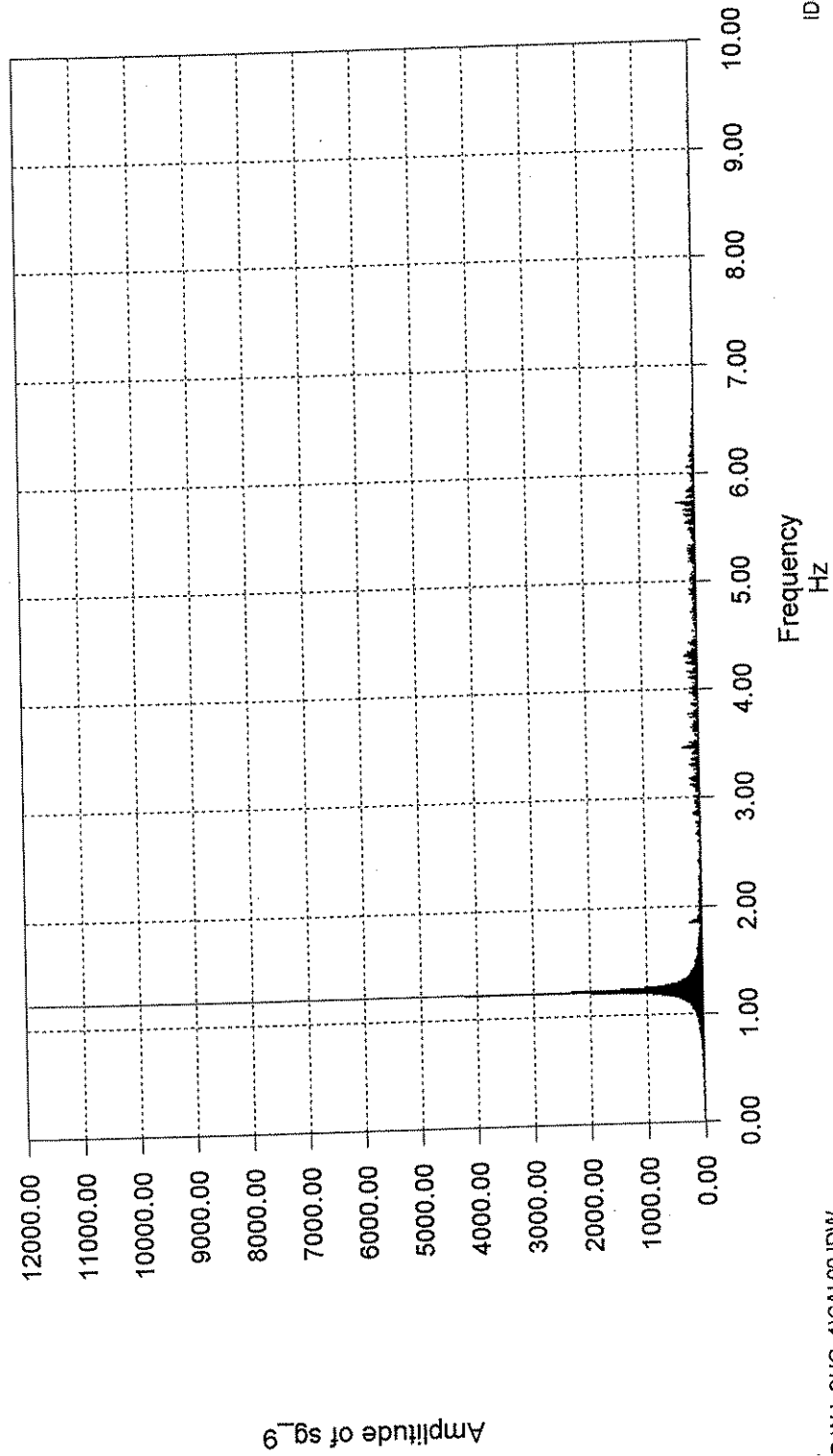


Figure 3-22 FFT Indicating Natural Frequency in the "Hatchet Mode".

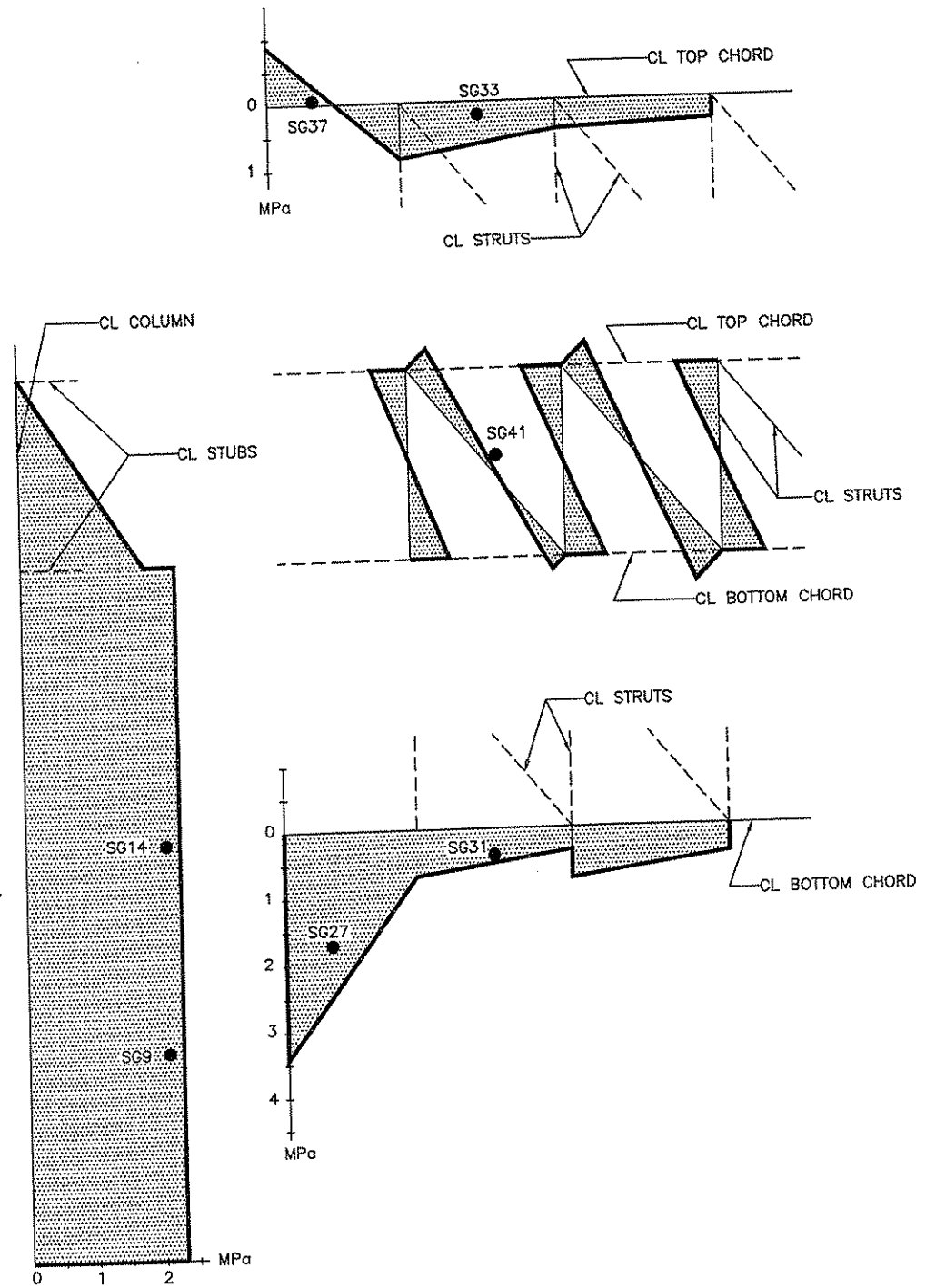


Figure 3-23 Stress in Structure from a 1 kN Load

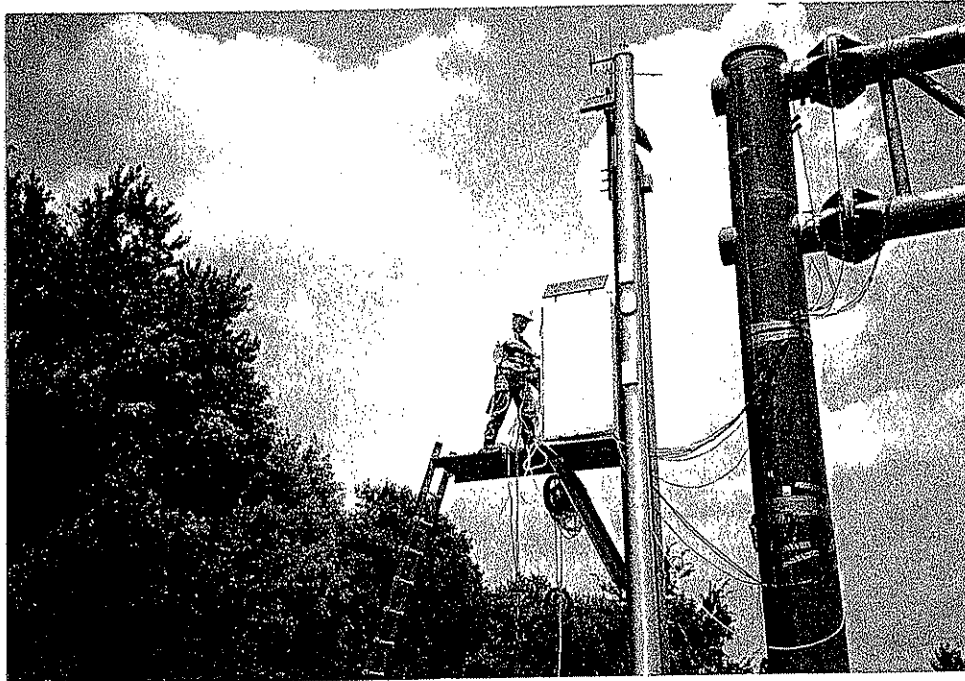


Figure 3-24 Enclosure for Data Acquisition Equipment During the Long-term Testing.

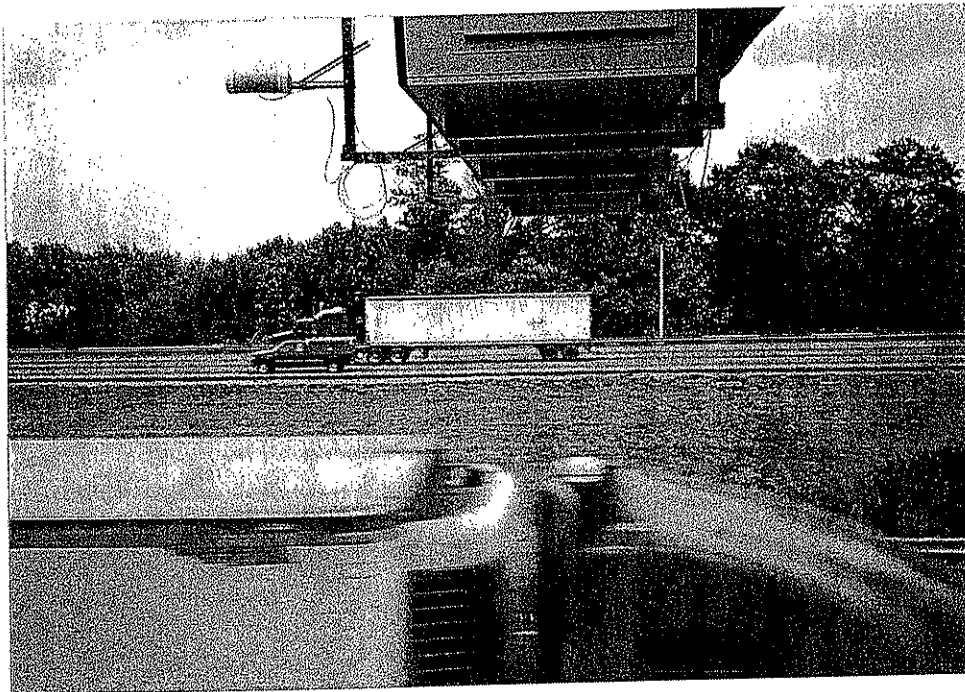
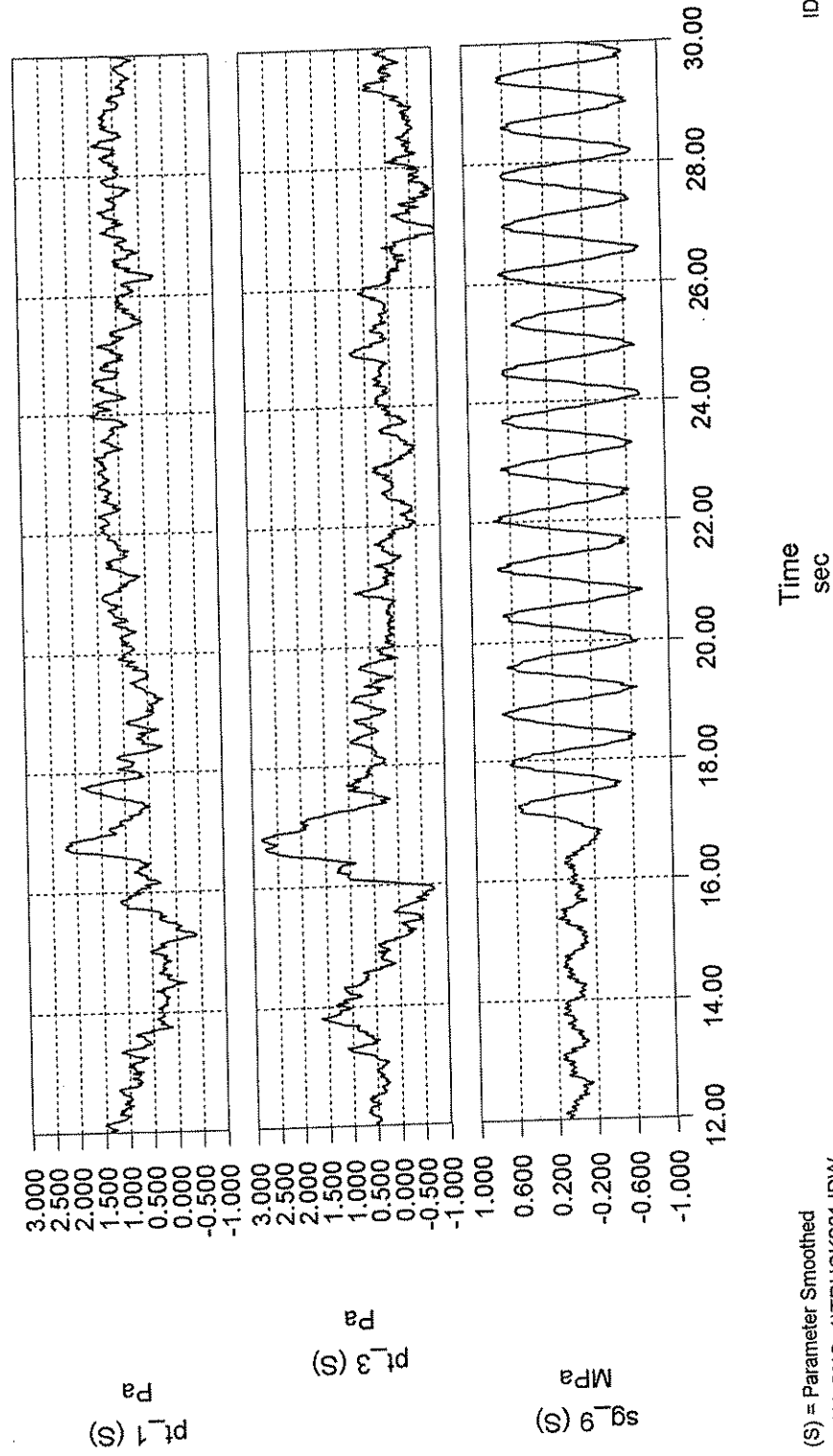


Figure 3-25 Random Trucks Under VMS Causing Gusts.

Gusts from Truck Test One

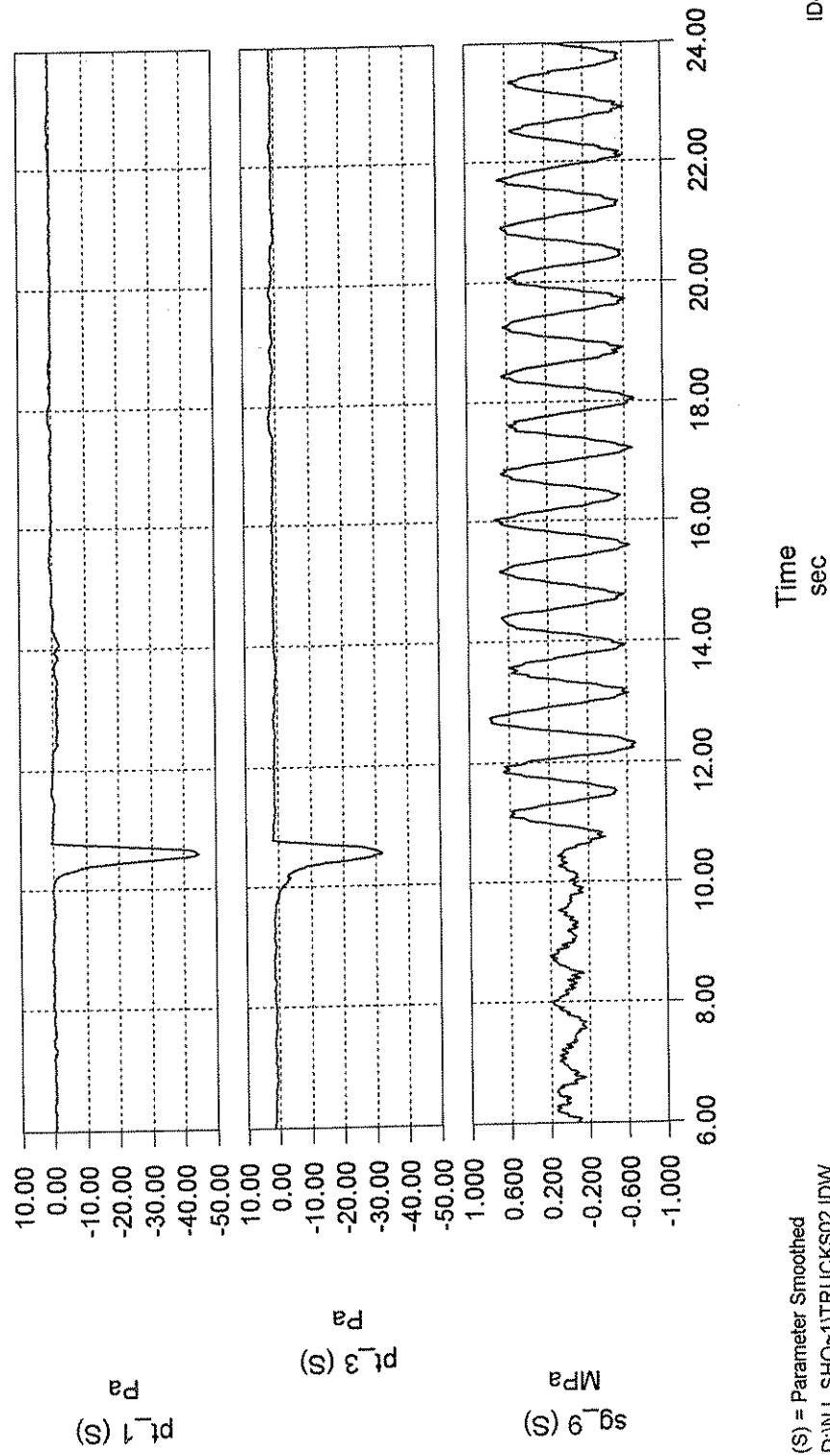


(S) = Parameter Smoothed
D:\NJ_SHO~1\TRUCKS01.IDW

ID-2000

Figure 3-26 Pressures From Truck Test One and the Corresponding Column Stress.

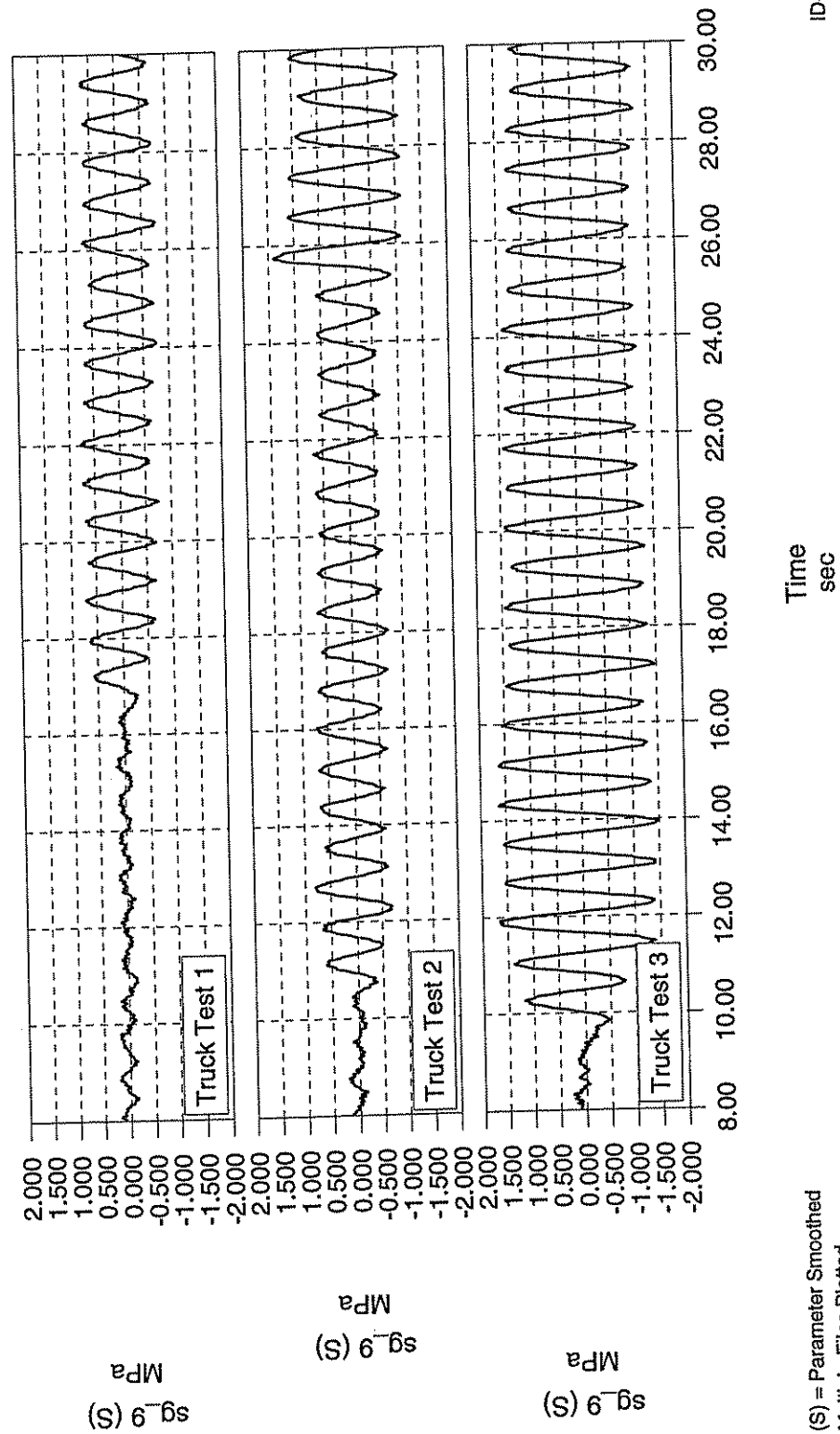
Gusts from Truck Test Two



ID-2000

Figure 3-27 Pressures From Truck Test Two and the Corresponding Column Stress.

Column Strain Gage Response to Various Test Truck Configurations

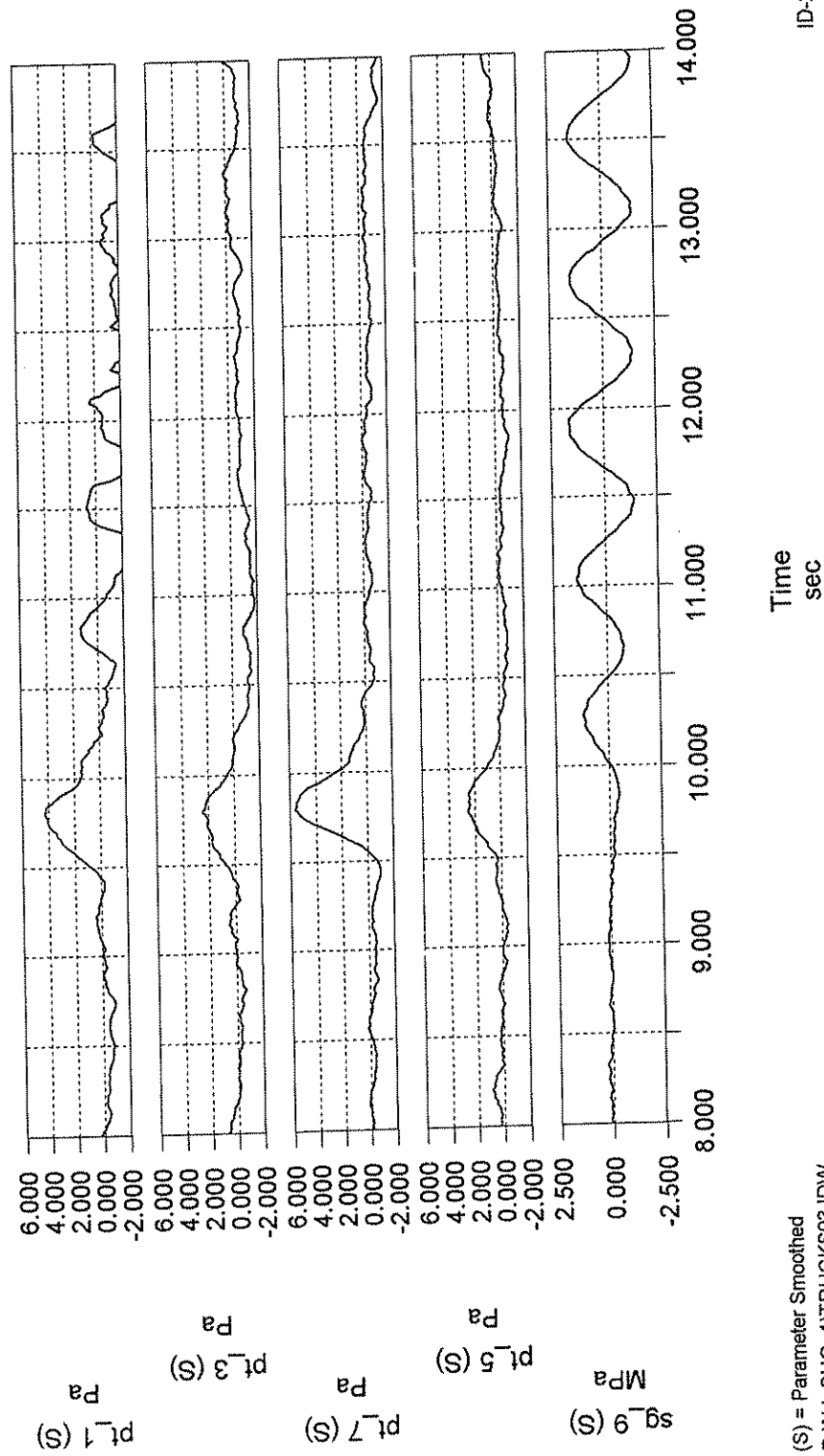


(S) = Parameter Smoothed
Multiple Files Plotted

ID-2000

Figure 3-28 Comparison of Column Response in All Three Truck Tests.

Pressure Gradient in Truck Test Three

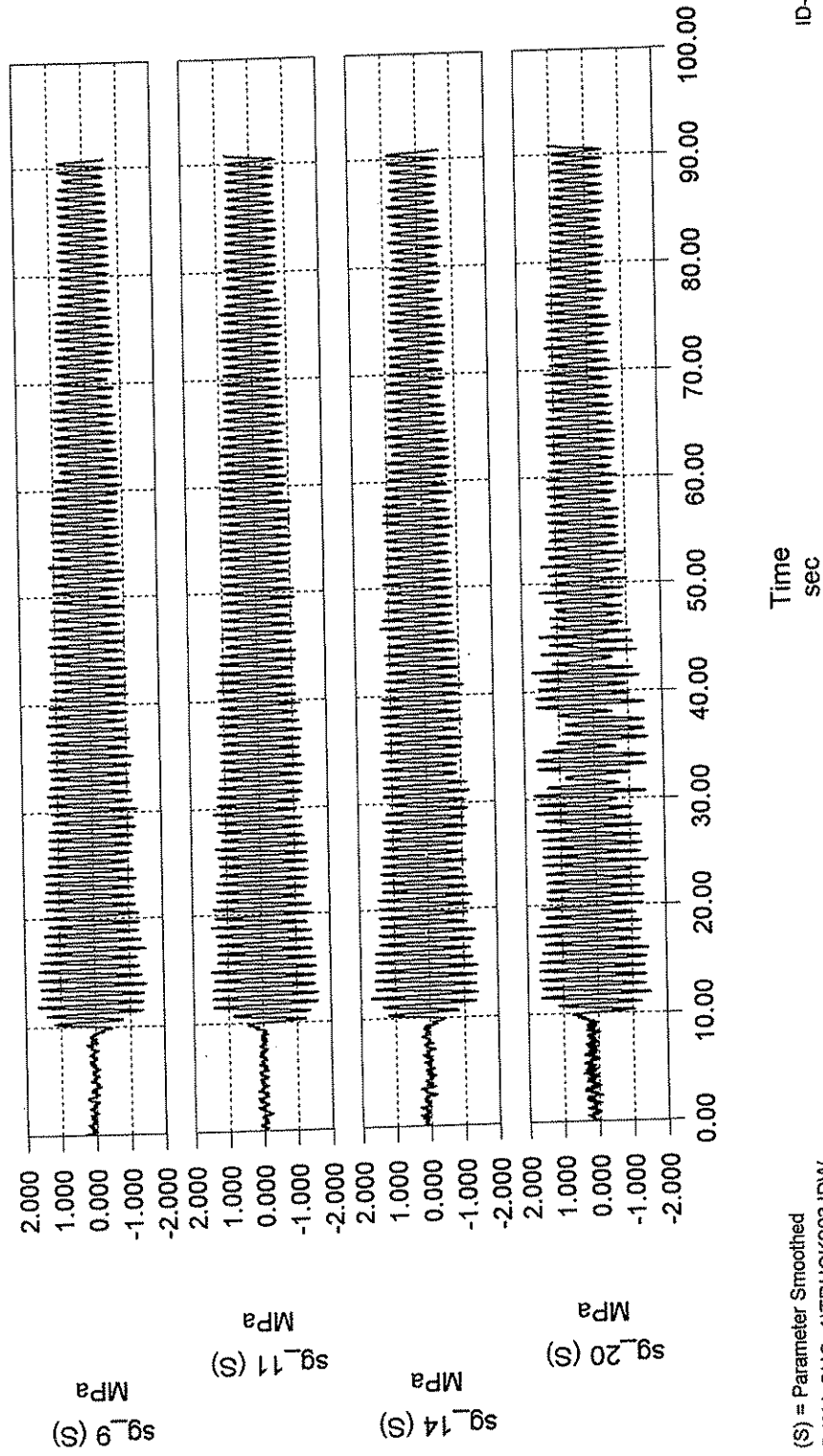


(S) = Parameter Smoothed
D:\NJ_SHO-1\TRUCKS03.IDW

ID-2000

Figure 3-29 Pressure Gradient in Truck Test Three.

Column Strain Gage Data From Test Truck Run 3



(S) = Parameter Smoothed
D:\NJ_SHO-1\TRUCKS03.IDW

ID-2000

Figure 3-30 Stress Range in Column from Truck Test Three.

Lower Stub and Chord Strain Gage Data From Truck Test Run 3

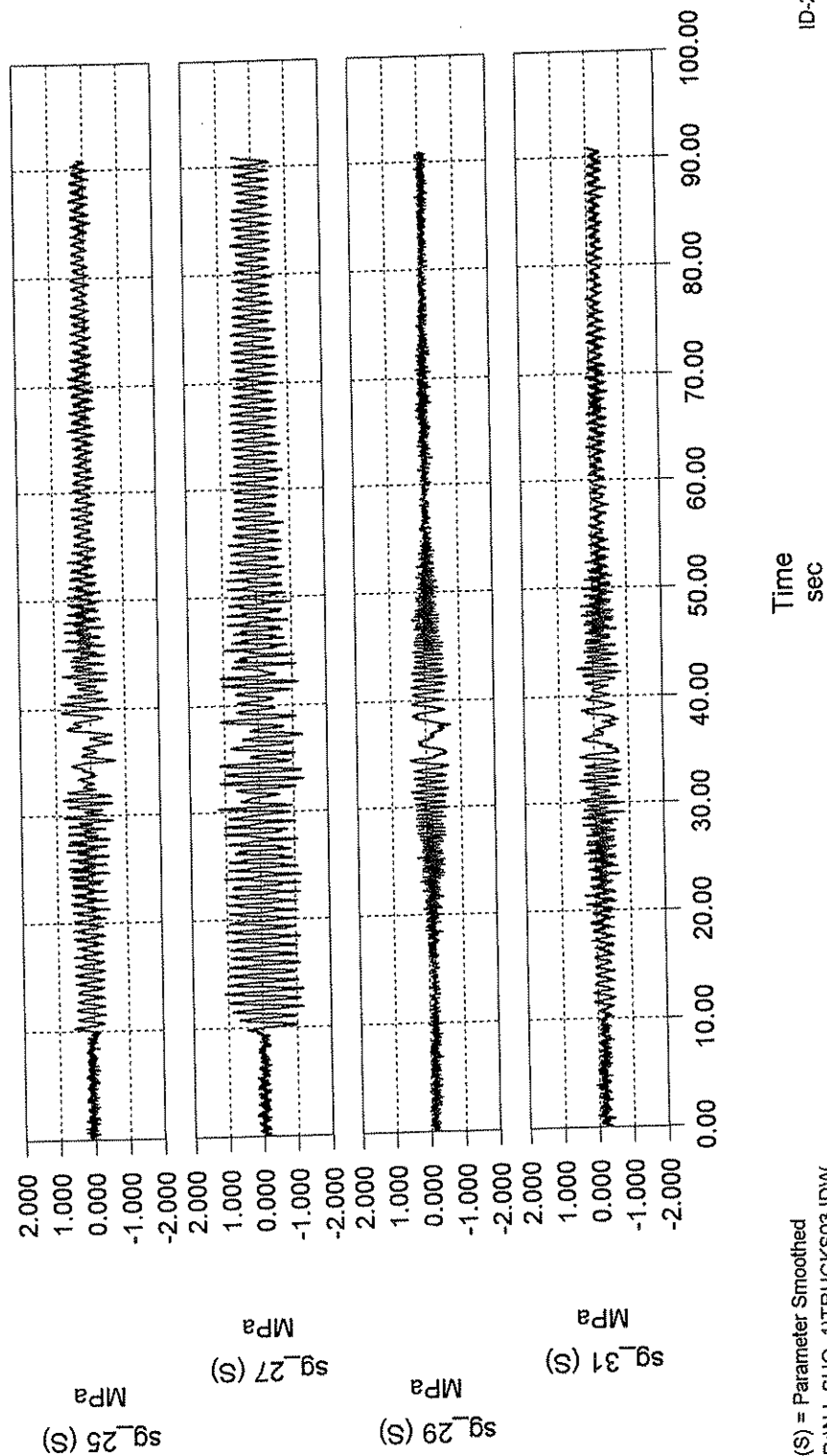
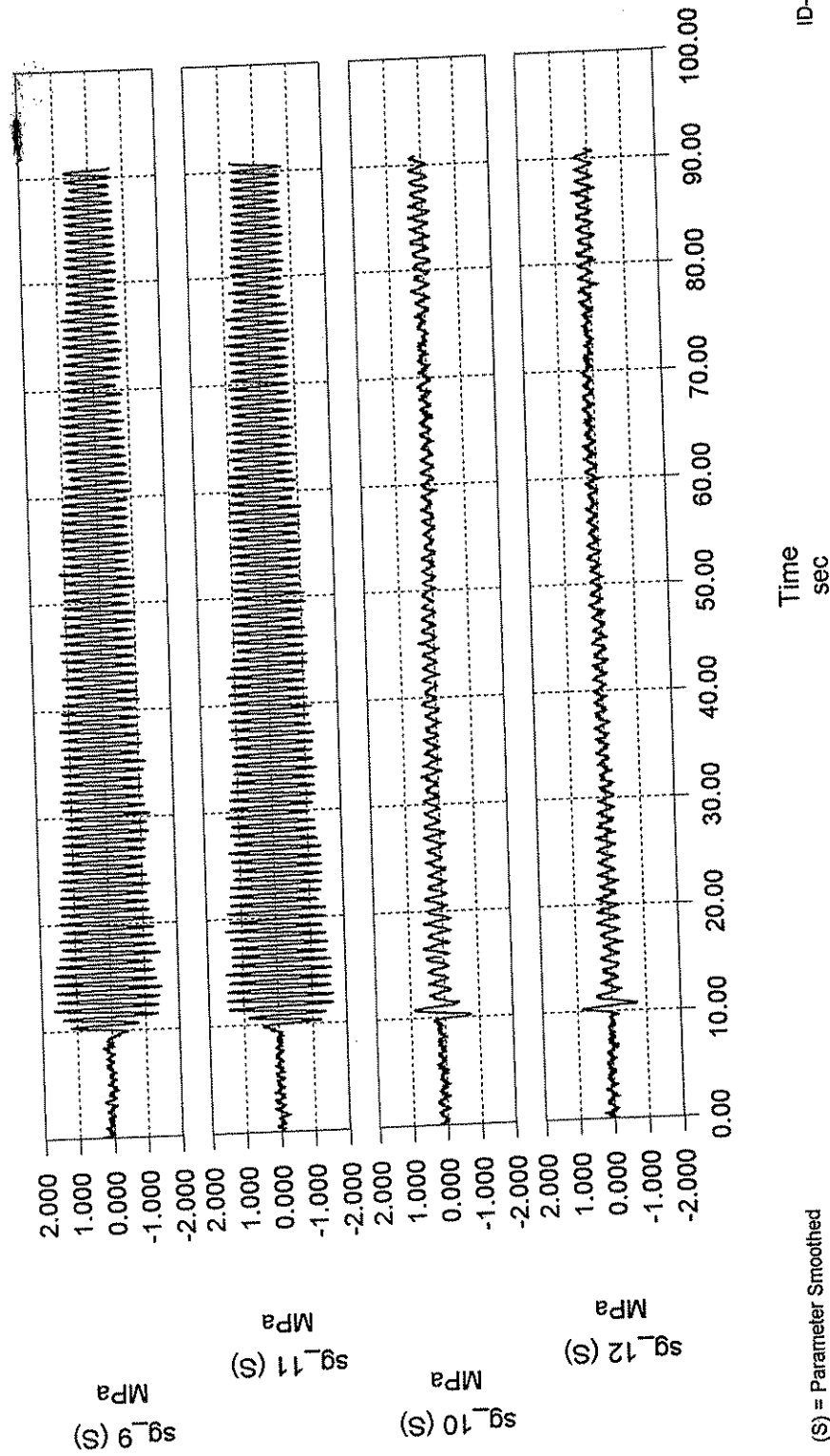


Figure 3-31 Stress Range in Lower Stub and Chord in Truck Test Three.

Column Gages Comparing "Hatchet" and "Twisting" Modes
From Test Truck Run 3 Gusts



(S) = Parameter Smoothed
D:\NJ_SHO~1\TRUCKS03.IDW

ID-2000

Figure 3-32 Comparison of Structure in "Twisting" and "Hatchet" Modes.

Typical Column Stress Ranges From
Random Truck Gusts

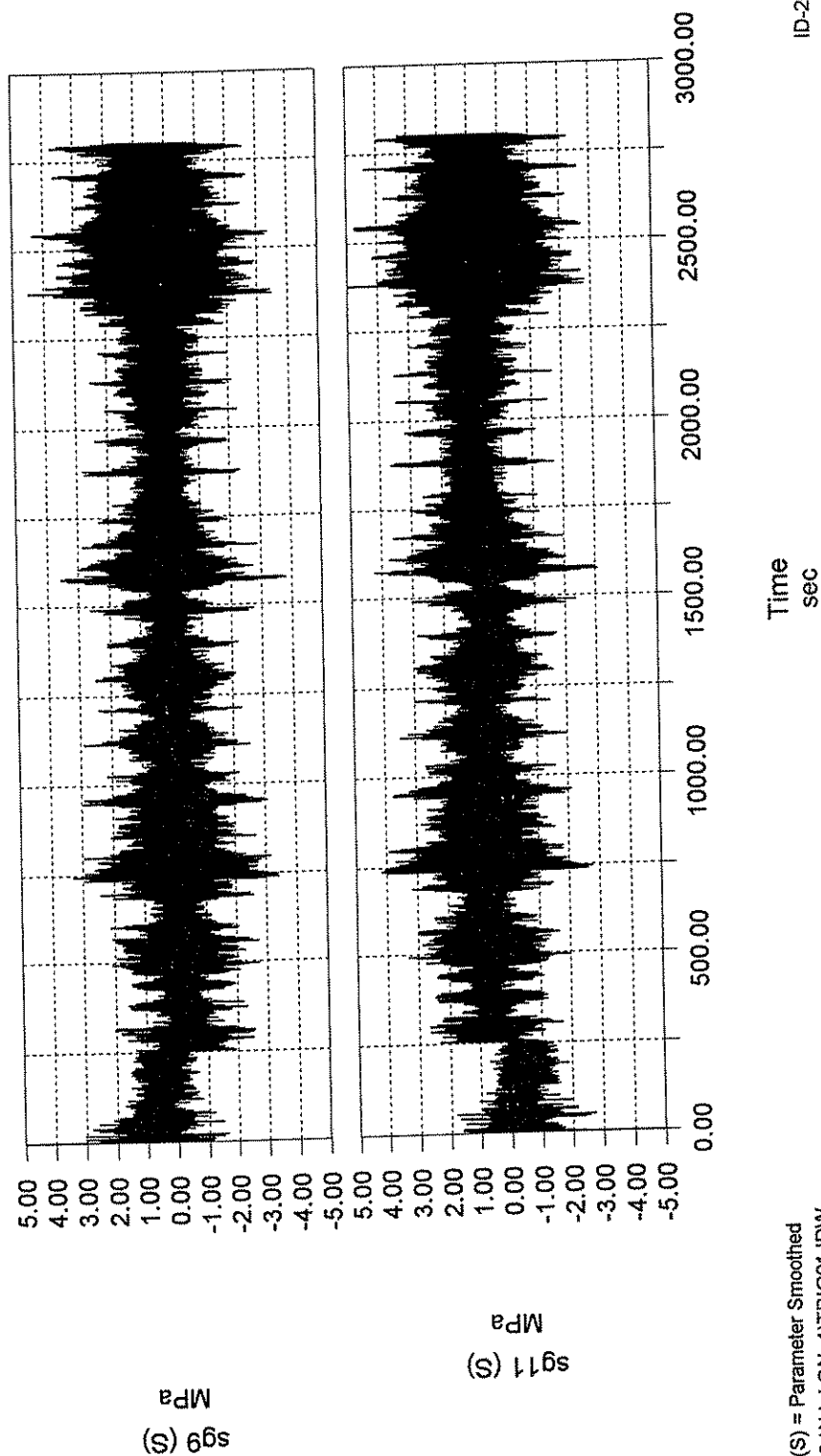
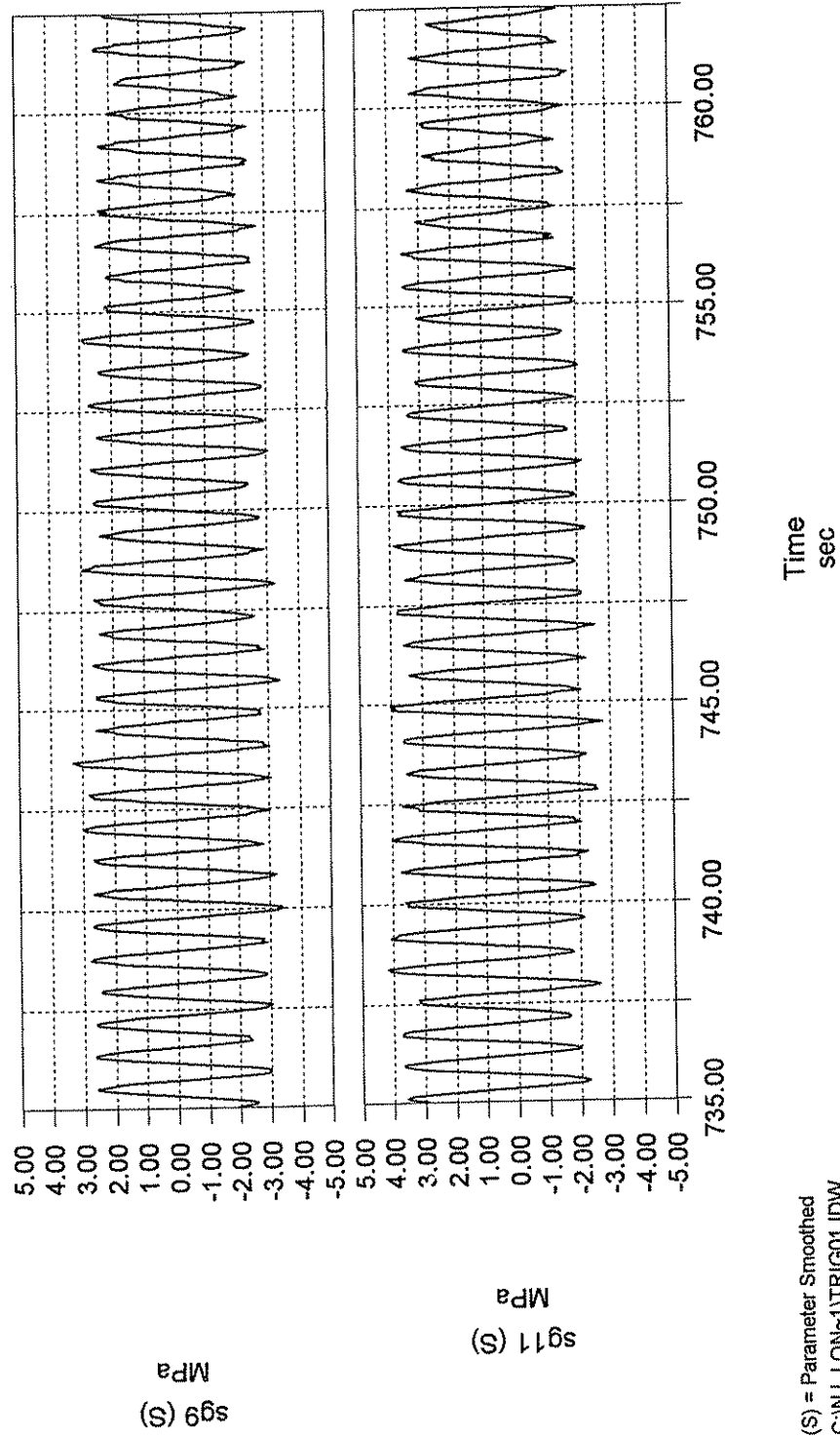


Figure 3-33 Random Data File from Long Term Monitoring.

Typical Column Stress Ranges From
Random Truck Gusts

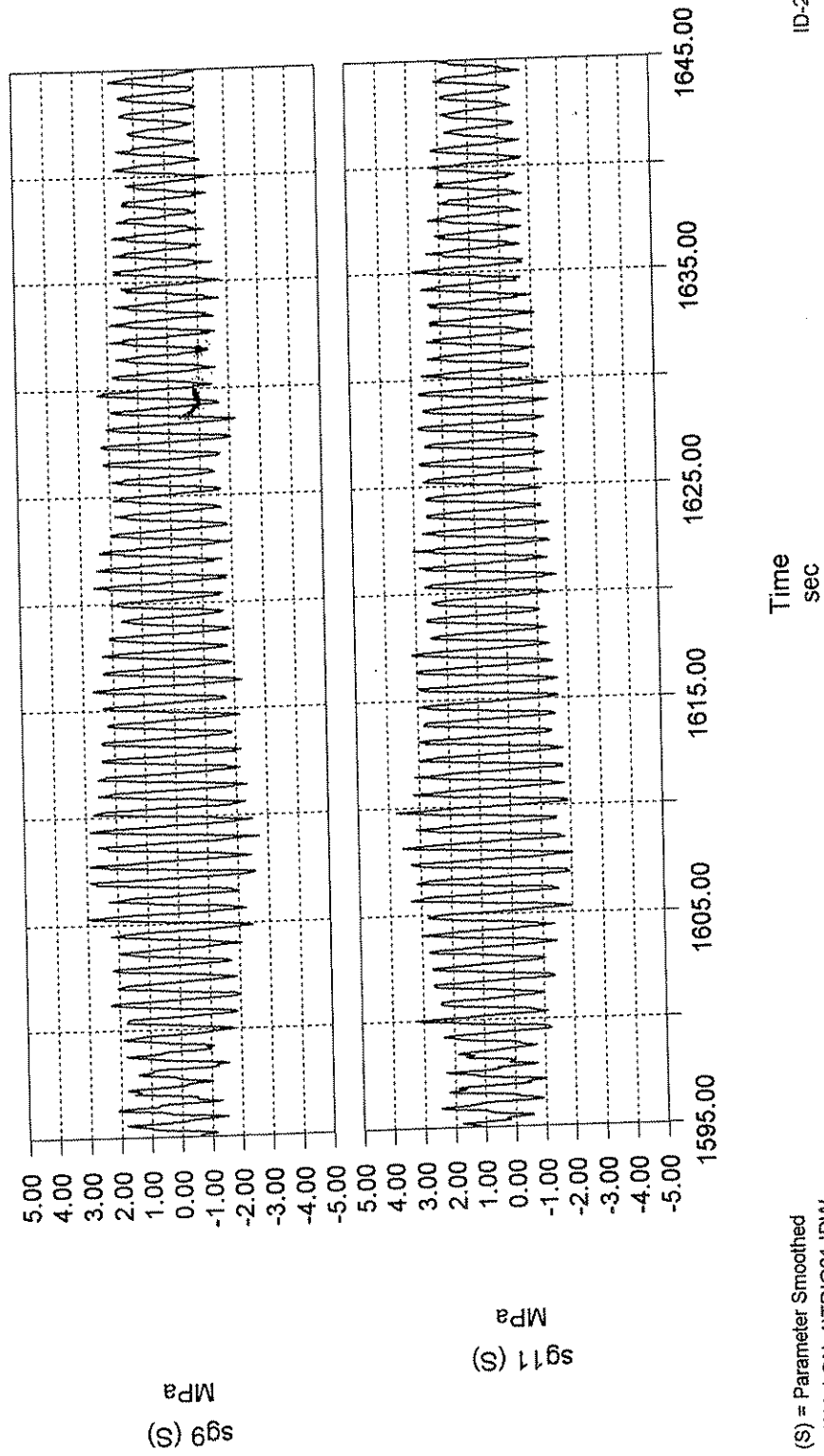


(S) = Parameter Smoothed
C:\NJ_LON-1\TRIG01.IDW

ID-2000

Figure 3-34 Close Up of Long Term Data.

Typical Column Stress Ranges From
Random Truck Gusts



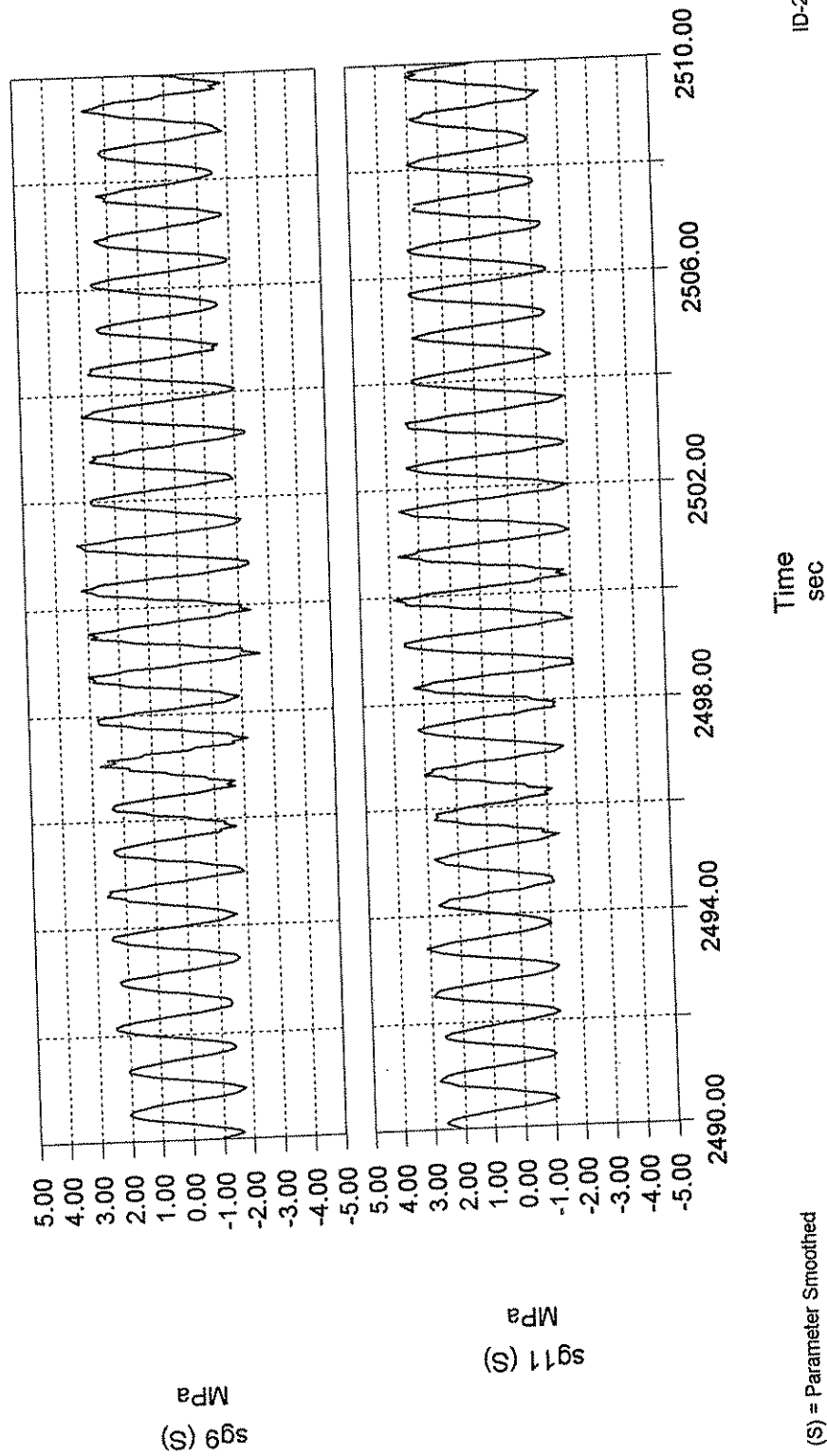
(S) = Parameter Smoothed
D:\NJ_LON-1\TRIG01.IDW

Time
sec

ID-2000

Figure 3-35 Close Up of Long Term Data.

Typical Column Stress Ranges From
Random Truck Gusts

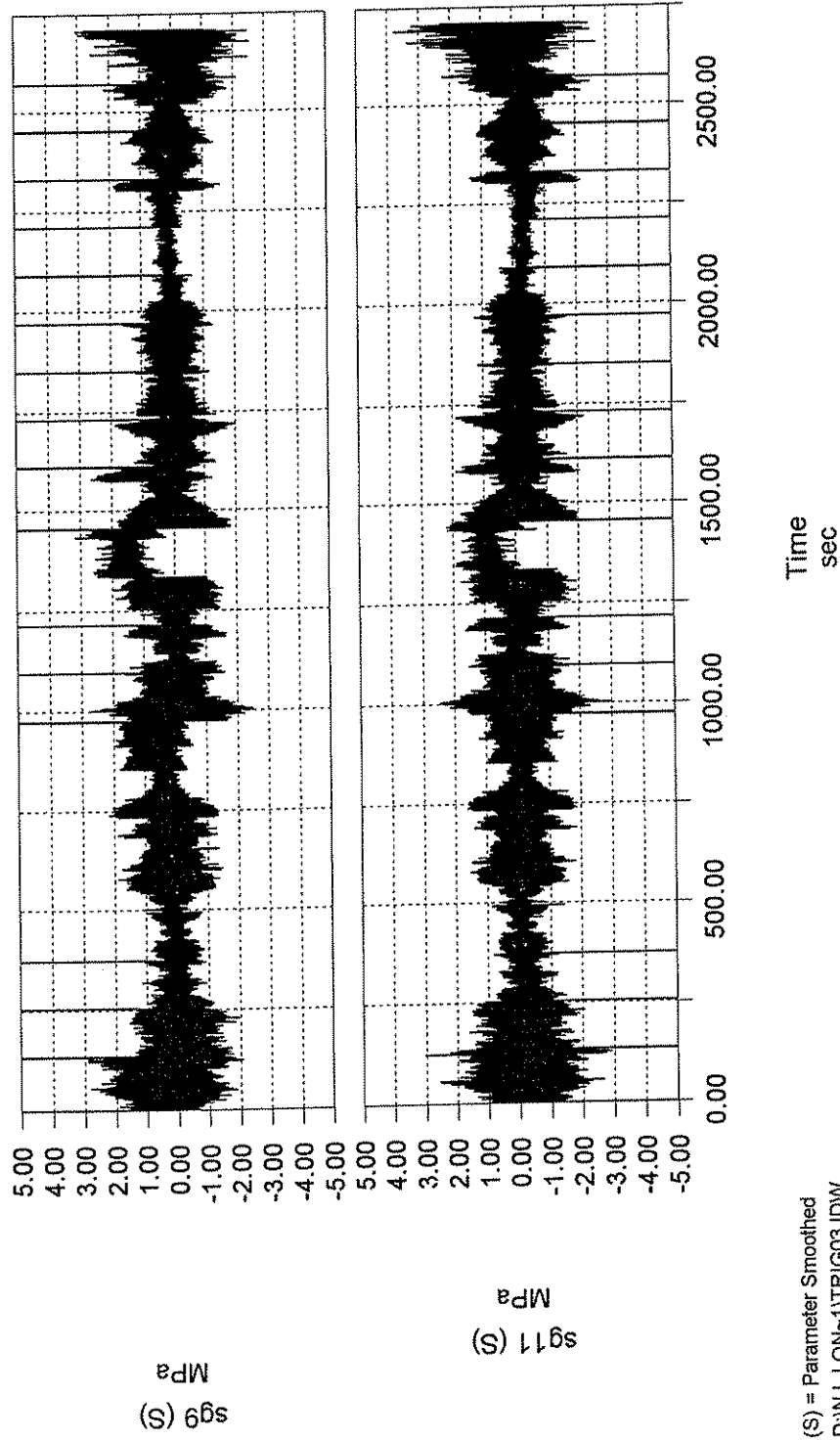


(S) = Parameter Smoothed
C:\NJ_LON~1\TRIG01.IDW

ID-2000

Figure 3-36 Close Up of Long Term Data.

Typical Column Stress Ranges From
Random Truck Gusts

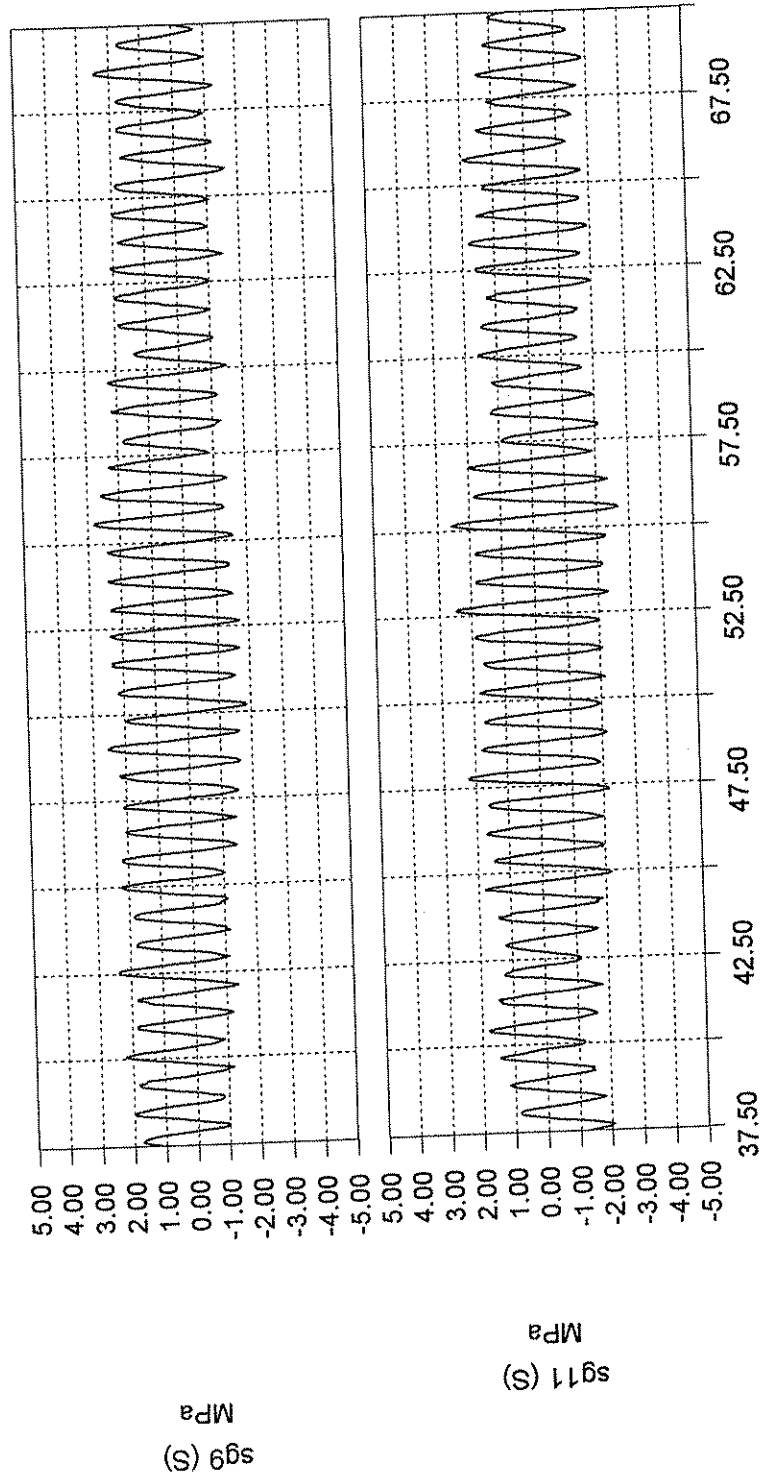


(S) = Parameter Smoothed
D:\NJ_LON~1\TRIG03.IDW

ID-2000

Figure 3-37 Random Data File from Long Term Monitoring.

Typical Column Stress Ranges From
Random Truck Gusts



Time
sec

(S) = Parameter Smoothed
D:\NJ_LON-1\TRIG03.IDW

ID-2000

Figure 3-38 Close Up of Long Term Data.

Typical Column Stress Ranges From
Random Truck Gusts

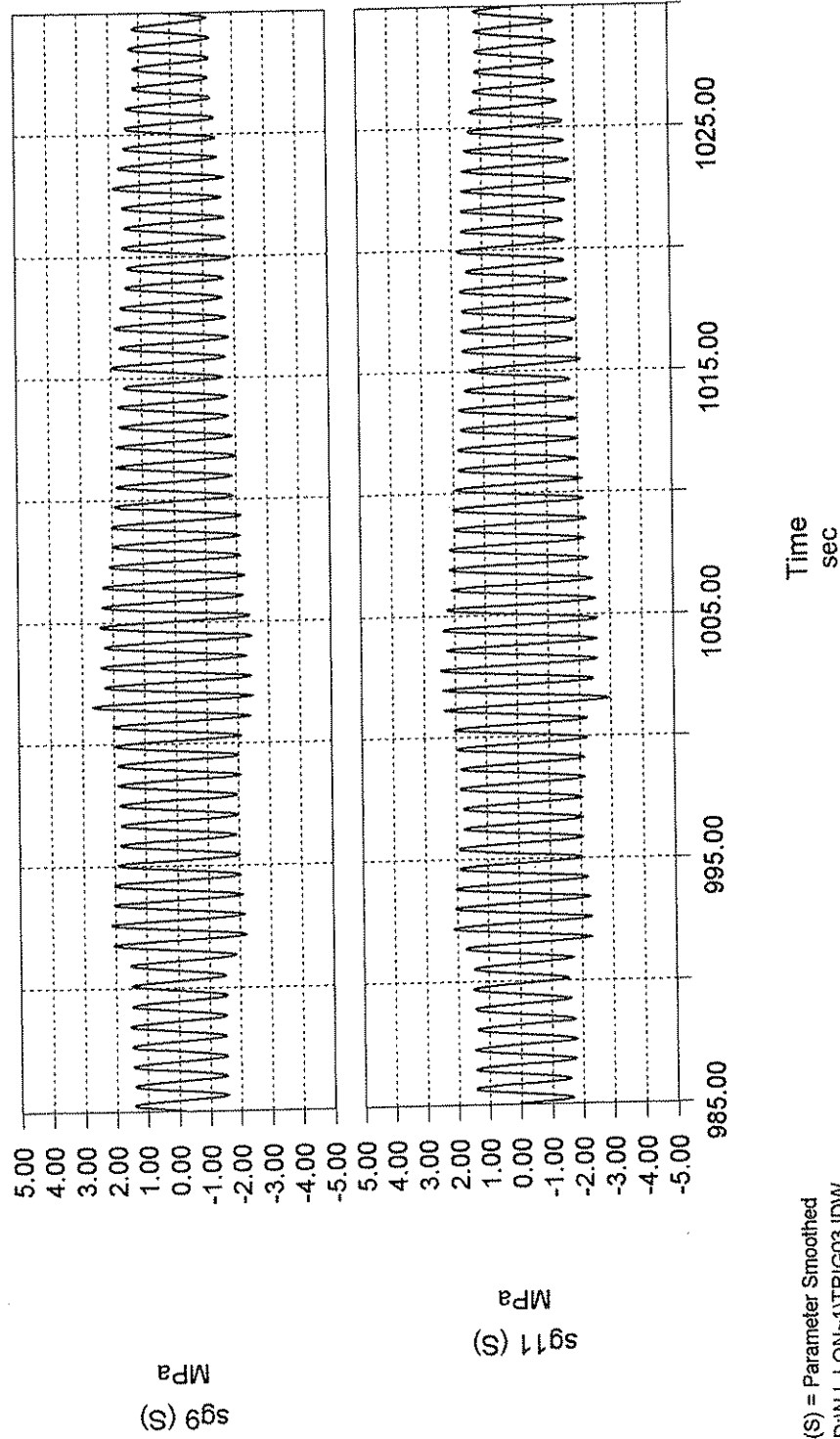
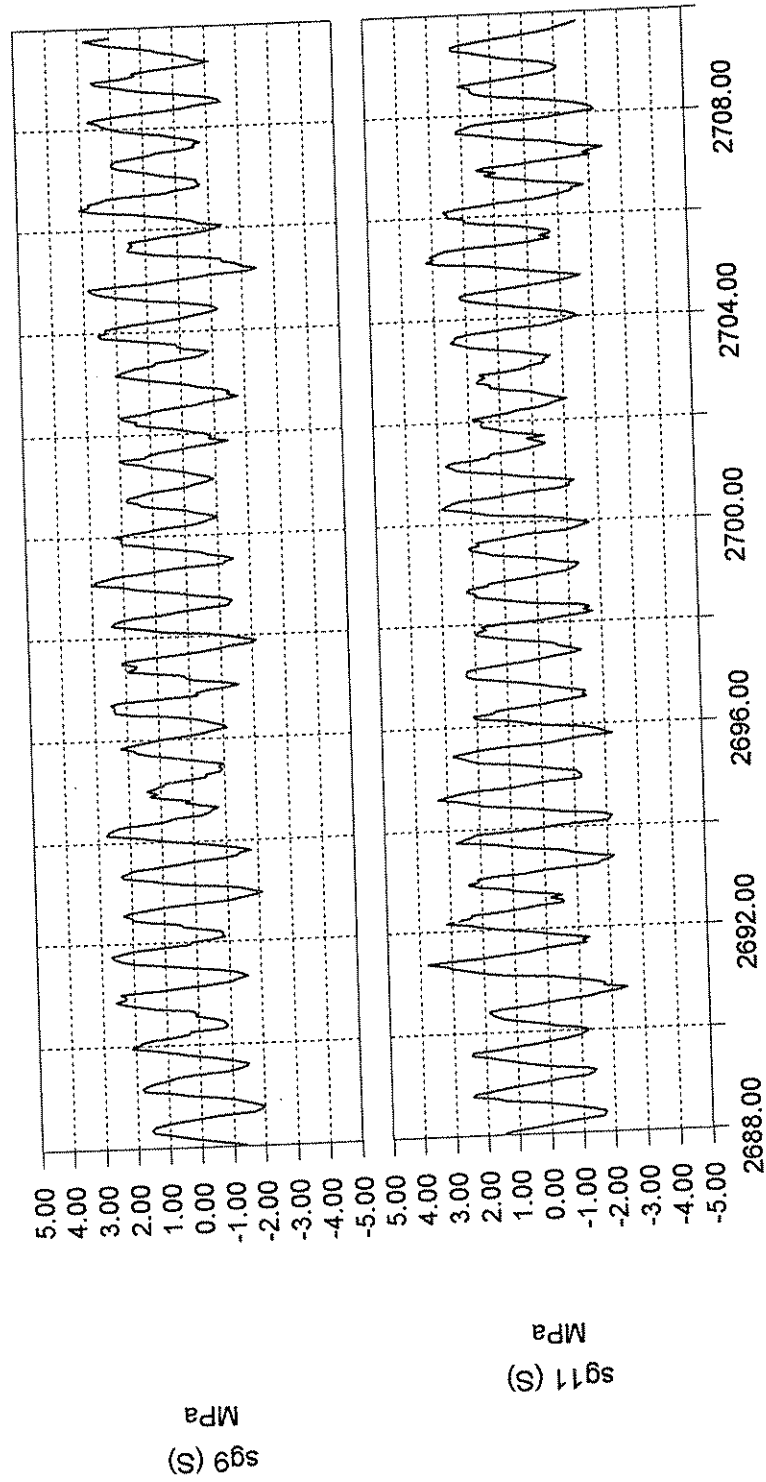


Figure 3-39 Close Up of Long Term Data

Typical Column Stress Ranges From Random Truck Gusts



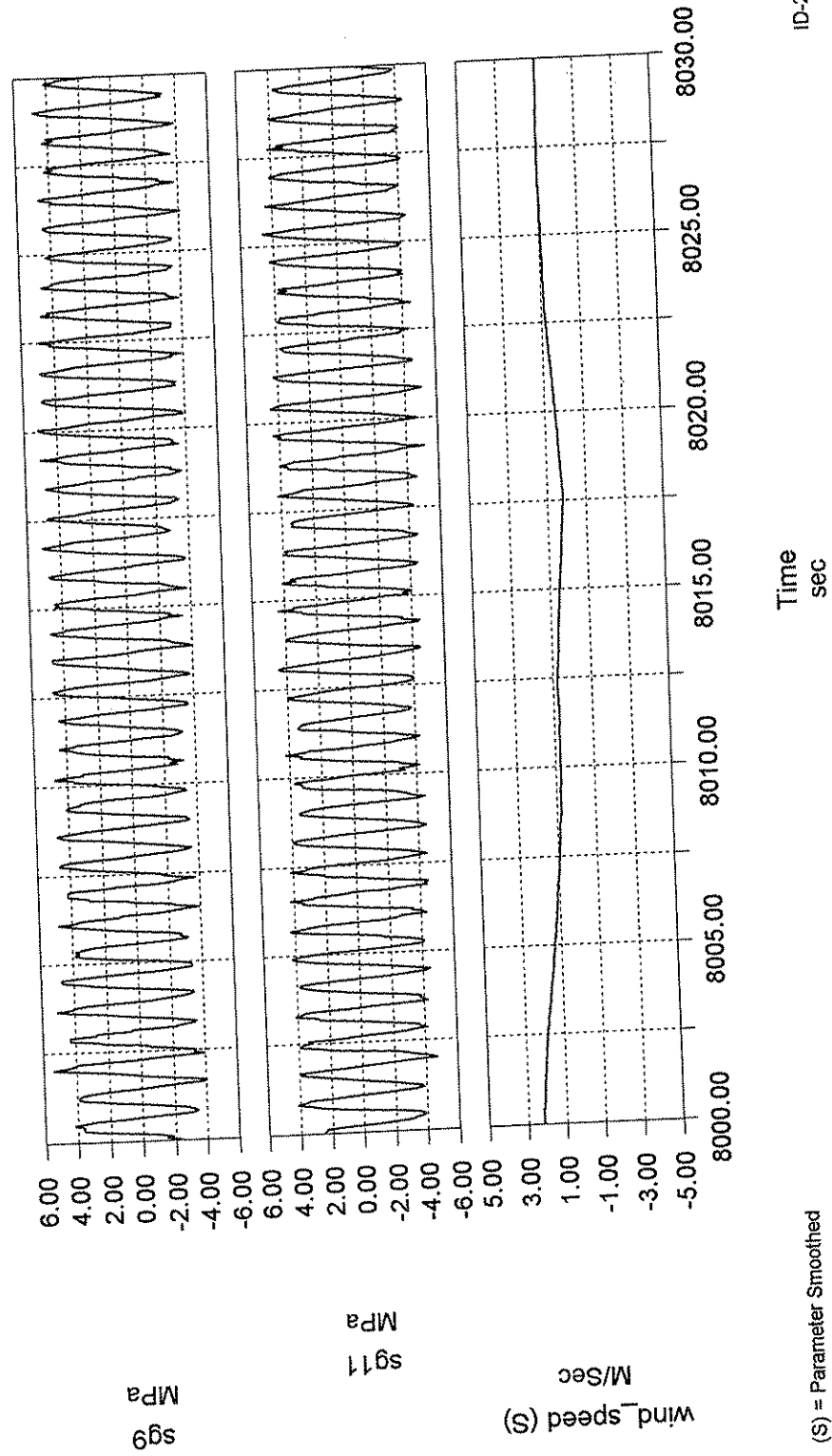
(S) = Parameter Smoothed
D:\NJ_LON-1\TRIG03.IDW

Time
sec

ID-2000

Figure 3-40 Close Up of Long Term Data

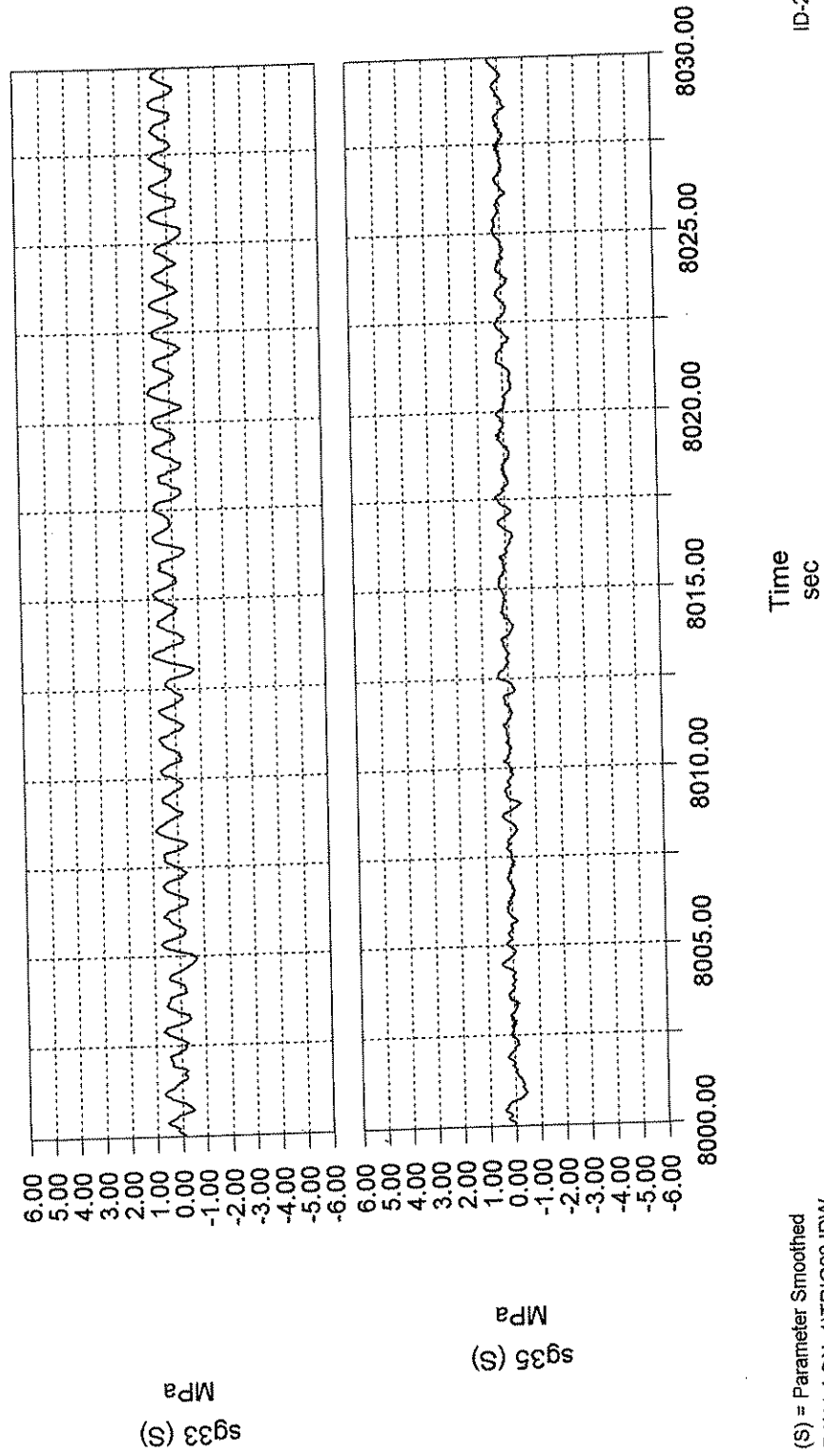
Maximum Recorded Stress Ranges in Column



(S) = Parameter Smoothed
D:\NJ_LON~1\TRIG08.IDW

Figure 3-41 Maximum Recorded Stress Ranges in Column and Natural Wind Speed.

Maximum Recorded Stress Ranges in Top Chord

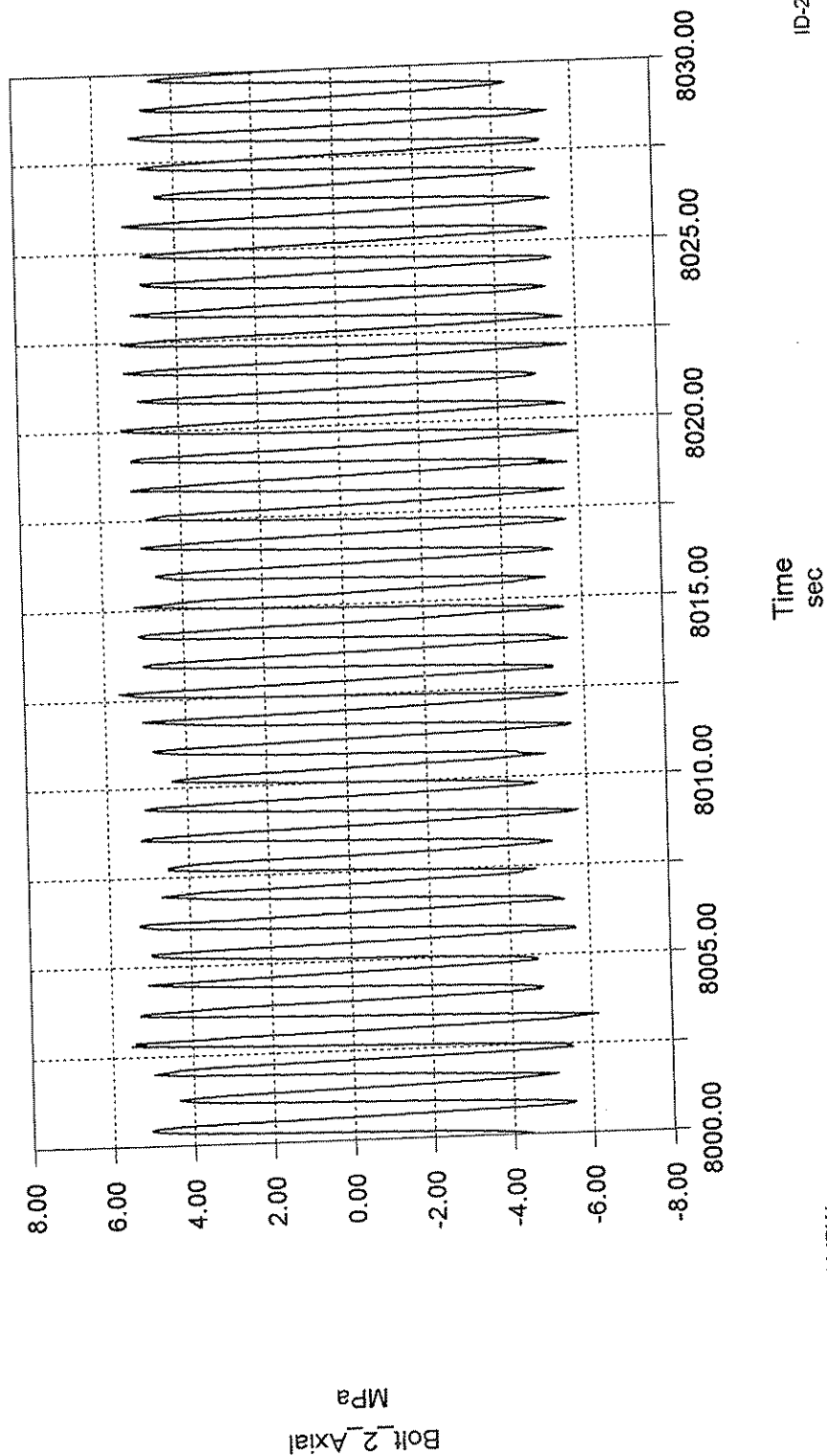


(S) = Parameter Smoothed
D:\NJ_LON~1\TRIG08.IDW

ID-2000

Figure 3-42 Maximum Recorded Stress Ranges in Top Chord.

Maximum Recorded Stress Ranges in Anchor Bolt 2

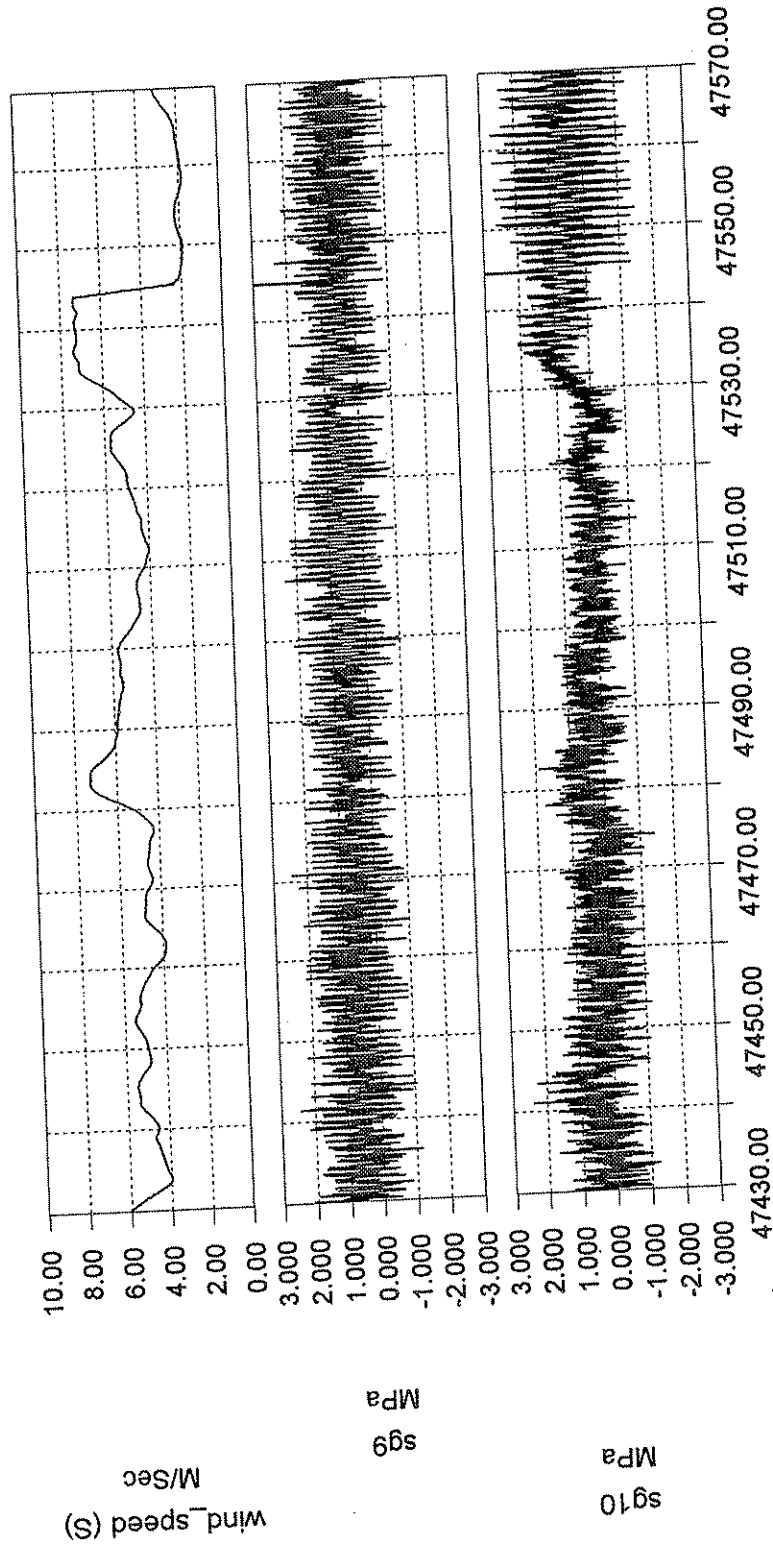


D:\NJ_LON~1\TRIG08.IDW

ID-2000

Figure 3-43 Maximum Recorded Axial Stress Ranges in Anchor Bolts.

Largest Recorded Wind Speed with Column Response



Time
sec

ID-2000

Figure 3-44 Maximum Wind Speed and Column Response.

(S) = Parameter Smoothed
D:\NJ_LON~1\TRIG08.IDW

Chapter 4: Recommendations and Conclusions

4.1 Design Load Recommendations

The results of the research reported herein indicates that the following fatigue design loads should be used for cantilevered VMS sign support structures:

4.1.1 Galloping

The VMS that was instrumented on Interstate 80 did not exhibit any signs of galloping in the three months it was monitored, however data from other studies indicates galloping can be a concern for cantilevered VMS support structures and could be designed for with the following loads.

- Cantilevered sign and signal support structures could be designed for galloping-induced loads using an equivalent static shear pressure range of 1000 Pa (21 psf) which is applied vertically to the vertically-projected area of any sign and/or signal attachments rigidly mounted to the horizontal mast-arm. Equation 4-1 indicates the appropriate pressure from galloping

$$P_G = 1000I_F \quad (\text{Pa}) \quad (4-1)$$

where I_F is the importance factor based on the environment of the VMS.

4.1.2 Truck-Induced Gusts

Truck-induced gusts were measured during the monitoring of the VMS on Interstate 80 and have been determined to be a potential concern for cantilevered VMS support structures. Truck-induced gusts could be designed for with the following loads.

- Sign and signal support structures could be designed for truck-induced gust loads using an equivalent static pressure of "TG" Pa times the drag coefficient, which is applied vertically to the horizontally-projected area of the structural members and any attachments mounted to the horizontal mast-arm along a length of the mast arm which is the greater of the length of the sign or 3.7 m (12 ft). Equation 4-2 indicates the appropriate pressure from truck-induced wind gusts

$$P_{TG} = (TG)C_dI_F \quad (\text{Pa}) \quad (4-2)$$

where TG is the appropriate value from Table 4-1, C_d is the appropriate drag coefficient from table 1.2.5C of the AASHTO specification and I_F is the

importance factor based on the environment of the VMS. There is no lane-load reduction factor to be considered with truck-induced gusts.

Table 4-1: Truck-Induced Gust Values	
Elevation Above Road Surface	Value of "TG"
6 m or less	1760 Pa
6.1 m to 7 m	1530 Pa
7.1 m to 8 m	1150 Pa
8.1 m to 9 m	690 Pa
9.1 m to 10 m	380 Pa
10.1 m or above	0 Pa

4.1.3 Natural Wind Gusts

There were no significant natural-wind gusts that occurred during the monitoring of the VMS on Interstate 80, however data from other studies indicates natural wind gusts can be a concern for cantilevered VMS support structures and could be designed for with the following loads.

- All types of cantilevered sign and luminaire support structures could be designed for natural-wind-gust loads using an equivalent static pressure range of 250 Pa (5.2 psf) times the drag coefficient which is applied horizontally to the horizontally projected area of any exposed portions of the structure and the attachments. Equation 4-3 indicates the appropriate pressure from natural wind gusts

$$P_{NW} = 250C_dI_F \quad (\text{Pa}) \quad (4-3)$$

where C_d is the appropriate drag coefficient from table 1.2.5C of the AASHTO specification and I_F is the importance factor based on the sign environment.

4.2 Conclusions

The following conclusions were drawn from the findings of monitoring the cantilevered VMS on Interstate 80 west bound at mile marker 48.5 in northern New Jersey.

- The recommended design loads from NCHRP 10-38 were modified based on the knowledge obtained in this research. These modified design loads

were recommended for use in the design of cantilevered VMS support structures.

- No substantial changes are needed in the design of the present NJDOT cantilevered support structures to resist the recommended design loads. However, there are five critical locations that require better detailing for this structure to comply with the recommended fatigue design loads (Figure 4-1). The redesigned standards for cantilevered sign support structures, which incorporate the improved fatigue details recommended in NCHRP 10-38 have corrected the five problem areas. As long as the improved fatigue details are properly sized for each structure, there should be no fatigue-related problems at these joints.
- The existing structure can be used at its location on Interstate 80, since the monitoring has proved that this location does not experience the worst-case loading.

Although the measured truck-induced gusts were significantly lower at the 48.5 mile marker of Interstate 48.5 west bound, it does not seem unreasonable to use the design value of 1760 Pa. The displacement of this structure prior to removal from route 17 was consistent with the larger recommended design load range.

Using the above recommended fatigue design loads, there are some details that are currently not adequately designed for fatigue on the structure that was monitored on interstate 80. Better fatigue details that will improve these locations were implemented in the metrification project for overhead and cantilevered sign support structures. Figure 4-1 shows the stress ranges at the critical locations of the sign support structure. The only member that may be required to increase in section size is the column. The current column thickness is 15.9 mm (0.625 in.); there are columns that are used in the metric standards as thick as 22.2 mm (0.875 in.), this column thickness may need to be used for the cantilevered VMS sign support structures. Structural analysis indicates that the truck-induced wind loading is what governs the fatigue design of all the critical details and deflection of this particular sign support structure. The deflection at the tip is 3.03 in.; this is not an excessive amount of deflection and could probably be tolerated.

Based on the field test data and the previous research, it was recommended that the fatigue design load ranges suggested in Project 10-38 be used for design with only slight modification to the truck-induced gusts, as mentioned above. The recommended design value of 1760 Pa for truck-induced gusts is about 3.3 above what was measured on the VMS on interstate 80. Given that there has been at least one cantilevered VMS support structure in Florida, which was reported to have failed due to truck-induced gusts, it is not clear if during the monitoring period the worst case loading was observed. For one thing, the large-amplitude displacements that were observed on Route 17 were not encountered. It could be that the worst case loading occurs when there are significant natural wind gusts acting together with the truck induced wind gusts. Large

natural wind gusts did not occur during the period the structure was monitored. Therefore, it is prudent to stay with the larger design loads recommended in Project 10-38. Furthermore, calculations with the support structure show that even if the value of the design truck-gust pressure were decreased, galloping would probably then control and a lighter structure would probably not result.

4.3 Recommendations for Future Research

Future research that is to be done concerning the long-term monitoring of sign support structures could be benefited by these suggestions.

4.3.1 Power Supply

The power supply that was used for the long-term monitoring was insufficient for the magnitude of monitoring that was to be performed. Two 20-watt solar panels were not adequate to keep the marine batteries charged, even in the middle of summer. Much larger solar panels would be needed to adequately keep the batteries charged. A third battery may even be considered to increase the reserve of power on hand. If this type of monitoring were to be performed in the winter months the economic considerations could become extremely high just for solar panels alone. The best way to be sure of the power supply is to get a reliable source of 120-volt AC power. Use on or two marine batteries as backups incase of power interruptions, but rely on AC power for the main supply.

4.3.2 Communication

The cellular phone communication link was unsuccessful. A higher power transceiver and modem designed for wireless transfer of data needed to be investigated further. Recommendations are being made to use a Sierra Wireless modem. These modems have a 3 watt transceiver built in and are specifically designed for wireless transfer of data.

The size of the files that were being sent was very large for the present technology. Most people consider a one Meg file to be a large file for data transfer through a modem. The data files that needed to be retrieved were in the 40 Meg range. Some modem experimentation performed after the actual testing using LAN lines was only able to transfer data at the rate of around one Meg in 15 minutes. At this rate it would have taken a 10-hour phone call to retrieve the data. If data is to be transferred through modems, measures must be taken to ensure that the communication link is excellent, preferably through a LAN line and that the files are kept small enough to transmit relatively quickly. The longer the call lasts the more the chance of the data transfer being interrupted and corruption of the file occurring.

4.3.3 Pressure Measurements

Pitot tubes were connected to pressure transducers in an attempt to measure truck-induced wind gust pressures. This application of pitot tubes and pressure transducers is not recommended for future research. The pitot tubes should be used in a condition with laminar flow, which is not experienced in the conditions that were tested. The inherent swirling of the air as it comes off the truck and toward the end of the pitot tube make it impossible to get consistent results. If the swirl happens to be directed in an upward path as it just approaches the tip of the tube the results will be favorable, however if the swirl is approaching the tip of the tube at an angle the measurements will be incorrect. As was described in section 3.4, a better approach is to simply back calculate a pressure based on strain gage measurements in the column. This method represents an integration of the truck-gust pressure over the entire soffit area of the VMS box and any attachments instead of just a single point in space. For future pressure measurements it is recommended to rely on the strain gage data and not even install pressure transducers.

4.3.4 Strain Measurements

The strain gage locations that were used on the structure in this project were not located to pick up a lot of the bending in the truss (Figure 3-11). An improved strain gage layout is presented in Figure 4-2. This figure reflects the redesign of the VMS support structures with a tube-to-gusset detail in the truss. The new gage locations should increase the ability to measure the bending components in the truss.

4.3.5 Additional Truck-Gust Measurements

The truck tests that were performed were able to give some data on the truck gust phenomenon, however there was not adequate time to perform enough tests to draw any hard conclusions. The repeatability of the data is easily questionable due to the scant number of times the tests were permitted on that day. Additional truck tests could be performed in a different manner. Instead of hiring trucks to drive under the sign with lanes closed specifically for them, use trucks that are in the regular traffic flow. During non-rush hour traffic the trucks were able to obtain reasonably high speeds and cause significant gusting. By recording the truck's speed, which lane it is in and the shape of the truck additional conclusions could possibly be made on this phenomenon. By doing this additional testing on several different occasions the probability of getting a day with significant head winds on the truck is increased. The synergetic effect of a high head wind are not well known at this time and is part of the reason for a high factor of safety on the truck-induced gust design pressure.

4.3.6 Wind Induced Vibrations

This project was carried out in the summer months, which are not typically the months of strong winds in northern New Jersey. Future research should consider the fact that the strongest winds in northern New Jersey are typically in the winter and spring. Historical wind records from nearby weather stations and airports should be able to help confirm the best times of year to monitor wind data in this area. These records will also indicate the predominant direction of the winds. Future structures that are monitored should be oriented perpendicular to the direction of wind flow. The best situation would be to have the natural wind gusts be a head wind for traffic. This would help to better quantify the synergetic effects of natural wind gusts and truck-induced gusts.

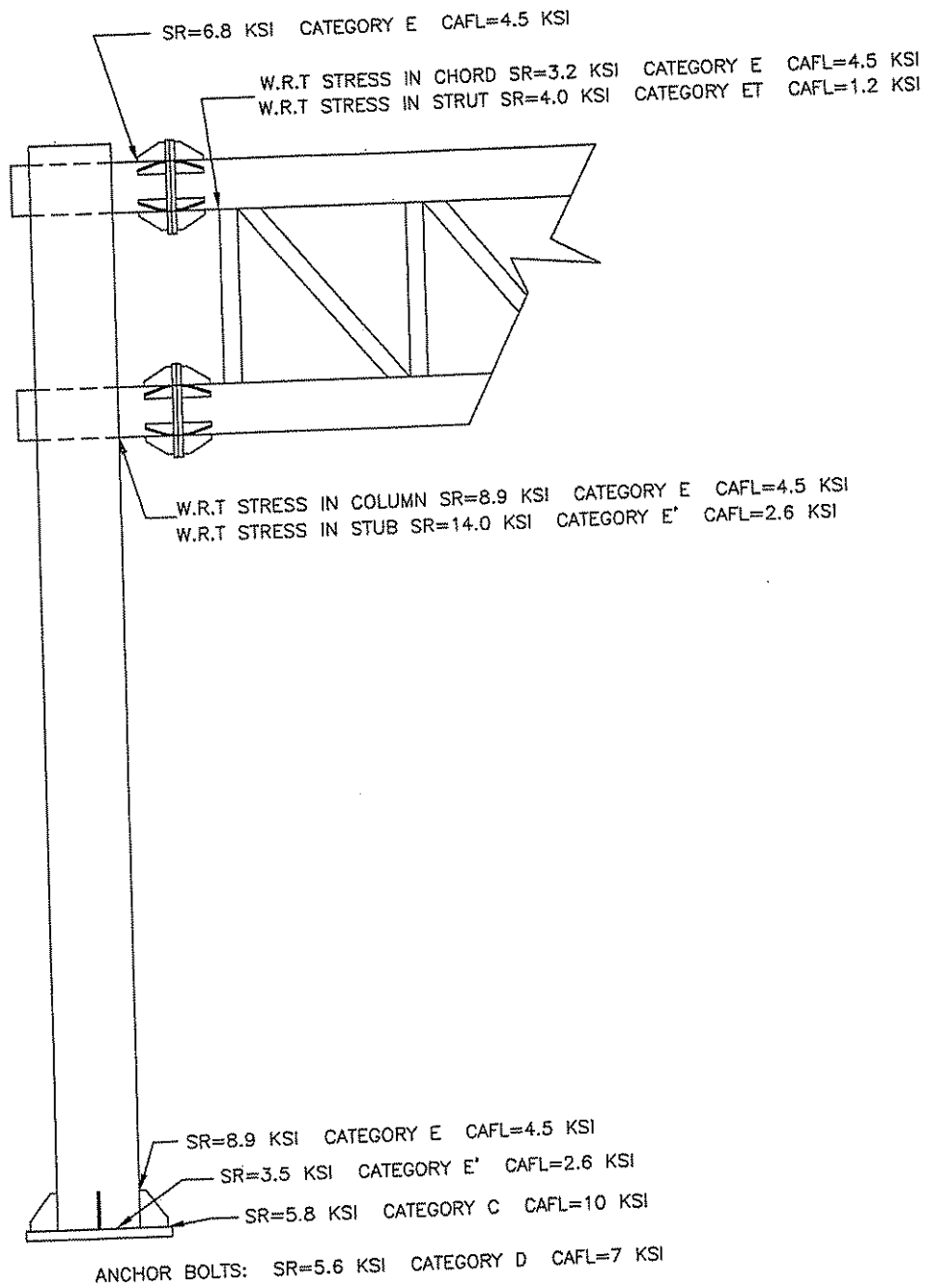


Figure 4-1 Critical Location Stress Ranges on I-80 Structure.

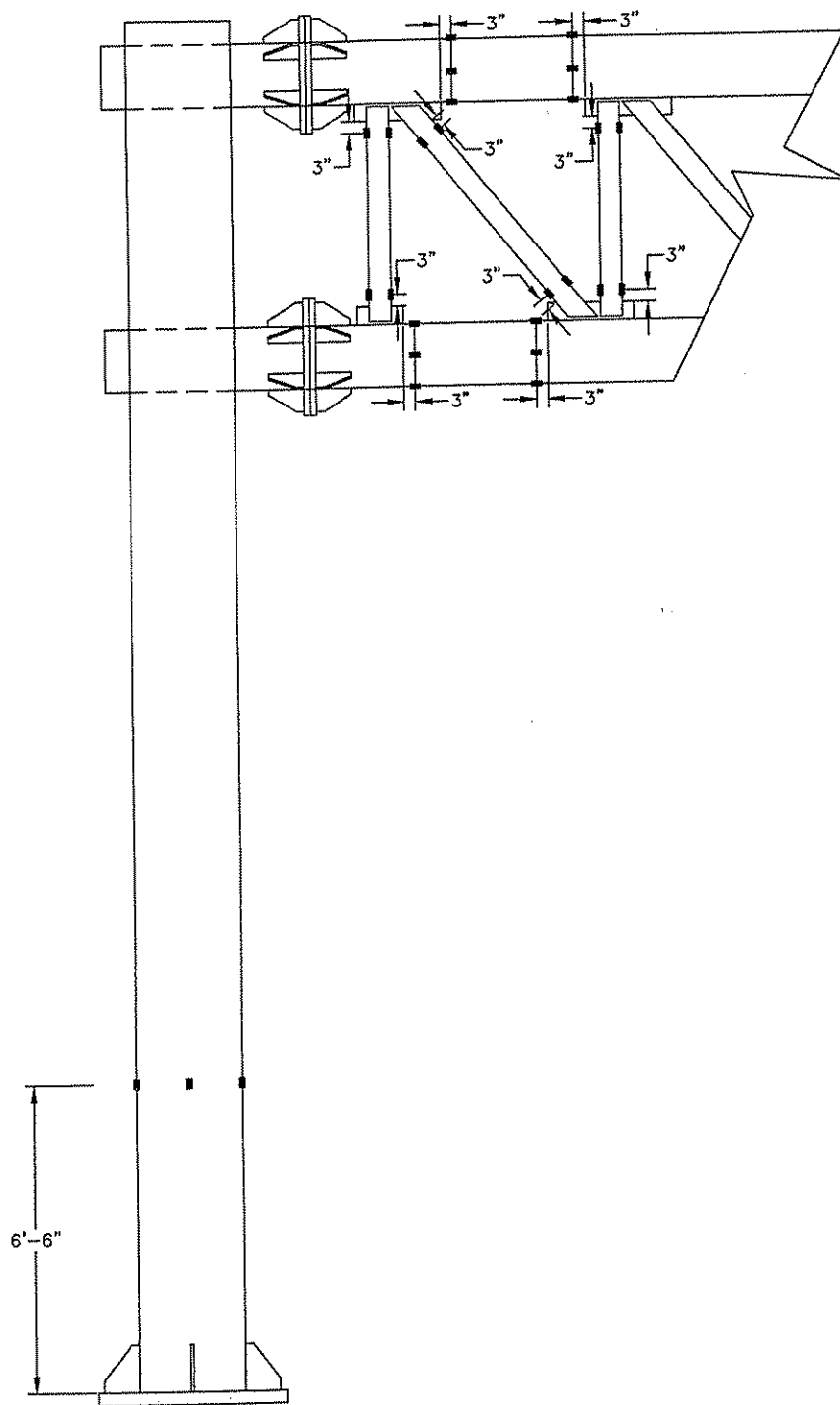


Figure 4-2 Improved Strain Gage Layout for Future Monitoring.

References

1. Irwin, H. P., Peeters, M. An Investigation of the Aerodynamic Stability of Slender Sign Bridges, Calgary, National Research Council Canada, National Aeronautical Establishment, July 1980.
2. Novak, M., "areoelastic Galloping of Prismatic Bodies," Journal of the Engineering Mechanics Division, ASCE, Vol. 95, No. EM1, 1969.
3. Den Hartog, J.P., Mechanical Vibrations, Fourth Edition, McGraw-Hill, New York, NY, 1956.
4. Novak, M., "Galloping Oscillations of Prismatic Structures," Journal of the Engineering Mechanics Division, ASCE, Vol. 98, No. EM1, 1972.
5. McDonald, J.R., et al., Wind Load Effects on Signals, Luminaires and Traffic Signal Structures, Report 1303-1F, Wind Engineering Research Center, Texas Tech University, Lubbock, TX, 1995.
6. Kaczinski, M.R., et al., Fatigue-Resistance Design of Cantilevered Signal, Sign, and Light Supports, National Cooperative Highway Research Program, Final Report - NCHRP Project 10-38, Transportation Research Board, Washington D.C., 1996.
7. Davenport, A.G., The Spectrum of Horizontal Gustiness Near the Ground in High Winds, Quarterly Journal, Royal Meteorological Society Vol. 87, London 1961.
8. Lundquist, R.C., et al., Aerodynamically Induced Stresses in Traffic Signals and Luminaire Supports, Mechanics Research Report MRI-TR-2430-1, Bridge Department, California Division of Highways, 1972.
9. Liu, H., Wind Engineering - A Handbook for Structural Engineers, Prentice Hall, Englewood Cliffs, NJ, 1991.
10. Simiu E., et al., Wind Effects on Structures: An Introduction to Wind Engineering, John Wiley & Sons, NY, 1996.
11. Cook, R.A., et al., Wind Load Data for Variable Message Signs, Florida Department of Transportation, Final Project Report - State Study No. 0728, April 1996.

12. Cali, P.M., Interim Report on the Effects of Truck Induced Gusts on Overhead Highway Sign Structures, Report 110-79-2, Center for Transportation Engineering Studies, North Carolina State University at Raleigh, Raleigh, NC, 1984.
13. Creamer, B.M., Frank, K.H. and Klingner, R.E., Fatigue Loading of Cantilever Sign Structures from Truck Wind Gusts, Report No. FHWA/tx-79/10+209-1f, Center for Highway Research, University of Texas, Austin, 1979.
14. Edwards, J.A., et al., Deflection Criteria for Wind-Induced Vibrations in Cantilever Highway Sign Structures, Report 110-79-2, Center for Transportation Engineering Studies, North Carolina State University at Raleigh, Raleigh, NC, 1984.
15. McCrum, R.L. (Michigan DoT) , Letter report to M. Kaczinski of Lehigh University dated December 22, 1993.
16. DeSantis, P.V. and Haig, P., "Unanticipated Loading Causes Highway Sign Failure," Proceedings of ANSYS Convention, 1996.
17. "Winds Blow I-15 Sign Down," Engineering News Record, December 11, 1995.
18. Dexter, R. J. and Fisher J. W., Fatigue and Fracture – Chapter 8, Steel Design Handbook LRFD Method, Tamboli, A. R. (ed.), McGraw Hill, 1997.
19. Research Council on Structural Connections, Specifications for Structural Joints Using ASTM A325 or A490 Bolts, RCSC, 1996.
20. ENV 1993-1-1, "Eurocode 3: Design of Steel Structures-Part 1.1: General Rules and Rules for Buildings", European Committee for Standardization (CEN), Brussels, April 1992.
21. Dexter R. J., and Fisher J. W., Fatigue and Fracture - Chapter 24, Handbook of Structural Engineering, Chen, W. S. (ed.), CRC Press LLC, Boca Raton, FL, 1997.

Appendix A – Fatigue Design Load Application

1. General

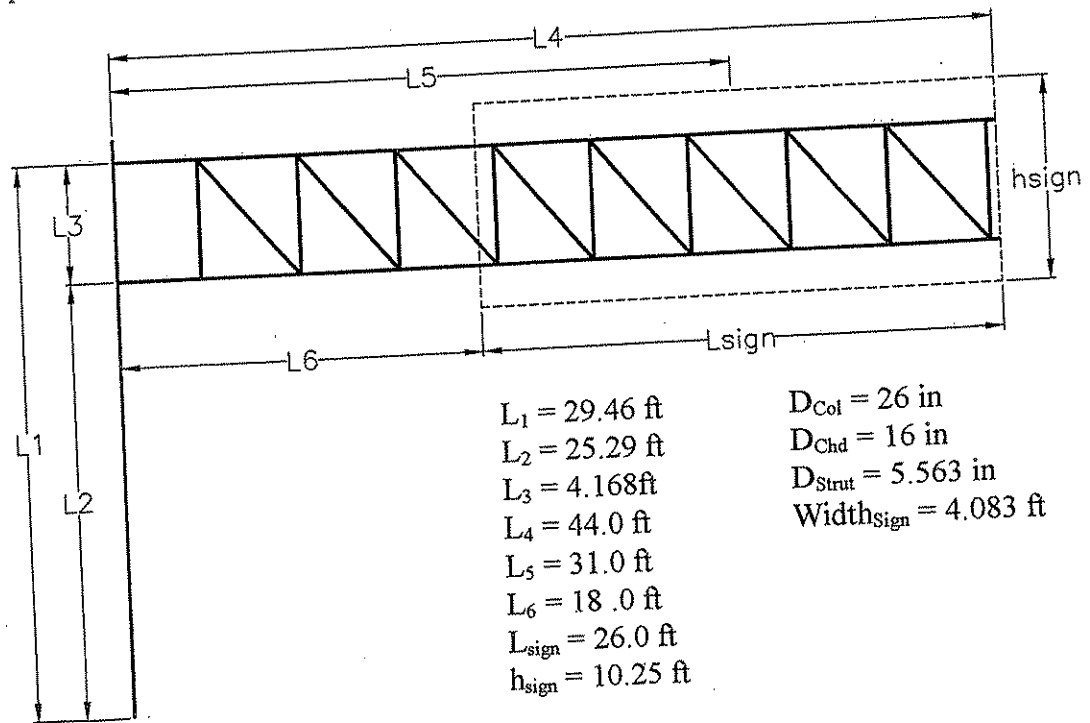
The following appendix details select, necessary calculations that need to be performed on cantilevered VMS sign support structures in order to evaluate their fatigue strength.

1.1 Description

The structure in this appendix is the one that was instrumented on Interstate 80, mile-marker 48.5, westbound, in northern New Jersey. The sign was checked for fatigue sensitive areas based on the loads recommended in this report and Section 1.9.6 of the AASHTO Specifications. Because the structure is over an interstate highway, the importance factor is 1 in all calculations (Table 1.9.6.1 AASHTO). Because the structure was originally designed using English units all calculations are performed in English units.

1.2 Dimensions

The following dimensions represent the centerline measurements for the VMS sign support structure that was monitored in New Jersey.



2. Calculations of Limit State Fatigue Loads

This section illustrates the application of the three wind loading phenomena that are applicable to a cantilevered VMS sign support structures, i.e. natural wind gusts, galloping, and truck-induced wind gusts.

2.1 Galloping

The support structure is checked using the equivalent static shear pressure range of 21 psf for galloping

$$P_G = 21I_F = (21)(1.0) = 21 \text{ psf}$$

where I_F is the importance factor.

The frontal area of the sign projected on a vertical plane is calculated by:

$$A_{\text{Front}} = L_{\text{sign}}h_{\text{sign}} = (10.25 \text{ ft})(26 \text{ ft}) = 266.5 \text{ ft}^2$$

The equivalent static shear load range to be applied to the face of the sign is calculated by:

$$F_G = P_G A_{\text{Front}} = (21 \text{ psf})(266.5 \text{ ft}^2) = 5.6 \text{ kips}$$

2.2 Natural Wind Gusts

Because there were no significant wind events that occurred during the monitoring of this structure it is assumed that the annual mean wind velocity is 5 m/s at the location of the sign. The structure is checked using the equivalent static pressure range of 5.2 psf times the drag coefficient for natural wind gusts

$$P_{\text{NW}} = 5.2C_dI_F$$

where C_d is the appropriate drag coefficient from table 1.2.5C of the AASHTO Specification. The pressures for the different components of the structure are calculated by:

Sign

$$(P_{\text{NW}})_{\text{Sign}} = (5.2)(1.19)(1.0) = 6.19 \text{ psf}$$

where 1.19 is the appropriate C_d for this geometry of sign.

Tubes

$$(P_{NW})_{Tube} = (5.2)(1.10)(1.0) = 5.72 \text{ psf}$$

where 1.10 is the appropriate C_d for a tube.

The areas of the different components of the structure are calculated by:

$$A_{Front} = L_{Sign}h_{Sign} = (10.25 \text{ ft})(26 \text{ ft}) = 266.5 \text{ ft}^2$$

$$A_{Chord} = L_{\phi}D_{Chd} = (18 \text{ ft})(16 \text{ in}) = 24 \text{ ft}^2 \text{ per chord}$$

$$A_{Strut} = L_{Strut}D_{Strut} = (7.75 \text{ ft})(5.563 \text{ in}) = 3.6 \text{ ft}^2 \text{ per strut}$$

$$A_{Col} = L_1D_{Col} = (29.46 \text{ ft})(26 \text{ in}) = 63.83 \text{ ft}^2$$

The equivalent static load range applied to the sign is calculated by:

$$(F_{NW})_{Sign} = (P_{NW})_{Sign}A_{Front} = (6.19 \text{ psf})(266.5 \text{ ft}^2) = 1.7 \text{ kips}$$

$$(F_{NW})_{Chd} = (P_{NW})_{Tube}A_{Chd} = (5.72 \text{ psf})(24 \text{ ft}^2) = 0.14 \text{ kips per chord}$$

$$(F_{NW})_{Strut} = (P_{NW})_{Tube}A_{Strut} = (5.72 \text{ psf})(3.6 \text{ ft}^2) = 0.02 \text{ kips per strut}$$

$$(F_{NW})_{Col} = (P_{NW})_{Tube}A_{Col} = (5.72 \text{ psf})(63.83 \text{ ft}^2) = 0.365 \text{ kips}$$

2.3 Truck Gusts

The support structure is checked using the equivalent static pressure range of 36.6 psf for truck-induced wind gusts

$$P_{TG} = 36.6C_dI_F$$

where C_d is the appropriate drag coefficient from table 1.2.5C of the AASHTO Specification. The pressures for the different components of the structure are calculated by:

Sign

$$(P_{TG})_{Sign} = (36.6)(1.45)(1.0) = 43.55 \text{ psf}$$

where 1.19 is the appropriate C_d for this geometry of sign.

Tubes

$$(P_{TG})_{Tube} = (36.6)(1.10)(1.0) = 40.26 \text{ psf}$$

where 1.10 is the appropriate C_d for a tube.

The areas of the different components of the structure are calculated by:

$$A_{Soffit} = L_{Sign} \text{Width}_{Sign} = (26 \text{ ft})(4.083 \text{ ft}) = 106.2 \text{ ft}^2$$

$$A_{Chord} = *L_{Sign}D_{Chord} = (26 \text{ ft})(16 \text{ in}) = 34.67 \text{ ft}^2 \text{ per chord}$$

* Only the length of the chord above the traffic lanes is used in this calculation. In this case that length is also the length of the sign.

The equivalent static load range applied to the sign is calculated by:

$$(F_{TG})_{Sign} = (P_{TG})_{Sign}A_{Soffit} = (43.55 \text{ psf})(106.2 \text{ ft}^2) = 5.64 \text{ kips}$$

$$**(F_{TG})_{Chord} = (P_{TG})_{Tube}A_{Chord} = (40.26 \text{ psf})(34.67 \text{ ft}^2) = 1.4 \text{ kips per chord}$$

** Only apply this force to the bottom chord.

3. Bending Moment Calculations

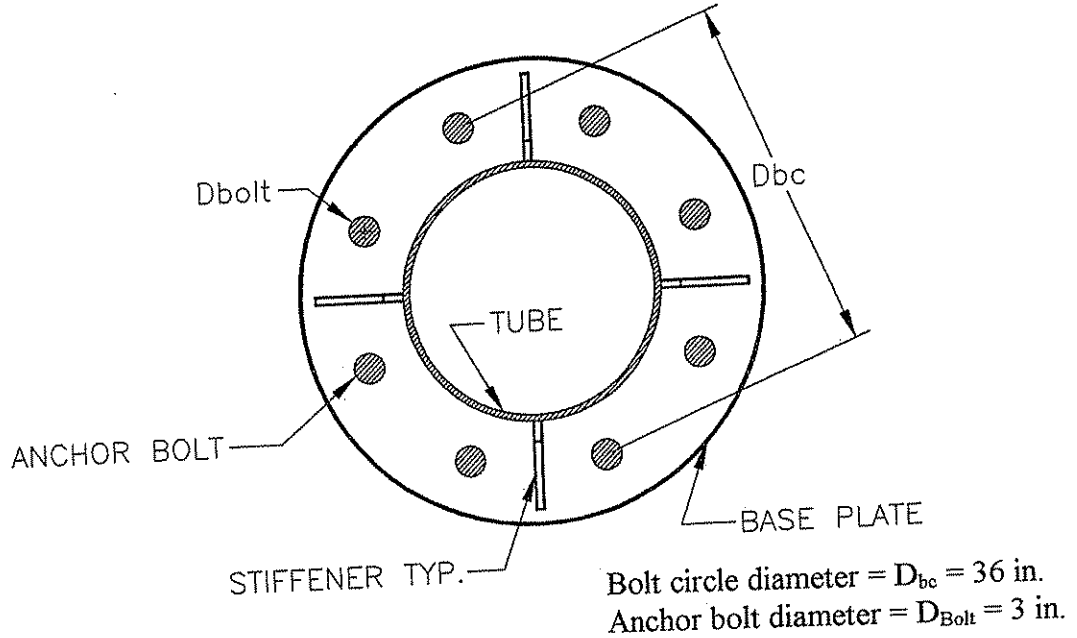
All bending moment calculations are performed using a simple first order analysis. The load case that gives the worst case bending moment at all critical locations is truck-induced wind gusts.

4. Stress Range Calculations

The stress ranges for all fatigue sensitive locations are checked in this section.

4.1 Anchor Bolts

Details of the anchor bolt group are provided below:



4.1.1 Moment of Inertia of the Bolt Group

The centroidal distance to each of the anchor bolts is calculated by:

$$\bar{x}_1 = \left(\frac{D_{bc}}{2}\right)(\cos 22.5^\circ) = \left(\frac{36in}{2}\right)(0.9239) = 16.63in$$

$$\bar{x}_2 = \left(\frac{D_{bc}}{2}\right)(\sin 22.5^\circ) = \left(\frac{36in}{2}\right)(0.3827) = 6.89in$$

The tensile area of each anchor bolt is calculated by:

$$A_T = \frac{\pi}{4} \left(D_{Bolt} - \frac{0.9743}{n} \right)^2 = \frac{\pi}{4} \left(3in - \frac{0.9743}{13} \right)^2 = 6.72in^2$$

where A_T is the tensile area of each bolt, D_{Bolt} is the diameter of a single bolt, and n is the number of threads per inch.

The moment of inertia of the bolt group is calculated by:

$$I_b = \sum A_T \bar{x}^2 = 4[(6.72 \text{ in}^2)(6.89 \text{ in})^2] + 4[(6.72 \text{ in}^2)(16.63 \text{ in})^2] = 8709.9 \text{ in}^4$$

4.1.2 Anchor Bolt Stress Range

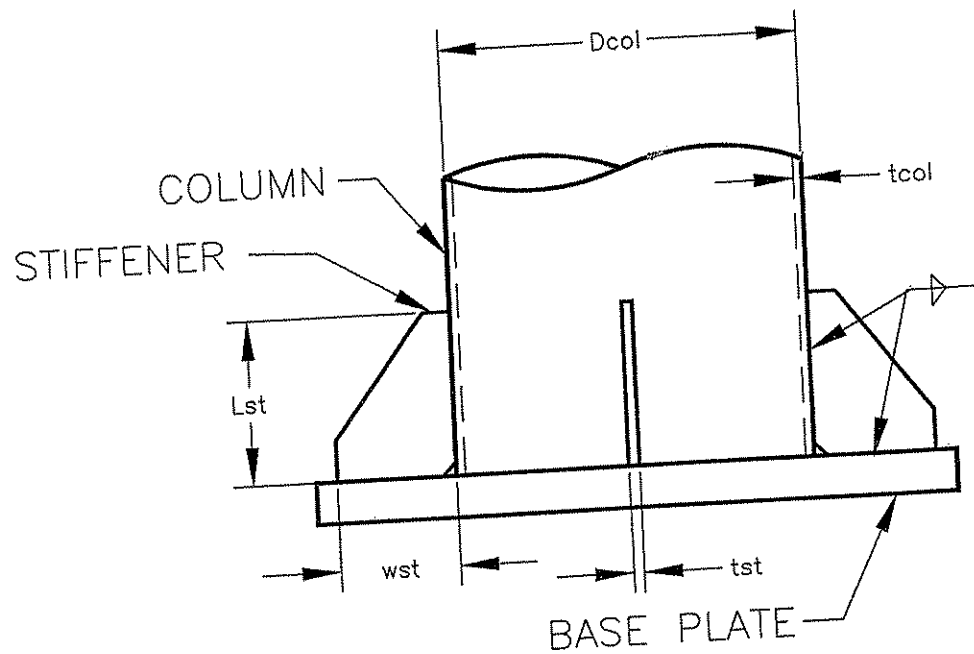
Based on the calculations of section 3 truck-induced gusts control the design of the anchor bolts. The axial stress range in each anchor bolt is calculated by:

$$(S_R)_{Bolt} = \frac{(M_z)_{TG} c}{I_b} = \frac{(228 \text{ kft})(12 \text{ in/ft})(18 \text{ in})}{8709.9 \text{ in}^4} = 5.6 \text{ ksi}$$

Anchor bolts are classified as a category D detail. The corresponding CAFL is 7 ksi. Since the calculated stress range (5.6 ksi) is less than the CAFL (7 ksi) the anchor bolts are adequately designed for fatigue.

4.2 Column to base plate connection

Details of the column to base plate connection are given below.



Column diameter = $D_{Col} = 26 \text{ in}$
 Column thickness = $t_{Col} = 0.625 \text{ in}$
 Stiffener length = $L_{st} = 12 \text{ in}$
 Stiffener width = $w_{st} = 8.75 \text{ in}$
 Stiffener thickness = $t_{st} = 0.75 \text{ in}$

4.2.1 Moment of Inertia

The moment of inertia of the column is calculated by:

$$I_{Col} = \frac{\pi}{64} [D_{Col}^4 - (D_{Col} - 2t_{Col})^4] = \frac{\pi}{64} [(26in)^4 - (26in - 2 * 0.625in)^4] = 4012.6in^4$$

The area of the stiffener is calculated by:

$$A_{st} = w_{st}t_{st} = (8.75 in)(0.75 in) = 6.563 in^2$$

The centroidal distance to each stiffener is calculated by:

$$\bar{x} = \frac{D_{Col}}{2} + \frac{w_{st}}{2} = \frac{36in}{2} + \frac{8.75in}{2} = 21.75in$$

The moment of inertia of the column base is calculated by:

$$*I_{cb} = I_{Col} + \sum A_{st} \bar{x}^2 = 4012.6 in^4 + 2(6.563 in^2)(21.75 in^2) = 10221.5 in^4$$

*Note that the moment of inertia of the individual stiffeners is ignored in the calculation of the moment of inertia at the column to baseplate connection.

4.2.2 Stress Range at Column to Baseplate Connection

Based on the calculations in section 3 truck-induced wind gusts control the column to baseplate connection. The stress range at the column to baseplate connection was calculated by:

$$(S_R)_{Col-BP} = \frac{(M_Z)_{TG} c}{I_{cb}} = \frac{(228kft)(12in / ft)(13in)}{10221.5in^4} = 3.5ksi$$

The column was fillet welded to the base plate and was therefore a category E' detail. The corresponding CAFL was 2.6 ksi. Since the calculated stress range (3.5 ksi) was greater than the CAFL (2.6 ksi) the column to baseplate connection was inadequately designed for fatigue.

4.3 Stiffener to Baseplate Connection

The details of the stiffener to baseplate connection are the same as those given in section 4.2 Column to Baseplate Connection and will not be repeated here.

4.3.1 Moment of Inertia

The moment of inertia of the column base was calculated in section 4.2.1, only the result is repeated here.

$$I_{cb} = 10221.5 \text{ in}^4$$

4.3.2 Stress Range at Stiffener to Baseplate Connection

Based on the calculations in section 3 truck-induced wind gusts control the stiffener to baseplate connection. The stress range at the stiffener to baseplate connection was calculated by:

$$(S_R)_{st-BP} = \frac{(M_Z)_{TG} c}{I_{cb}} = \frac{(228 \text{ kft})(12 \text{ in / ft})(21.75 \text{ in})}{10221.5 \text{ in}^4} = 5.8 \text{ ksi}$$

According to AASHTO page 6-28 the CAFL of this connection is based on the thickness of the stiffener. The CAFL is dependent upon the thickness of the plates:

If $t_{st} > .5$ in then the fatigue strength is the lesser of ΔF_n or the CAFL for a category C detail i.e. 10 ksi. ΔF_n is calculated by:

$$\Delta F_n = \Delta F_n^C \left(\frac{0.06 + 0.79 \left(\frac{H}{t_{st}} \right)}{1.1 t_{st}^{\frac{1}{6}}} \right) = 10 \text{ ksi} \left(\frac{0.06 + 0.79 \left(\frac{1.25 \text{ in}}{0.75 \text{ in}} \right)}{(1.1)(0.75 \text{ in})^{\frac{1}{6}}} \right) = 13.13 \text{ ksi}$$

where ΔF_n is the modified fatigue strength, ΔF_n^C is the CAFL for a category C detail, H is the effective weld throat, and t_{st} is the stiffener thickness.

The stiffener to baseplate connection is a category C detail. By the results of the above calculations there is no reduction in fatigue strength for this particular detail. The corresponding CAFL is 10 ksi. Since the calculated stress range (5.8 ksi) is less than the CAFL (10 ksi) the stiffener to baseplate connection is adequately designed for fatigue.

4.4 Top of Stiffeners

The details of the top of stiffener to column connection were shown in section 4.2 and will not be repeated here.

4.4.1 Moment of Inertia

The moment of inertia at the top of the stiffeners is the moment of inertia of the column and is calculated by:

$$I_{Col} = \frac{\pi}{64} [D_{Col}^4 - (D_{Col} - 2t_{Col})^4] = \frac{\pi}{64} [(26in)^4 - (26in - 2 * 0.625in)^4] = 4012.6in^4$$

4.4.2 Stress Range at Tops of Stiffeners

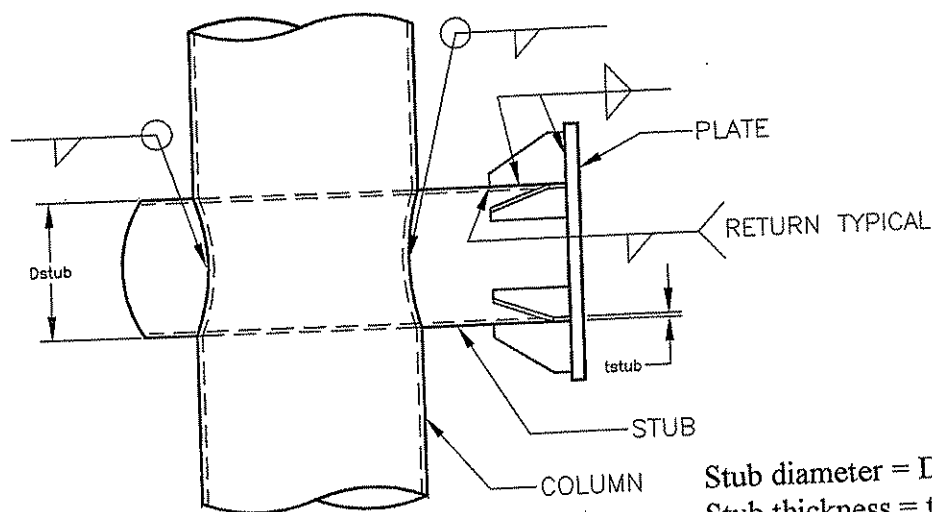
Based on the calculations in section 3 truck-induced wind gusts control the top of stiffener to column connection. The stress range at the top of stiffener to column connection is calculated by:

$$(S_R)_{st-Col} = \frac{(M_z)_{TG} c}{I_{Col}} = \frac{(228kft)(12in/ft)(13in)}{4012.6in^4} = 8.9ksi$$

The top of stiffener to column connection is a category E detail. The corresponding CAFL is 4.5 ksi. Since the calculated stress range (8.9 ksi) is greater than the CAFL (4.5 ksi) the column to base plate connection is inadequately designed for fatigue.

4.5 Column to Stub Connection

The details of the column to stub connection are given below. Because both of the members in the connection are subject to loads the detail must be checked with respect to the stress in each member.



4.5.1 With Respect to Stress in Column

The following calculations determine the fatigue strength of the column to stub connection with respect to the stress in the column.

4.5.1.1 Moment of Inertia

With respect to the stress in the column the moment of inertia needed is that of the column. The column's moment of inertia is calculated in section 4.2.1; therefore, only the result is shown here.

$$I_{Col} = 4012.6 \text{ in}^4$$

4.5.1.2 Stress Range in Column

Based on the calculations in section 3 truck-induced wind gusts control the column to stub connection. The stress range in the column is calculated by:

$$(S_R)_{Col-stub} = \frac{(M_Z)_{TG} c}{I_{Col}} = \frac{(228 \text{ kft})(12 \text{ in / ft})(13 \text{ in})}{4012.6 \text{ in}^4} = 8.9 \text{ ksi}$$

With respect to the stress in the column the column to stub connection is a category E detail. The corresponding CAFL is 4.5 ksi. Since the calculated stress range (8.9 ksi) is greater than the CAFL (4.5 ksi) the column to stub connection is inadequately designed for fatigue.

4.5.2 With Respect to Stress in Stub

The following calculations determine the fatigue strength of the column to stub connection with respect to the stress in the stub.

4.5.2.1 Moment of Inertia and Area

The moment of inertia and area of the stub are respectively calculated by:

$$I_{stub} = \frac{\pi}{64} [D_{stub}^4 - (D_{stub} - 2t_{stub})^4] = \frac{\pi}{64} [(16 \text{ in})^4 - (16 \text{ in} - 2 * 0.5 \text{ in})^4] = 732.0 \text{ in}^4$$

$$A_{stub} = \frac{\pi}{4} [D_{stub}^2 - (D_{stub} - 2t_{stub})^2] = \frac{\pi}{4} [(16 \text{ in})^2 - (16 \text{ in} - 2 * 0.5 \text{ in})^2] = 24.35 \text{ in}^2$$

4.5.2.2 Stress Range in Stub at Column Face

Based on the calculations in section 3 truck-induced wind gusts control the column to stub connection. The stress range in the stub is calculated by:

$$(S_R)_{stub-Col} = \frac{Axial_{TG}}{A_{stub}} + \frac{(M_z)_{TG}c}{I_{stub}} = \frac{31.7k}{24.35in^2} + \frac{(48.5kft)(12in/ft)(8in)}{732.0in^4} = 14.0ksi$$

With respect to the stress in the stub, the column to stub connection is a category E' detail. The corresponding CAFL is 2.6 ksi. Since the calculated stress range (14.0 ksi) is greater than the CAFL (2.6 ksi) the column to stub connection is inadequately designed for fatigue.

4.6 End of Stiffener on Stub

The details of the end of the stiffener on the stub are shown in section 4.5 above.

4.6.1 Moment of Inertia and Area

The moment of inertia and area of the stub were calculated in section 4.5.2.1 and therefore only their respective values are given here.

$$I_{stub} = 732.0 \text{ in}^4$$

$$A_{stub} = 24.35 \text{ in}^2$$

4.6.2 Stress Range at End of Stiffener on Stub

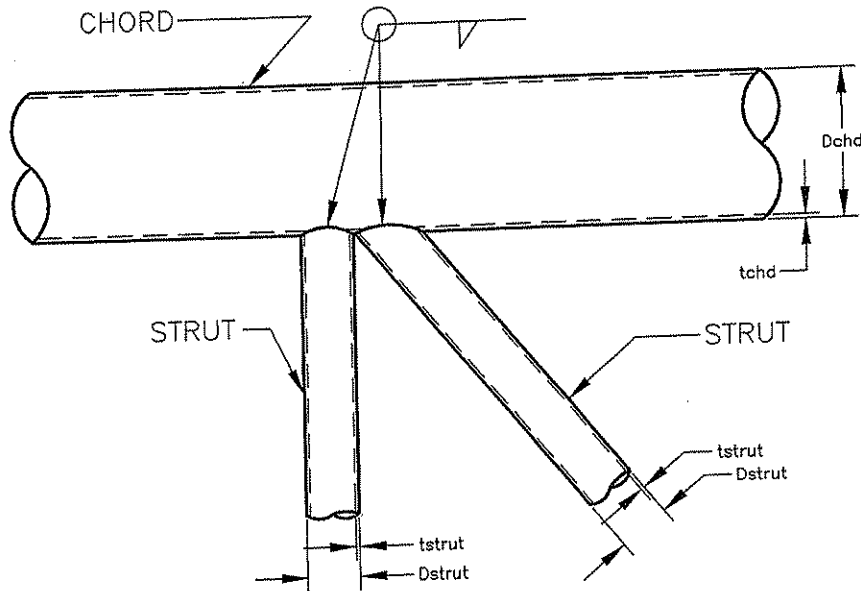
Based on the calculations in section 3 truck-induced wind gusts control the end of stiffener to stub connection. The stress range in the stub at the end of the stiffener is calculated by:

$$(S_R)_{stub-st} = \frac{Axial_{TG}}{A_{stub}} + \frac{(M_z)_{TG}c}{I_{stub}} = \frac{31.7k}{24.35in^2} + \frac{(20.84kft)(12in/ft)(8in)}{732.0in^4} = 6.8ksi$$

Because the stiffener is greater than four inches the connection is a category E detail. The corresponding CAFL is 4.5 ksi. Since the calculated stress range (6.8 ksi) is greater than the CAFL (4.5 ksi) the stiffener to stub connection is inadequately designed for fatigue.

4.7 Strut to Chord Connection

The details of the strut to chord connection are shown below. Because both of the members in the connection are subject to loads the detail must be checked with respect to the stress in each member.



Chord diameter = $D_{chd} = 16$ in
 Chord thickness = $t_{chd} = 0.5$ in
 Strut diameter = $D_{strut} = 5.563$ in
 Strut thickness = $t_{strut} = 0.375$ in

4.5.1 With Respect to Stress in Chord

The following calculations determine the fatigue strength of the strut to chord connection with respect to the stress in the chord.

4.5.1.1 Moment of Inertia and Area

The moment of inertia and area of the chord are respectively calculated by:

$$I_{chd} = \frac{\pi}{64} [D_{chd}^4 - (D_{chd} - 2t_{chd})^4] = \frac{\pi}{64} [(16in)^4 - (16in - 2 * 0.5in)^4] = 732.0in^4$$

$$A_{chd} = \frac{\pi}{4} [D_{chd}^2 - (D_{chd} - 2t_{chd})^2] = \frac{\pi}{4} [(16in)^2 - (16in - 2 * 0.5in)^2] = 24.35in^2$$

4.7.1.2 Stress Range in Chord

Based on the calculations in section 3 truck-induced wind gusts control the strut to chord connection. The stress range in the chord is calculated by:

$$(S_R)_{chd-strut} = \frac{Axial_{TG}}{A_{chd}} + \frac{(M_z)_{TG} c}{I_{chd}} = \frac{31.7k}{24.35in^2} + \frac{(7.0kft)(12in/ft)(8in)}{732.0in^4} = 3.2ksi$$

With respect to the stress in the chord the strut to chord connection is a category E detail. The corresponding CAFL is 4.5 ksi. Since the calculated stress range (3.2 ksi) is less than the CAFL (4.5 ksi) the strut to chord connection is adequately designed for fatigue.

4.7.2 With Respect to Stress in Strut

The following calculations determine the fatigue strength of the strut to chord connection with respect to the stress in the strut.

4.7.2.1 Moment of Inertia and Area

The moment of inertia and area of the strut are respectively calculated by:

$$I_{strut} = \frac{\pi}{64} [D_{strut}^4 - (D_{strut} - 2t_{strut})^4]$$

$$I_{strut} = \frac{\pi}{64} [(5.563in)^4 - (5.563in - 2 * 0.375in)^4] = 20.67in^4$$

$$A_{strut} = \frac{\pi}{4} [D_{strut}^2 - (D_{strut} - 2t_{strut})^2] = \frac{\pi}{4} [(5.563in)^2 - (5.563in - 2 * 0.375in)^2] = 6.11in^2$$

4.5.2.2 Stress Range in Stub at Column Face

Based on the calculations in section 3 truck-induced wind gusts control strut to chord connection. The stress range in the strut is calculated by:

$$(S_R)_{strut-chd} = \frac{Axial_{TG}}{A_{strut}} + \frac{(M_z)_{TG} c}{I_{strut}} = \frac{11.6k}{6.11in^2} + \frac{(0.65kft)(12in/ft)(2.782in)}{20.67in^4} = 4.0ksi$$

With respect to the stress in the strut, the strut to chord connection is a category ET detail. The corresponding CAFL is 1.2 ksi. Since the calculated stress range (4.0 ksi)

is greater than the CAFL (1.2 ksi) the strut to chord connection is inadequately designed for fatigue.

